DEVELOPMENT OF PHASE-RESOLVED PATTERN DATABASE TO IDENTIFY PARTIAL DISCHARGE ACTIVITIES IN SOLID DIELECTRICS

A thesis submitted in partial fulfilment of the degree of Master of Electrical Engineering

By

PAYEL BANERJEE

Examination Roll No.: M4ELE19005

Registration No.: 140664 of 2017-2018

Under the guidance of

Dr. Kesab Bhattacharyya

Professor

Department of Electrical Engineering

Faculty of Engineering and Technology

Jadavpur University

Kolkata, India

&

Dr. Biswendu Chatterjee

Associate Professor

Department of Electrical Engineering

Faculty of Engineering and Technology

Jadavpur University

Kolkata, India

Department of Electrical Engineering

Faculty of Engineering and Technology

Jadavpur University

Kolkata - 700032

JADAVPUR UNIVERSITY
KOLKATA- 700032, INDIA

FACULTY OF ENGINEERING AND TECHNOLOGY

CERTIFICATE OF RECOMMENDATION

This is to certify that the thesis titled "**Development of Phase-resolved Pattern Database to Identify Partial Discharge Activities in Solid Dielectrics**", submitted by Payel Banerjee (Registration No.140664 of 2017-2018 and Exam Roll No. M4ELE19005) has been carried out under our supervision and be accepted in partial fulfilment of the requirement of the degree of "Master of Electrical Engineering" of Jadavpur University.

Prof. Kesab Bhattacharyya
Head, Dept. of Electrical Engineering,
Faculty of Engineering and Technology,
Jadavpur University

Dr. Biswendu Chatterjee
Associate Professor,
Dept. of Electrical Engineering,
Faculty of Engineering and Technology,
Jadavpur University

Prof. Kesab Bhattacharyya
Head, Dept. of Electrical Engineering,
Faculty of Engineering and Technology,
Jadavpur University

Prof. Chiranjib Bhattacharjee
Dean,
Faculty of Engineering and Technology,
Jadavpur University

JADAVPUR UNIVERSITY
KOLKATA- 700032, INDIA

FACULTY OF ENGINEERING AND TECHNOLOGY

CERTIFICATE OF APPROVAL*

The thesis titled "**Development of Phase-resolved Pattern Database to Identify Partial Discharge Activities in Solid Dielectrics**", submitted by Payel Banerjee (Registration No.140664 of 2017-2018 and Exam Roll No. M4ELE19005), for the award of Master of Engineering Degree in Electrical Engineering with specialization in "High voltage engineering" during 2017-2019 at Jadavpur University, is hereby approved as a credible study of an engineering subject carried out and presented in a manner satisfactory to warrant its acceptance as a prerequisite to the degree for which it has been submitted. It is understood that by this approval the undersigned does not necessarily endorse or approve any statement made, opinion expressed or conclusion therein but approve this thesis only for the purpose for which it is submitted.

_____

Signature of the Supervisor

_____ _____

Signature of the Examiner(s) Signature of the Supervisor

*Only in case the thesis is approved

JADAVPUR UNIVERSITY
FACULTY OF ENGINEERING AND TECHNOLOGY

Declaration of Originality and Compliance of Academic Ethics

I, hereby declare that the thesis entitled "**Development of Phase-resolved Pattern Database to Identify Partial Discharge Activities in Solid Dielectrics**" contains a literature survey and original research work as part of the course of Master of Engineering studies.

All the information in this document has been obtained and presented in accordance with academic rules and ethical conduct.

I, also declare that the materials and results that are not original to this work have been fully cited and referenced as required by the rules and conduct.

Name	:	Payel Banerjee
Exam Roll No.	:	M4ELE19005
Registration No.	:	140664 of 2017-2018
Title of the Thesis	:	Development of Phase-resolved Pattern Database to Identify Partial Discharge Activities in Solid Dielectrics
Signature with date	:	

ACKNOWLEDGEMENT

I would like to express my sincere gratitude and indebtedness to my project supervisors, **Dr. Kesab Bhattacharyya** Professor, Department of Electrical Engineering, Jadavpur University and **Dr.Biswendu Chatterjee**, Associate Professor, Department of Electrical Engineering, Jadavpur University for their continuous support, the immense share of knowledge, patience and motivation during the course of the research work. This thesis work would not have been possible without their valuable help and guidance.

I would like to express my deep sense of gratitude to **Dr. Sovan Dalai** and **Dr. Arpan Kumar Pradhan**, Department of Electrical Engineering, Jadavpur University, for their insightful comments, encouragement and active support in this thesis work. I would like to extend my gratitude to the **High Tension Laboratory** of Jadavpur University, Kolkata, for providing excellent facilities to conduct the research work smoothly.

I am grateful to **Dr. Kesab Bhattacharyya**, Head, Department of Electrical Engineering, Jadavpur University, for providing the necessary facilities for carrying out this research work.

I would like to take this opportunity to express my indebtedness to my friends and colleagues **Mr. Arup Kumar Das**, **Mr. Sanjoy Pondit** and **Mr. Syed Sharif Alam,** P.G. Scholars, E.E. Department, for their constant assistance, stimulating discussions and encouragement. I would like to convey my soulful thankfulness to the rest of the P.G.Scholars of E.E. department for their moral support during the course of the research work.

Last but not least, I would like to express my profound gratitude to my family for the continuous encouragement throughout my years of study and through the process of researching and writing this thesis. This accomplishment would not have been possible without them.

Payel Banerjee
Department of Electrical Engineering
Jadavpur University

CONTENTS

CONTENTS

CONTENTS

CONTENTS

ABSTRACT

With the rapid increase in power demand and development of power systems, it is essential for the various electrical systems to operate reliably. The reliability of these essential electrical devices is of utmost importance as failure results in an interruption to electrical power delivery. Now, for reliable performances, these electrical devices are heavily dependent on its insulation system. Most of the high voltage equipment consists mainly of solid insulations. Now, generally due to the bulk transmission of power these solid insulation system of the electrical devices are constantly under different stresses like electrical, thermal, mechanical, etc. which degrades the properties of the insulation ultimately leading to the breakdown of insulation. Moreover, real solid dielectrics used in the insulation systems consist of voids, impurities, etc that causes internal discharges. These internal discharges are the underlying reasons for its breakdown. Thus, early detection of these various causes is imperative to prevent the failure of insulation. Many diagnostic methods are applied to monitor the actual condition of the insulation. Amongst the various diagnostic methods partial discharge (PD) measurement of the insulation has been considered as a promising tool as it gives a brief idea about the aging condition of the insulation sample and location of the PD source in the dielectric. In this work, partial discharge activities in different solid dielectrics are studied and a database is developed based on the phase-resolved PD pattern obtained. From these PD activities a brief idea about the ability of the insulation to be a suitable insulation for practical purposes could be found.

NOMENCLATURE

V	Voltage
i_{pol}	Polarization current
i_{depol}	Depolarization current
t_{pol}	Charging time
$f(t)$	Polarization function
σ_0	D.c. conductivity
PI	Polarization index
tanδ	Dielectric dissipation factor
I_R	Resistive current
I_C	Capacitor current
ω	Frequency of the applied voltage
T1	Front time of a partial discharge signal
T2	Tail time of a partial discharge signal
ε_r	Relative Permittivity
$\boldsymbol{L}$	Inductance
C	Capacitance
R	Resistance
ϕ	Phase angle
q	Charge magnitude of a signal
n	Rate of pulse count
I_{max}	Maximum magnitude of current
I_{known}	Known magnitude of a current signal
μ	Mean value
σ	Standard deviation
S_k	Skewness
K_u	Kurtosis

LIST OF FIGURES

LIST OF FIGURES

LIST OF FIGURES

LIST OF FIGURES

LIST OF TABLES

METHODS ADOPTED TO ASSIGN NUMBERS TO FIGURES, TABLES AND EQUATIONS

Figures, tables and equations have been numbered in accordance with the chapters in which they appear in the thesis. Each figure, table and equation have two distinct digits. The first one specifies the serial number of the chapter and the second digit denotes to the actual number of the figure, table or equation in that chapter.

REPRESENTATION OF REFERENCES

The list of references has been furnished at the end of the thesis. These references have been represented by the respective name of the author(s) along the year of publication.

CHAPTER - 1

Introduction

Chapter 1

1.1 BACKGROUND

The insulation forms the backbone of a functional electrical system. Insulation is used in almost all electrical devices and the life expectancy of the electrical apparatuses depends predominantly on the condition of their insulation system. Failure in insulation leads to catastrophic failures in the various high voltage equipment, which engenders widespread interruption in the service and sometimes service break. For the reliable and durable performance of these electrical devices, proper insulation selection is important. It is thus essential to know the property of the insulating medium for an optimum solution in terms of insulating capability and cost [1,2].

Generally, the solid insulation is preferred over liquid and gaseous dielectrics as it not only possesses the properties which exist in liquid and gaseous dielectrics but also provides better dielectric strength and mechanical support. From the very first day in the line of service, these solid insulations are subjected to various stresses like electrical, thermal, mechanical which after prolonged operation affects the insulation and the properties of the dielectric would get degraded. However, real solid dielectrics contain voids, cavities, and other manufacturing defects. Under normal working stress itself, the voltage across the cavities may exceed the breakdown value and initiate internal breakdown and thus insulation degradation takes place. Therefore, a lot of research activities are directed towards a better understanding of the breakdown process of solid insulation [3].

To assure reliable and long-lasting operation of electrical equipment, preventive measures are taken with the help of various condition monitoring tools. Condition monitoring maximizes the performance of the insulation material and helps to improve the longevity of the equipment. Now, amongst the various diagnostic methods, partial discharge (PD) measurement of the insulation has been considered as a promising tool [3,4].

The PD measurement is a non-destructive, non-intrusive diagnostic method and also produces insights for the identification of the defects in the insulation system. This diagnosis, reports the various characteristics of the material which helps in keeping the occurrence of various faults viz insulation degradation, etc in check. The PD measurement has been used as the quality control test of any new equipment. It has been a tedious job to carry out real-time diagnostic tests on the insulation system in service, thus samples are

collected and studied. The analyzed results help in providing useful information about the actual condition of the sample insulation. In the case of the electrical method of detection of PD, the characteristics of the PD have been studied with the help of phase-resolved partial discharge (PRPD) distribution.

In this thesis, condition monitoring of various common solid insulation has been performed with the PD measurement as the diagnostic method and a comparative study has been drawn for different sets of samples. Also, condition monitoring of these samples was performed and analyzed based on the dissipation factor (tanδ) and the insulation resistance (IR) of these insulation samples [5,8].

1.2 AIM OF THE THESIS

The PD measurement is an important diagnostic tool to ascertain the condition of the insulation system. The aim is to assemble an experimental set up in the laboratory, for the measurement of PD data for various solid insulation samples such that the cost of the system can be optimized without compromising the precision and quality of data collection technique.

A typical PD pulse has a time duration of some nanoseconds, which needs high- end oscilloscopes to measure. This, in turn, makes the overall PD measurement system very costly. On the other hand, low-end oscilloscopes with higher time per division involve a much lower cost in acquiring PD data. However, this system has a typical limitation that individual PD pulses cannot be segregated. Instead, the system captures an aggregate of the few pulses as one pulse. If a suitable algorithm can be applied then this lower order aggregated partial discharge pulse can also give the measure of the partial discharge activities in the sample. By suitable multiplication factor, the quantitative PD activity in both the systems can be made very close with respect to the apparent charge. Since the main target was to identify the deterioration rate in the sample with respect to the PD activity, if there was a close match of apparent partial discharge between the high and low-end systems, then this process could be a low cost but effective alternative to high-end PD analyzers or sensors. From another viewpoint, it has been observed that the frequency range PD activity spans from KiloHertz (kHz) to MegaHertz (MHz). The PD in the lower frequency range can give a reflection of the condition of the sample under use, results of which are expected to be almost identical if PD is captured in the higher frequency range.

To overcome the limitations of the method, PD calibrator has been used to fine tune the algorithm.

PD data collected via the phase-resolved PD technique has been studied, analyzed and an attempt has been made to draw a comparative study among the samples. The PRPD pattern for every sample is unique and the aim of this thesis work has been to report these distribution patterns for different conditions of the sample.

In parallel, the characteristics of the samples were studied based on the dissipation factor (tanδ) and IR measurement to give a brief idea about the deterioration of the insulation samples. All these diagnostic methods were adapted for quality control and to have a brief idea about the condition of the sample.

1.3 CONTENT OF THE THESIS

The whole thesis has been divided into two parts. In the first part, the experimental set up was prepared to carry out the PD measurement procedure of the insulation samples. The measurement of the tanδ and IR of the sample are also performed. In the second part, quantification of the PD data has been done and a comparative analysis was drawn based on the PD data. Based on the tanδ and IR measurement comparative study was made about the samples. The main objectives of the work are

- To assemble all the components and devices required for the experimental process to perform the PD measurement tests on various solid insulation samples.
- To develop an algorithm to compute the partial discharge inception voltage of each sample during the experiment.
- To develop an algorithm to detect the PRPD patterns, which have been later analyzed to have an idea about the deterioration rate of the insulation.
- To develop an algorithm to calibrate the current signals obtained during PRPD analysis with a known signal and quantification of these current signal into charge magnitude to have an idea about the amount of discharge.
- To provide a comparative study based on PD monitoring for all the samples. The unique PRPD patterns for different samples are reported. The PRPD data for each and every sample has been analyzed and compared to give an estimation of the quantity of PD.

- To provide a comparative study of the sample based on the tanδ and IR to produce insight into the deterioration of the sample.
- To compute a few statistical operators applying standard statistical analysis for the characterization of several uni-variate PRPD distributions.

1.4 ORGANIZATION OF THE THESIS

The entire thesis work has been documented chronologically in eight chapters. The mentioned Chapters are as follows

Chapter 1 comprises of background, aim, and content of the thesis which gives a brief insight into the thesis work.

Chapter 2 describes the purpose of using solid insulation in different high voltage equipment and states their advantages and drawbacks. Varied insulation samples along with their features and applications have been produced here.

Chapter 3 describes the necessity of condition monitoring of insulation samples using various diagnostic methods. The reason behind the selection of PD measurement as the diagnostic method has been explained here.

Chapter 4 explains PD occurrence, mechanism and principal measurement technique using the concept of apparent charge. The description of a typical PRPD distribution has been presented.

Chapter 5 discusses the processes of sample preparation and assembling the experimental set-up for the PD measurement. It chronicles the processes required for acquiring the PD data, tanδ value, IR value for each sample.

Chapter 6 prepares a database of different insulation samples based on the characteristics of PD Pattern. A comparative study has been also prepared based on the tanδ and IR values of the insulation samples.

Chapter 7 explains the characterization of PRPD patterns based on statistical analysis. It also provides a complete 3-D representation of a ϕ-q-n graph of a sample.

Chapter 8 provides the conclusion and explains the future scope of the thesis in brief.

CHAPTER - 2

Solid Insulating Materials

Chapter 2

2.1 INTRODUCTION

The reliability of high voltage electrical devices is largely determined by the quality of the insulation materials used. The insulation system is composed of a unique combination of materials that have been verified for chemical compatibility when used at certain maximum temperatures. These combinations are arranged and applied as an insulation system for motors, transformers, relays solenoids, etc. electrical insulation plays an important role in high voltage equipment safety. There are diverse insulating materials and the engineers need to comprehend which insulating material would go best for what type of electrical equipment.

Each insulating material has its own unique properties which vary from one another based on their composition, electrical properties, breakdown strength, ability to withstand thermal pressure ,electrical and mechanical stresses, etc. This chapter documents the different types of dry-type insulating materials used in the Electrical system [5,8,24].

2.2 THE PURPOSE OF ELECTRICAL INSULATION

The insulation materials must be able to reliably withstand the numerous mechanical, thermal, electrical, chemical and climatic loads when in operation. The preponderant cause of equipment failure is dependent on insulation faults. The primary use for insulation in electrical apparatuses is to separate electrical circuits and conducting parts of different voltages. Thus, insulation has a great responsibility for providing reliable and successful operation of the electrical apparatus [21,23].

2.3 GENERAL CONSIDERATION FOR INSULATION SELECTION

The insulation must meet several important requirements but these primary characteristics determine the effectiveness of the insulation. It must have a satisfactory level of dielectric breakdown strength, high electrical resistivity, and suitably low dielectric loss. Moisture resistance has been a highly desirable property in most electrical insulation. Insulation must also fulfil many important physical properties that help in withstanding physical forces under operating conditions. Physical characteristics that are important comprises of compressive strength, flexural property, tear strength, tensile strength, resistance to abrasion, etc. The insulation should be capable of retaining its characteristics even after

reasonable deformation. Thermal conductivity of insulation and chemical resistance are vital. The practical design of equipment generally involves considerable compromise as there is no universal insulating material present and no single insulating material has all the desired properties [23,24].

An increase in the working temperature of insulation has great practical significance. In electrical machines, the extension of the temperature rise, which is usually limited by insulating materials, makes it possible to raise the capacity of an electrical machine without changing its dimensions or to reduce its size and lower the cost keeping the same power rating [3,4].

As recommended by IEC 60085, the insulating materials used in electrical equipment are classified according to their thermal endurance [22]. Each insulation class is assigned a certain temperature limit for long time service under normal working conditions as given in Table 2.1.

TABLE 2.1 THERMAL CLASSIFICATION OF INSULATING MATERIALS [22].

Sl.No	Class of Insulation	Temperature Limit
1	Y	90°C
2	A	105°C
3	E	120°C
4	B	130°C
5	F	155°C
6	H	180°C
7	C	>180°C

Operation of insulating materials at such temperatures ensures a desirable life for electrical equipment from technical and economic consideration.

2.4 INSULATING MATERIALS AND THEIR CHARACTERISTICS

The different dry type solid insulating materials used for the experiment are listed here. A few important characteristics have been mentioned in the subsequent sub-sections.

2.4.1 PRESSBOARD [25,26]

Here two types of pressboards have been used based on thickness. The thicknesses of the Pressboards are 0.89mm and 1.8mm.

- **Description:** Pressboard is produced from pure unbleached cellulose from softwood pulp. Layers of wet boards are pressed under heat and pressure and then dried simultaneously to form a laminate. The cellulose fibers are processed into various grades and thickness in the form of sheets. These are non-toxic in nature.
- **Features:** Good dimensional stability, good dielectric strength, high mechanical strength, excellent flexibility, low cost, easy to fabricate, stable density.
- **Application:** Power and distribution transformers, instrument transformers, shunt reactors, inductors, capacitors.
- **Class of Insulation:** A.
- **Dielectric Strength:** 12kV/mm (0.89mm), 14kV/mm (1.81mm) at a temperature of 25°C.

2.4.2 LEATHEROID PAPER [27]

- **Description:** It is double layer insulation made of polyester film with insulating press paper overlay on one side for insulation.
- **Features:** High tensile and tear strength, high dielectric strength, good dimensional stability, compatibility with impregnating varnishes and oil.
- **Application:** Slot insulation, slot closure, layer insulation in electric motor, chokes and small transformers.
- **Class of Insulation:** B.
- **Dielectric Strength:** 20kV/mm at a temperature of 25°C.

2.4.3 NOMEX FILM

Here, two types of nomex films have been used based on thickness. The thicknesses of the nomex films are 0.15mm and 0.25mm.

- **Description:** It is a composite of polyester and nomex laminates (three-ply laminate with nomex paper between two layers of the polyester film).
- **Features:** Good mechanical stability, excellent thermal and chemical stability, excellent electrical property, and heat resistant.

- **Application:** Used in motors and generators as slot insulation, phase insulation, interphase insulation. In dry-type transformers, it is used as layer insulation for coils. Also used in choke coils. They are commonly used in class H generators and motors and also largely in class F motors [29].
- **Class of Insulation**: C.
- **Dielectric Strength:** 30kV/mm (0.15mm) and 32kV/mm (0.25mm) at a temperature of 25°C.

2.4.4 NOMEX PAPER

- **Description**: Nomex paper has a composition of poly-aramid poly-meta-phenylene isophthalamide.
- **Features:** Outstanding thermal stability and mechanical toughness, excellent inherent dielectric strength, flame resistance, and chemical compatibility make Nomex paper ideal as dry-type transformer insulation. The use of Nomex paper for motor insulation can help prevent premature motor failure and equipment downtime because Nomex does not shrink, embrittle, soften or melt during short-term exposure to temperatures.
- **Application:** In dry-type transformers, it is used as turn and conductor insulation, layer and barrier insulation, core insulation, lead and tap insulation, end filler, channel and washer, radial and axial spacers. It is used in almost all kinds of motors - AC Industrial (class F and class H), low voltage traction (random wound), high voltage traction (form wound), high voltage motor, automotive starter, automotive alternator, automotive motor for EV/HEV, d.c. traction motors. It's usage also extends to slot liners, wedges, and mid sticks, phase insulation, conductor insulation, coil separators, pole insulation, turn insulation, main wall insulation in all these motors [28].
- **Class of Insulation:** C.
- **Dielectric Strength:** 35kV/mm (3mil) at a temperature of 25°C.

2.4.5 KRAFT PAPER

- **Description:** The usual electrical grade kraft paper is made of very high quality unbleached, the kraft-processed, long-fibered pulp with high porosity.

- **Features:** It has high tensile strength and durability. It is heat resistant and has good dielectric properties.
- **Application**: In electrical motors, it is used as electrical insulation between layers of wound coils. In current transformers and power transformers, it is used in the windings. Other than these, it is also used in the transformer bushing [41].
- **Class of Insulation:** A
- **Dielectric Strength:** 8kV/mm at a temperature of 25°C.

2.5 ADVANTAGES OF USING DRY-TYPE INSULATIONS [30,31,32,33]

- Dry-type insulation offers enhanced safety because there is no fluid spill, explode or burn.
- Dry-type transformers and motors using Nomex paper and laminates as the insulation medium can be located close to their loads. Hence, dry type insulation based electrical devices are located inside factories, schools, hospitals, and apartments.
- Dry-type transformers insulated with thermally high graded dry-type insulation can be designed for temperature rise, requiring less conductor and core steel, which can result in a lower initial cost. The reduced size and weight contribute to ease of installation and the smaller cores result in lower no-load losses.
- The overload capabilities of electrical machines increase when suitable dry type insulations are used.
- Some of the dry-type insulations are moisture resistant, thus electrical devices incorporating these insulations can be used in humidity prone areas such as in marine application.
- Suitable for use in lower ambient temperature makes them extremely utilitarian.

2.6 DISADVANTAGES OF USING DRY-TYPE INSULATIONS [30,31,32,33]

- For same power and voltage rating, electrical machines using dry type insulation is costlier than the oil cooled machines.
- Electrical machines using dry type insulation are long-lasting, but if there is an insulation failure the whole set up needs to be changed.

- Electrical machines eg. Transformers using dry type insulation, due to lack of constant cooling medium comes under the effect of environmental conditions, and thus the span of life decreases.

CHAPTER - 3

Condition Monitoring of the Solid Insulating Material

Chapter 3

3.1 INTRODUCTION

Power Transformers, CTs, PTs, motors, generators form the integral components of the Power System. The failure of these electrical devices leads to potentially widespread interruption of service and high replacement cost, so condition monitoring of this equipment deserves more attention. For reliable and efficient operation, the insulation system of these components needs to be in the first-rate condition. From the very day of this equipment in service, different stresses like electrical, thermal, mechanical, chemical and other environmental condition affect the insulation system of these components. Partial discharge, hotspots, etc degrades the quality of the insulation and eventually leads to the breakdown of the insulation. At the initial stage, degradation of the quality of the insulation is slow, but the rate of deterioration increases rapidly in due course of time which ultimately leads to insulation failure of the system. So, to avoid this situation continuous monitoring is required to take preventive measures. Now, it is always not easy to dismantle electrical equipment for condition monitoring, hence a sample specimen of the insulation is tested and the condition of the equipment is decided based on that. Condition monitoring saves the equipment from catastrophic failure which provides economic benefits [4,6,10,12].

3.2 PURPOSE OF CONDITION MONITORING [6,10]

Capabilities of Condition Monitoring include high-resolution data acquisition, sophisticated alarming, exception reporting, and user notification capabilities. Data acquisition and subsequent signature analysis is a critical component of an overall electrical asset predictive maintenance program.

- Early detection of equipment degradation or impending failure helps to reduce maintenance costs. Limiting unplanned failures or significant degradation leads to increased productivity and thus increasing the lifespan of the machinery.
- Outage duration can be decreased if a thorough understanding of the equipment condition is available from beforehand.
- Continued operation of degraded equipment is possible by continuous critical observation of the asset such that continued production is possible while necessary

repairs are pre-planned. Performing repairs at a more convenient time minimize production losses and increase profitability.

- Condition monitoring based on several diagnostic methods helps in optimizing the equipment performance and hence helps in the better economic performance of various utilities.

3.3 A BRIEF THEORY ON BREAKDOWN IN SOLIDS [5,8]

Solid dielectric materials are used in all kinds of electrical circuits and devices to insulate one current carrying part from another when they operate at different voltages. Generally solid insulating materials possess all the qualities that are already there in liquid and gaseous dielectrics and in addition, it has higher breakdown strength along with better mechanical and bonding properties. Thus solid insulating materials are a good choice and always preferred.
Now, studies of the breakdown of solid dielectrics are of extreme importance in insulation studies.

Usually, a small number of conduction electrons are present in the solid dielectrics along with imperfections. When a certain range of the applied electric field is exceeded, these electrons creates electron avalanche leading to the breakdown of the solids. This phenomenon is known as an intrinsic breakdown. In the case of electro-mechanical breakdown when solid dielectrics are subjected to high electric fields, failure occurs when electrostatic compressive forces exceed the mechanical compressive strength of the material. The thermal breakdown is extremely common in case of solid dielectrics. When an electric field is applied to a dielectric, a small amount of conduction current flows and due to this heat is generated in the solid and heats up the material. When the heat generated in the dielectrics is greater than the heat dissipated thermal breakdown of the solid takes place. Solid dielectrics in the presence of air and gases undergo chemical changes when subjected to electrical stresses which eventually reduces the service life of the solid dielectric. No single mechanism can explain the breakdown phenomenon in solid dielectrics, as at the time of application of voltage, the different mechanism becomes active. [8,10]

In practice there are certain types of breakdown which do not fall under the above mechanisms. These breakdowns occur due to internal discharges, after prolonged operation. These are commonly known as ‘Treeing’ and ‘Tracking’. The conducting paths

may be formed on the insulator surfaces or there may be discharges due to the presence of voids in the solid which may lead to breakdown after a long time. These mechanisms for the generation of PD are elucidated in Chapter 4.

3.4 CONDITION MONITORING OF SOLID INSULATION

As previously mentioned in section 3.1, condition monitoring of high voltage devices is absolutely necessary. The insulation used in electrical devices is mainly solid. The presence of oxygen and moisture, electro-mechanical stress, thermal stress, etc., are strong contributors to the degradation as well as the aging process of the overall insulation of an electrical system. Since the aging of the insulation system can affect its electrical as well as its chemical properties, few diagnostic methods are applied for condition monitoring [8,10].

3.4.1 DIAGNOSTIC METHODS

Few of the diagnostic methodologies are applied to check and monitor the actual condition of the insulation and detect changes in the insulation structure or condition. Electrical tests involve assessing the electrical properties of the dry type solid insulation. Many of these tests fall under the routine test performed on these devices [8,14].

3.4.1.1 Polarization and Depolarization Current (PDC) Measurements

This measurement process includes applying a step voltage source on the dielectric sample for a large time span of $0 \leq t \leq t_{pol}$ in order to initiate the polarization process. The current during this time span can be termed as charging current or polarization current (i_{pol}). If charging time span (t_{pol}) is very large in order of 1000s -10000s, then polarization current become steady and only conduction current flows. If the applied voltage is removed and the sample is shorted at $t=(t_{pol})$, then the sample starts to discharge and the current recorded is termed as depolarization or discharging current (i_{depol}). Depolarization current is also termed as Isothermal current if the temperature remains constant during the depolarization process. The i_{depol} is directly proportional to the dielectric response function [*f(t)*]. So from PDC measurement, the time response of the dielectric can be calculated and the d.c. conductivity (σ_0) can also be derived from the difference between

i_{pol} and i_{depol}. Based on these two the extent of aging and moisture content of the overall sample can be investigated [4].

3.4.1.2 D.C. High-Potential (Hi-Pot) Test

Hi-pot test is also known as Dielectric Withstand Test. This test checks for leakage current and is a non-destructive test that determines the adequacy of electrical insulation for the normally occurring over voltage transient. This is a high-voltage test that is applied to all devices for a specific time in order to ensure that the insulation is not marginal. Hi-pot test helps to find degraded insulation. As per IEC 60950, the basic test voltage for Hi-pot test is the 2×(Operating Voltage) + 1000V. The reason for using 1000V as part of the basic formula is that the insulation in any product can be subjected to normal day-to-day transient over-voltages [3,7].

3.4.1.3 Breakdown Strength and Tensile Strength Measurement

Breakdown tests are done to check the withstand capacity of the insulation system by applying high voltage which is greater than the rated service voltage. The main purpose of this test is to check the reliability of the paper insulation. The mechanical strength of the paper is determined by its tensile strength. The insulating paper provides both electrical as well as mechanical strength. Tensile strength is often regarded as breaking strength per unit cross-sectional area of the paper. It is able to determine the strength of the paper and predict the suitability of the insulation used. The major limitation of the above tests is that they are destructive in nature in the case where the insulation is non-self-restraining. These tests lead to the breakdown of the insulating material i.e. property of the insulation material could be destroyed. Breakdown voltage varies depending upon the size of the specimen, but dielectric strength is an intrinsic property of the dielectric material and hence does not vary with the size of the specimen [3,8].

3.4.1.4 Insulation Resistance (IR) Test

This method is non-destructive. The instrument used for conducting this test is a megohmmeter also known as megger. In the test, a relatively high d.c. voltage is applied to the sample. The current flowing in the circuit is then measured. The insulation resistance (indicates material's resistance in mega-ohm) at time *t* is given in equation 3.1.

$$R_t = \frac{V}{I_t} \quad (3.1)$$

where V is the applied d.c. voltage and I_t is the total current measured after t minutes, as the current is not usually constant. As the resistance of insulation material is temperature dependent, all readings need correction (temperature correction factor) to the standard temperature for the class of the equipment under test.

There are at least four currents that may flow when a d.c. voltage is applied to the winding. They include capacitive charging current, conduction current, leakage current, absorption current.

A good insulation system shows a continued increase in its resistance value over the period of time in which voltage is applied, and on the other hand, an insulation system that is contaminated with moisture, dirt, etc will show a continuous downward trend.

Therefore, engineers measure insulation resistance in four common methods. They are (a) short-time readings, (b) time-resistance readings, (c) polarization index test, and (d) step-voltage test - to check for deterioration in the insulation system [9].

3.4.1.5 Polarization Index (PI) Test

The PI test is performed in order to measure quantitatively the ability of an insulator to polarize. When an insulator polarizes, the electric dipoles distributes throughout the insulator align themselves with an applied electric field. A polarization current then gets adds to the insulation leakage current. When insulation is completely polarized, polarization current drops to zero. The PI test is typically performed at 500V, 1000V, 2500V and 5000V depending on the operating voltage of the equipment being tested. The duration of the test is 10 minutes. The PI value is calculated by diving the insulation resistance at 10 minutes by the resistance at 1 minute.

$$\mathrm{PI} = \frac{IR(10\,\mathrm{min})}{IR(1\,\mathrm{min})} \quad (3.2)$$

Insulators that are in good condition will show a high polarization index while insulators that are damaged will not. Dielectric absorption is the IR value at 3 minutes divided by IR value at 30 seconds [9,10].

3.4.1.6 Measurement of dielectric Dissipation Factor (tanδ)

Dielectric dissipation factor is one of the important measurement to check the quality of the dry type solid insulations used in electrical machines. It is also known as the loss

factor. This provides useful information about the causes of aging in the insulation system. A high dielectric loss will result in the thermal breakdown of the insulation. Dielectric dissipation factor is represented by tanδ. Where δ is the angle between capacitive voltage and voltage applied as shown in the Fig.3.1.

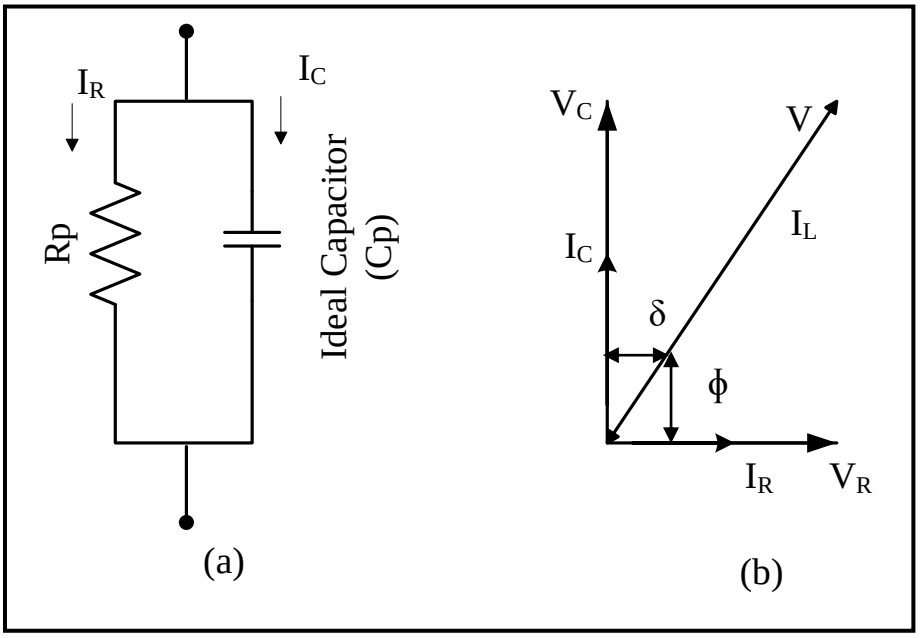

Fig. 3.1. Representation of a lossy dielectric (a) circuit representation and (b) Phasor Diagram.

Consider a dielectric medium in an a.c. circuit. The electrical representation of the insulation, in this case, would be a capacitor. If this dielectric medium is lossy, the capacitor is to be represented by a circuit in such a way that the active power dissipated by the circuit should be equal to the power dissipated in the capacitor dielectric, and the current should lead the voltage by the same angle as that observed in the dielectric under study. This equivalent circuit representation is done by modelling the lossy capacitor by an ideal capacitor (C_p) with a resistor (R_p) in parallel, as shown in Fig.3.1. So according to that if a voltage is applied across the insulator a current will flow through it. This total current can be divided into two components (i) Resistive Current (I_R=V/R) (ii) Capacitor Current (I_C=VωC). So as the resistive current increases the value of tan δ increases. It indicates that the insulation has deteriorated.

The expression for tan δ is given by

$$\tan\delta = \frac{I_R}{I_C} = \frac{1}{\omega RC} \qquad 3.3$$

Where ω is the frequency in rad/sec, C is the capacitance of the insulation in farad and R is resistance in ohms. In high voltage applications, insulation materials should possess low dissipation factor because it is directly related to energy loss in the dielectric [10,11,12].

3.4.1.7 Measurement of Partial Discharge (PD)

Amongst the various diagnostic techniques, PD measurement is considered as a promising tool for condition-based maintenance. Electrical breakdowns in a small region of the insulating system are called partial discharge. The following conditions can be determined during partial-discharge measurement:

- To determine whether a PD above a certain value has occurred in the transformer at a predefined voltage.
- To define the voltage values where the PD starts by increasing the applied voltage (PDIV) and the value where the PD ceases by decreasing the applied voltage (PDEV)
- To define the partial-discharge strength at a predefined voltage [13,15].

3.4.2 EMPHASIS ON PD MEASUREMENT AS THE DIAGNOSTIC METHOD

The appearance and the intensity of these PD pulses are a quality criterion for an electrical equipment rating and therefore an estimation of the condition of the insulation system can be done. So the partial discharge measurement has become a fixed part in industrial applications as a non-destructive high voltage test. It uses the different physical effects in different insulating systems to detect significant parameters to give directly or indirectly information about the equipment condition. PD provides information about the degradation stage of insulation defects due to the presence of voids, contaminations or moisture ingression. It acts as a forerunner for the aging phenomenon in electrical insulation. PD based diagnostic tool gaining importance, but it is useful when PD measurements are carried out with proper acquisition strategy with suitable instruments. In chapter 4, PD determination and measurement techniques in dry-type solid insulation sample will be discussed [13,15].

CHAPTER - 4

Theoretical Formulation

Chapter 4

4.1 INTRODUCTION

Insulation systems of electric machinery experience thermal, electrical, mechanical, and environmental stresses during operation. These stresses, individually or in combination, will age the insulation system and may lead to delamination of the insulation and other potential deterioration mechanisms. Sometimes, as a result of the initial manufacturing process, or because of the subsequent aging, Partial discharges (PD) may occur in the insulation of the machines. These various PD sites have the potential to cause deterioration to a greater or lesser extent and, in some cases, may ultimately result in an in-service failure. Experience has indicated that PD measurements can be useful for assessing the condition of the insulation. The number, magnitude, and polarity of these PDs can be a direct indication of the condition of the insulation system. In order to design a system to detect and locate the PD phenomenon within a high voltage system, it is important to understand the reason behind PD to occur and the methods to detect them. In this chapter, the basic idea of PD along with the mechanism of PD and measurement techniques are discussed [7,12,16].

4.2 PARTIAL DISCHARGE

A partial discharge, as defined by IEC 60270, is a "*localized electrical discharges that only partially bridge the insulation between conductors and which may or may not occur adjacent to conductors*". it is a partial breakdown in the insulation between two active conductors. Partial discharges can occur in any location where the local electrical field strength is sufficient to breakdown that particular portion of the dielectric material (whether it might be a deteriorated piece of insulation or an air cavity) [7].

The discharges generally appear as pulses with a typical duration of 1ns. While very short in duration, the energy present in the discharge can interact with the surrounding dielectric material resulting in further insulation degradation and eventually if left unchecked, failure of insulation takes place. Fig. 4.1 shows a typical partial discharge signal measured during experimental studies where T1 and T2 represent front time and tail time of PD signal respectively.

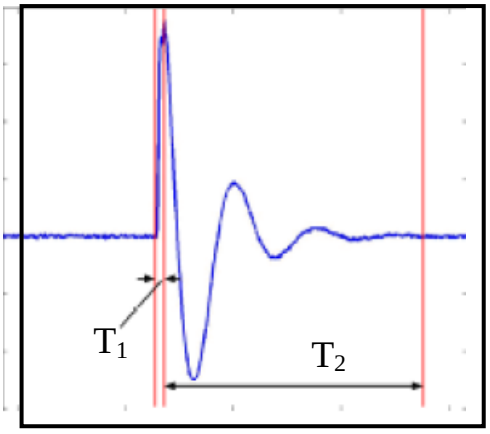

Fig. 4.1. Typical shape of PD Signal [7].

4.3 MECHANISM OF PARTIAL DISCHARGE

Some of the mechanisms to explain the breakdown in solid insulation due to the prolonged operation are explained in the subsequent subsection [8,10,17].

4.3.1 TREEING

When a solid dielectric insulator of thickness d_1 is placed between the sphere – plane electrodes as shown in Fig. 4.2, there is a possibility for two different dielectric media, i.e. a thin layer of air (thickness d_2) and the dielectric, to come in series. When voltage V is applied between the electrodes, a fraction V_2 of the applied voltage appears across the thin layer of air given by equation 4.2

$$V_2 = \frac{Vd_2}{d_2 + (\frac{1}{\varepsilon_r})d_1} \qquad 4.1$$

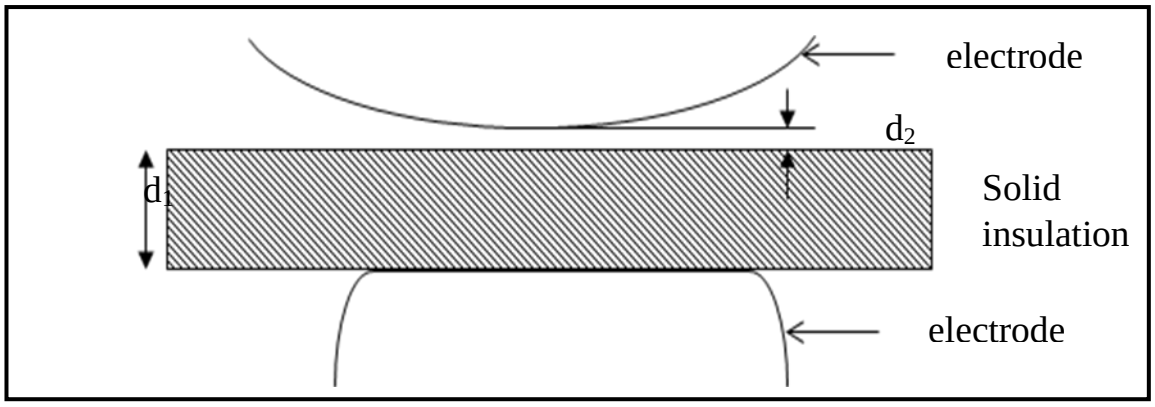

Fig. 4.2. Dielectric and electrode arrangement for the study of treeing [18].

Where ε_r is the relative permittivity of the solid insulation. The ratio of the dielectric stresses in the air gap E_2 and the solid E_1 is given by equation 4.2.

$$\frac{E_2}{E_1} = \varepsilon_r \qquad 4.2$$

Since ε_r >1, the stress in the air gap will exceed than that in the solid. This may result in a spark across the air-gap and thus charge accumulation takes place on the surface of the insulation. Sometimes erosion of the insulation surface takes place due to a spark. As time passes, breakdown channels spread through the insulation in an irregular fashion like the branches of a 'tree' resulting in the formation of a conducting channel throughout the insulation thickness. Hence care must be taken to see that no series air-gaps or weaker insulation gaps are formed.

4.3.2 TRACKING

Tracking is the formation of a permanent conducting path, usually carbon, across a surface of the insulation. This may result from the degradation of such insulation which contains some organic substance.

In the presence of moisture, leakage current flows through the pollution layer. This heats the surface which starts drying up and mall sparks are drawn between the separating moisture films. The heat resulting from these sparks causes carbonization at the region of sparking and the carbonized regions act as a permanent conducting channel. The electric stress over the rest of the region increases as the process acts effectively. Breakdown of the solid insulation occurs when the carbonized tracks bridge the gap between the electrodes and conduction paths are formed.

4.3.3 BREAKDOWN DUE TO VOIDS

Practical solid insulating materials contain voids or cavities. The voids are usually filled with a gaseous or liquid medium of lower breakdown strength than that of the solid. Also, the dielectric constant of the void medium is lower than that of the insulation. This results in higher electric field stress in the void compared to that in the solid. Accordingly, under normal working stress of the insulation, the field in the voids may exceed their breakdown value causing the breakdown of the voids.

It is possible to calculate the voltage across the dielectric which will initiate discharge in a gaseous cavity in a dielectric of thickness *'d'*. Fig. 4.3 shows the electrical equivalent circuit of a dielectric having a single void. The cavity is assumed to be in the form of a disc of thickness *'t'*, as shown in Fig. 4.3.

The insulating medium and the void may be represented by the three capacitances.

Cc -Capacitance of the void, *Cs* - Capacitance of the dielectric in series with the void, *Cr* - Capacitance of rest of the dielectric. This is shown in the equivalent electrical circuit in Fig. 4.3. So,

$$C_C = \frac{\varepsilon_0 A}{t} \ , \ C_C = \frac{\varepsilon_0 \varepsilon_r A}{d-t} \qquad 4.3$$

Where *A* is the cross-sectional area of the cavity disc, and ε_r is the relative permittivity of the solid

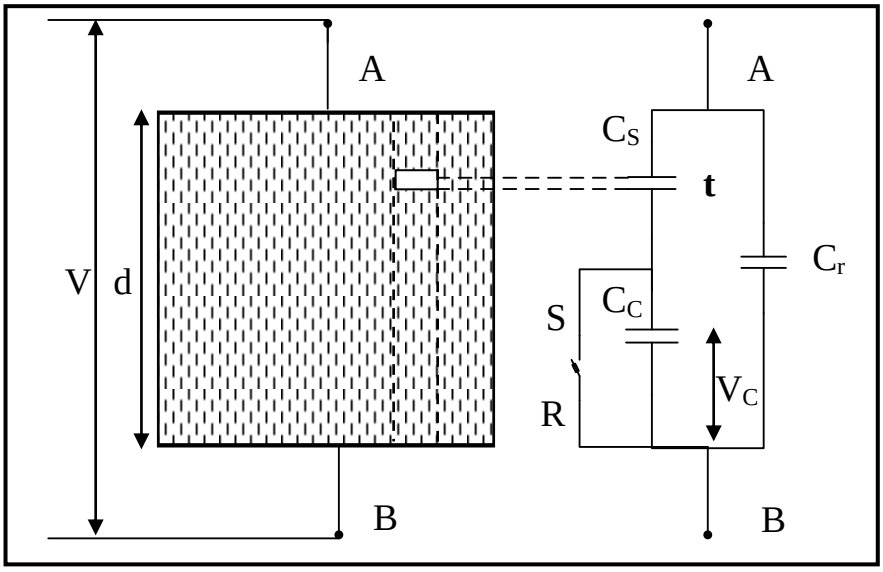

Fig. 4.3. Electrical equivalent circuit of a solid dielectric having a single void [18].

If a voltage *V* is applied across the dielectric, then the voltage across the void V_V is given by

$$V_V = \frac{C_S}{C_S + C_C} V = \frac{\frac{\varepsilon_r}{d-t}}{\frac{\varepsilon_r}{d-t} + \frac{1}{t}} V = \frac{V}{1 + \frac{1}{\varepsilon_r}(\frac{d}{t} - 1)}$$

$$\text{or} \quad V = V_V \{1 + \frac{1}{\varepsilon_r}(\frac{d}{t} - 1)\} \qquad 4.4$$

If the gaseous cavity has a breakdown strength of E_C, then the breakdown voltage across the cavity V_C , should be $E_C \times t$ and the dielectric voltage V_d required to cause the breakdown of the void is obtained by putting $V = V_d$ and $V_V = E_C t$ in the equation 4.4, i.e

$$V_d = E_C t\{1 + \frac{1}{\varepsilon_r}(\frac{d}{t} - 1)\} \qquad 4.5$$

So, when a voltage more than V_d is applied across the dielectric, breakdown of the gas in the void occurs. If an a.c. voltage is applied across the dielectric, the voltage across the void will also vary sinusoidally if there is no breakdown of the void. Fig. 4.4 shows the voltage V and V_V in the absence of any breakdown of the void.

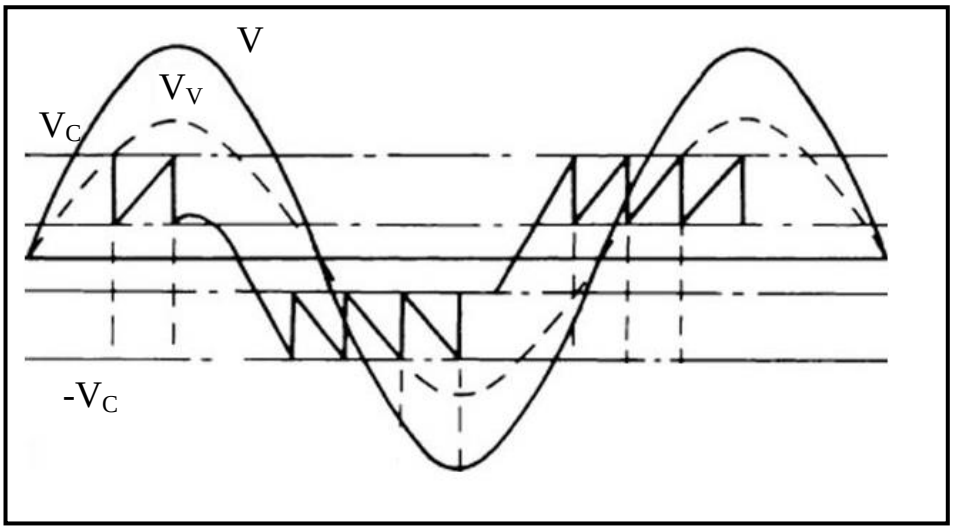

Fig. 4.4. The sequence of void breakdown under a.c. voltage [18].

From Fig. 4.4, it is seen that as V_V reaches the value V_C, a discharge takes place, the voltage V_V collapses and the spark gets extinguished. The voltage across the void then starts increasing again until it reaches V_C when a new discharge occurs. Thus several discharges may occur during the rising part of the applied voltage. Similarly in the negative half cycle of V, discharges in the void take place as V_V reaches - V_C. This discharge process is repeated in the void and it gives rise to positive and negative current pulses as shown in Fig. 4.4. These internal discharges are also known as the partial discharges (PD). During PD chemical bonds of the insulation gets broken at the void surfaces. Also, heat is produced in the discharge will carbonize the surface of the void and cause erosion of the material. These processes slowly degrade the insulation leading to a reduction in the dielectric thickness. The erosion roughens the surface and slowly penetrates the insulation

and later on it will increase channel propagation and 'tree-like' growth forms through the insulation. Ultimately breakdown of insulation will occur even at normal voltage application.

Thus in order for the PD to occur in a sample, the first criterion is that the electric field difference across the void must be higher than the breakdown value such that an electron can accelerate and produce more electrons in a chain like a process. The second criterion is that there must be a free electron present in the void.

4.4 MEASUREMENT OF PARTIAL DISCHARGE

PD measurement by electrical methods is not easy. The discharge takes place through impulses and the discharge quantity is also low. Measurement of these impulses is difficult due to electric noise originating from the adjoining circuits or from the test set-up itself. The fundamental principle of discharge measurements in solid insulation due to the void formation, when subjected to power frequency excitation, will be discussed in the following sub-sections.

4.4.1 CONCEPT OF APPARENT CHARGE

A dielectric system having a gas-filled cavity between electrodes *A* and *B* and the corresponding electrical equivalent circuit are shown in Fig. 4.3. The void will become a source of PD if the applied voltage is increased. The discharge characteristics with an a.c. voltage is shown in Fig. 4.4. It is these discharges which need to be measured. So the concept of apparent charges proportional to this discharge quantity has been applied and experimental techniques are adapted to measure these apparent charges to get an idea of partial discharge. The concept of apparent charges is discussed here.

The dielectric sample is shown in Fig. 4.3 is charged to a voltage *V*, but the terminals are disconnected from the voltage source. When the switch *S* is closed, the capacitor C_C discharges and the charge is lost in the whole system. This will cause a voltage drop of δV_C across the cavity and δV across the terminals *A* and *B*. δV_C will be distributed among C_S and C_r in series. So,

$$\delta V = \text{Voltage across } C_r = \delta V_C \frac{C_S}{C_S + C_r} \qquad 4.6$$

This voltage δV does not give any information about the charge discharged which is δq_c =

$C_C \delta V_C$. Moreover, it is proportional to C_S which increases with the diameter of the void. However, δV is a quantity which can be measured.

Let us now consider a test circuit shown in Fig. 4.5 is set up as shown in IEC 60270 where the test specimen is denoted by C_C connected through a filter to the high voltage source V to prevent external noises.

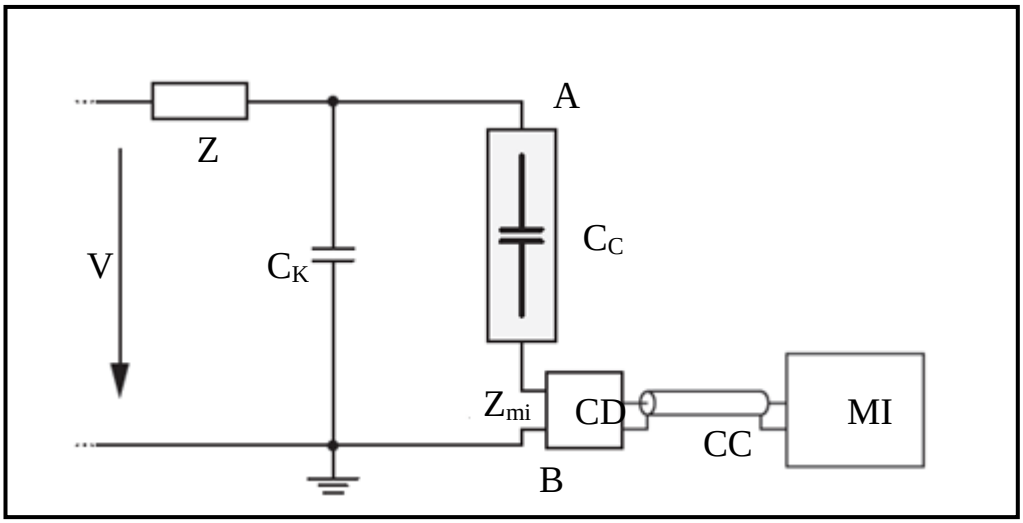

Fig. 4.5.The PD Measurement test circuit where coupling device is in series with the test object [7].

In Fig. 4.5, Z_{mi} is the input impedance of the measuring device, *CC* is the connecting cable, C_K is the coupling capacitor, the *CD* is the coupling device and *MI* is the measuring instrument [7].

During the short interval of cavity discharge, the capacitor C_K can only replenish the charge as the filter disconnects the test specimen from the source. So, it acts as a storage capacitor during the short period of the PD phenomenon. It releases a charge to the test specimen which tries to cancel the voltage drop δV across A and B.If $C_k >> (C_S + C_r)$, the voltage drop is completely compensated. The charge transferred by C_k is given by

$$q \approx (C_S + C_r)\, \delta V \qquad 4.7$$

Combing equations 4.6 and 4.7 ,

$$q = C_S\, \delta V_C \qquad 4.8$$

The charge q transferred by the capacitor C_k is called as the apparent charge which gives quantifies the discharge quantity of PD. This charge 'q' is measured in a PD measuring

device. Now, for the measuring of PD, a calibrator is used across the detector impedance Z_{mi} and the voltage pulse is calibrated in terms of the charge magnitude of the calibrator. This value is compared with the voltage pulse recorded to estimate the apparent charge.

4.5 PHASE RESOLVED PARTIAL DISCHARGE PATTERN (PRPD) [4]

The two most common types of PD data patterns used for the analysis and evaluation of PD are phase-resolved data and time-resolved data. The phase-resolved data analysis is employed for the electrical detection method.

The illustration of PD activity relative to the 360° degrees of an a.c. cycle is commonly known as phase-resolved partial discharge (PRPD) pattern which assists to find the prominent root cause of PD. In this detection method, the PD current waveforms are recorded and a 3-D '*q*-ϕ-*n*' pattern is obtained where 'ϕ' denotes the complete 360° degrees of an a.c. cycle, '*q*' gives the magnitude of the PD pulse and '*n*' being the repetition rate of PD pulses during one cycle of an a.c. waveform. The PD magnitude is related to the extent of damaging discharges occurring, therefore related to the amount of damage being inflicted into the insulation. The pulse repetition rate indicates the number of discharges occurring at the various maximum magnitude levels. Both play a role in determining the condition of the insulation under test. Fig. 4.6 shows a typical PRPD pattern of insulating material.

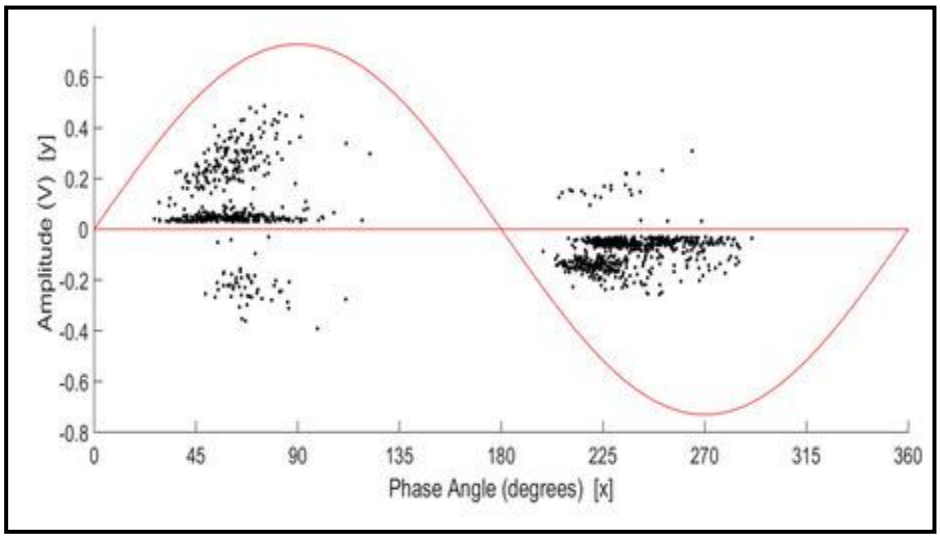

Fig. 4.6. A typical PRPD pattern of insulating material [19].

PD phase and charge magnitude can be obtained from PRPD data and statistical data can be obtained from the PRPD pattern, But the sequence of PD is lost in this pattern. In the

following chapters based on the PRPD pattern obtained for every sample, a comparative study is drawn [21].

CHAPTER - 5

Experimental Study

Chapter 5

5.1 INTRODUCTION

Life of a high voltage instrument is practically the life of its insulation. The requirement of the reliability of high voltage equipment has been emerging day by day, and thus condition monitoring of equipment has become imperative. The predictive maintenance done by condition monitoring has become one of the most sought after area at present which helps in preventing damages and increasing the life span of the equipment. Thus the revenues of the utilities have been benefited from that.

Condition monitoring of insulation involves both destructive and non-destructive methodologies. The non-destructive ways are always preferred as it does not involve shutting down and dismantling of electrical equipment. Detection and measurement of partial discharge (henceforth abbreviated as PD in this chapter) have been proved to be one of the most vital non-destructive diagnostic tools under condition monitoring. PD activity enhances the degradation of the insulation sample and hence the longevity of the electrical equipment get reduced. The sites where PD occur might deteriorate with time and eventually, the total failure of equipment may take place. The discharge occurs in an irregular pattern, which makes condition monitoring even more challenging.

This chapter describes the PD experiment that has been carried out in the High Tension Laboratory of Jadavpur University. The procedure of sample preparation, experimental setup, and the method adapted for the experiment are reported here [4,6,11].

5.2 SPECIFICATION OF THE SAMPLE

The samples used for the PD experiment are the most common, commercially available dry type insulation. They are listed in Table 5.1 with their specifications.

TABLE 5.1 LIST OF DRY TYPE INSULATION USED.

Sl.No	Insulation Type	Height (mm)	Diameter(mm)
1	Pressboard (Thin) single layer	0.89	10.5
2	Pressboard (Thin) double layer	1.81	10.5
3	Pressboard (Thin) triple layer	2.65	10.5
4	Pressboard (Thick) single layer	1.56	10.5
5	Pressboard (Thick) double layer	3.62	10.5

Sl.No	Insulation Type	Height (mm)	Diameter(mm)
6	Leatheroid Paper double layer	0.59	10.5
7	Leatheroid Paper triple layer	0.87	10.5
8	Nomex Film (Thick) double layer	0.38	10.5
9	Nomex Film (Thick) triple layer	0.57	10.5
10	Nomex Film(Thin) double layer	0.26	10.5
11	Nomex Film(Thin) triple layer	0.38	10.5
12	Nomex Paper double layer	0.11	10.5
13	Nomex Paper triple layer	0.16	10.5
14	8 fold Kraft paper	1.49	10.5

5.3 PREPARATION OF THE SAMPLE

The preparation of the sample prior to the experiment has been discussed here. The samples were prepared in two ways and data acquisition has been done on two sets of the sample. The samples were placed between two electrodes. There were impurities present in the sample, air gaps, micro-voids present between the layers and the electrode surface. With the application of high voltage on the sample, generation of PD the breakdown of voids under high electric field stress is a common phenomenon. To prevent any other discharges (e.g., surface and Corona discharges) to occur, the samples were cut in round shape having no sharp edges.

5.3.1 *SAMPLE PREPARATION FOR THE FIRST SET OF DATA*

The samples were arranged in both single as well as in multiple layers between the high voltage and low voltage electrodes. No artificial void had been created in the samples.

Fig. 5.1. Single layer thin Pressboard.

Fig.5.2. Double layer thin Pressboard.

Fig. 5.3. Triple layer thin Pressboard.

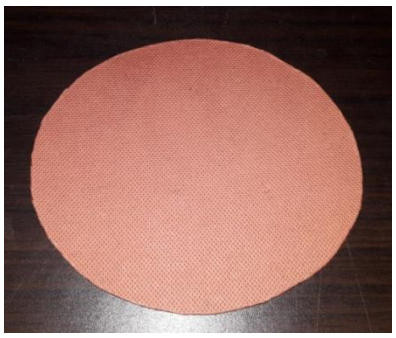

Fig. 5.4. Single layer thick Pressboard.

Fig. 5.5. Double layer thick Pressboard.

Fig. 5.6. Double layer Leatheroid paper.

Fig. 5.7.Single layer Nomex film(Thick).

Fig. 5.8.Single Layer Nomex film (Thin).

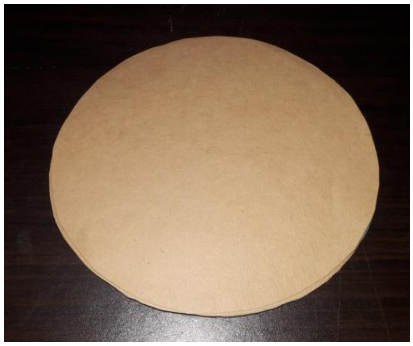

Fig. 5.9. Eightfold Kraft paper.

5.3.2 *SAMPLE PREPARATION FOR THE SECOND SET OF DATA*

The samples were stacked in a double layer between the high voltage and low voltage electrodes. The artificial void has been created in the sample such that a void is present in the center of the top layer of the sample. The area of the void was gradually increased in size and PD data were recorded. The list of the samples has been given in Table 5.2 [20].

TABLE 5.2 INSULATION SAMPLE WITH VOID DIMENSIONS.

Sl. No.	Sample Type	Void Area (sq.mm)	Width of the Void (mm)
1	Nomex Paper(Double Layer)	2×2 = 4	0.11
		3×3 =9	
		4×4=16	
		5×5=25	
2	Nomex Film Thin(Double Layer)	2×2 = 4	0.26
		3×3 =9	
		4×4=16	
		5×5=25	
3	Leatheroid Paper(Double Layer)	2×2 = 4	0.59
		3×3 =9	
		4×4=16	
		5×5=25	

The prepared samples with centrally placed void for Nomex film(thin), Leatheroid paper and Nomex paper are shown in Fig. 5.10, Fig. 5.11, and Fig. 5.12 respectively.

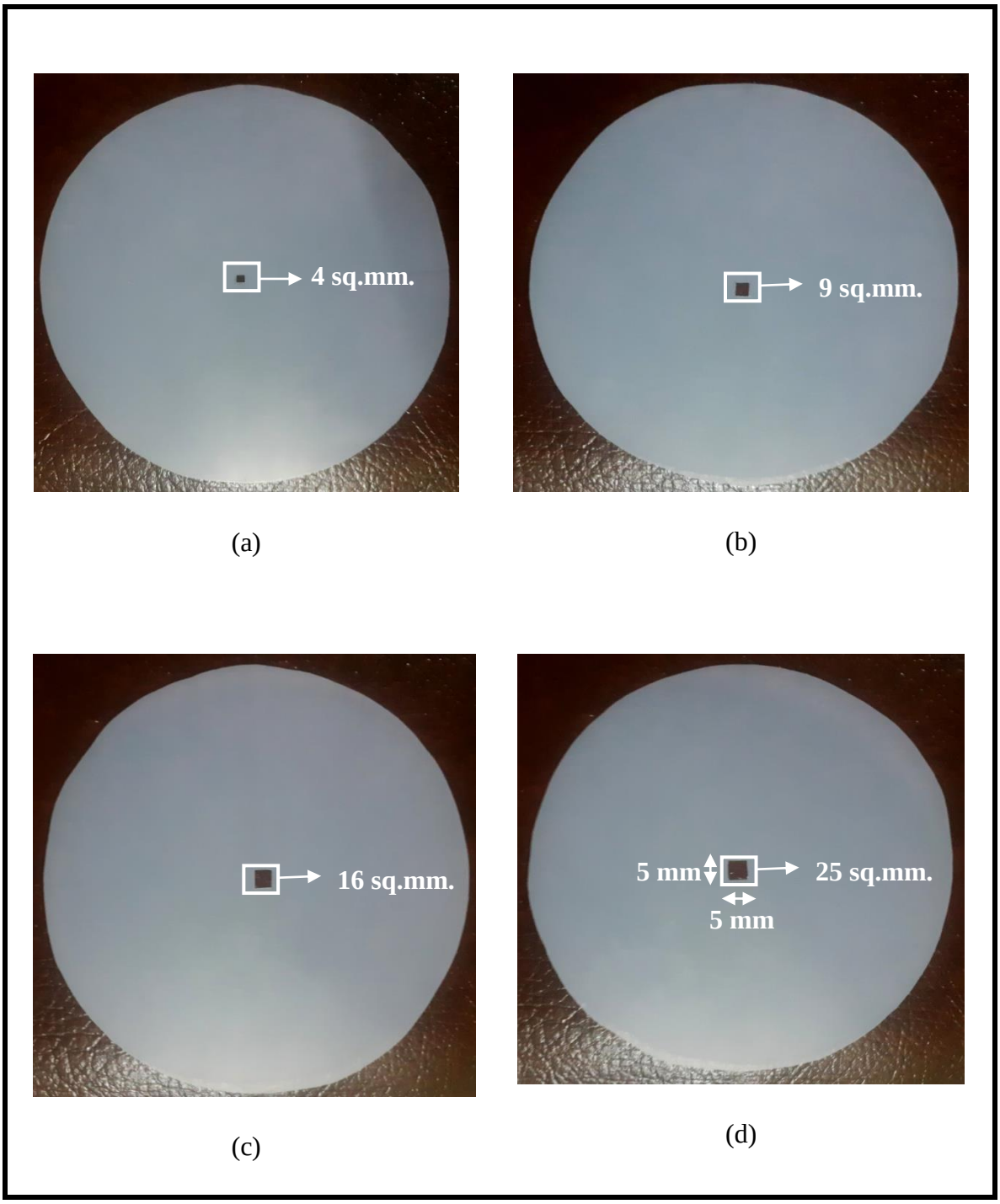

Fig. 5.10. Nomex film(thin) samples having voids of area (a) 4sq.mm , (b) 9sq.mm.,(c) 16sq.mm (d) and 25sq.mm.

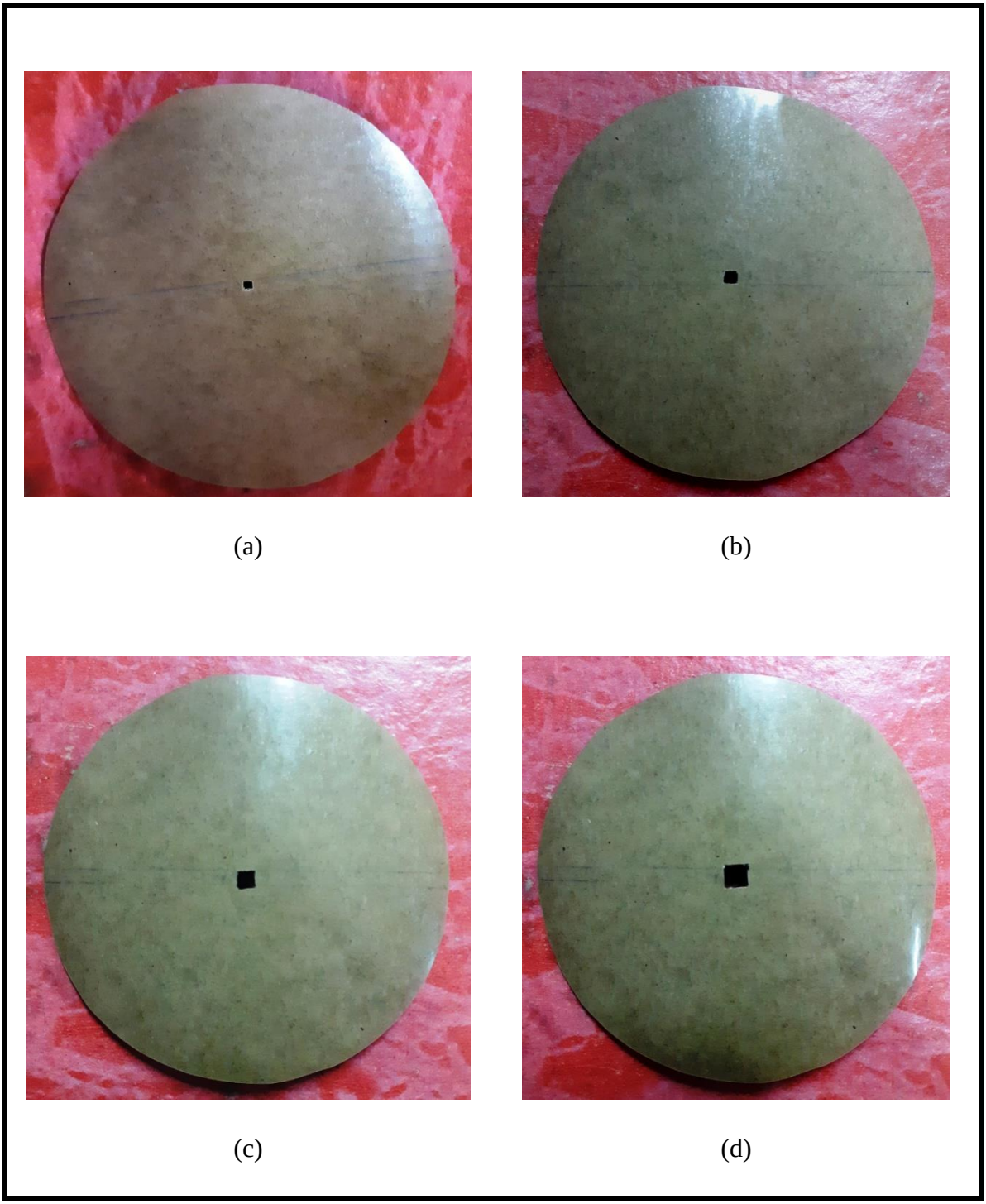

Fig. 5.11. Leatheroid paper samples having voids of area (a) 4sq.mm ,(b) 9sq.mm.,(c) 16sq.mm (d) and 25sq.mm.

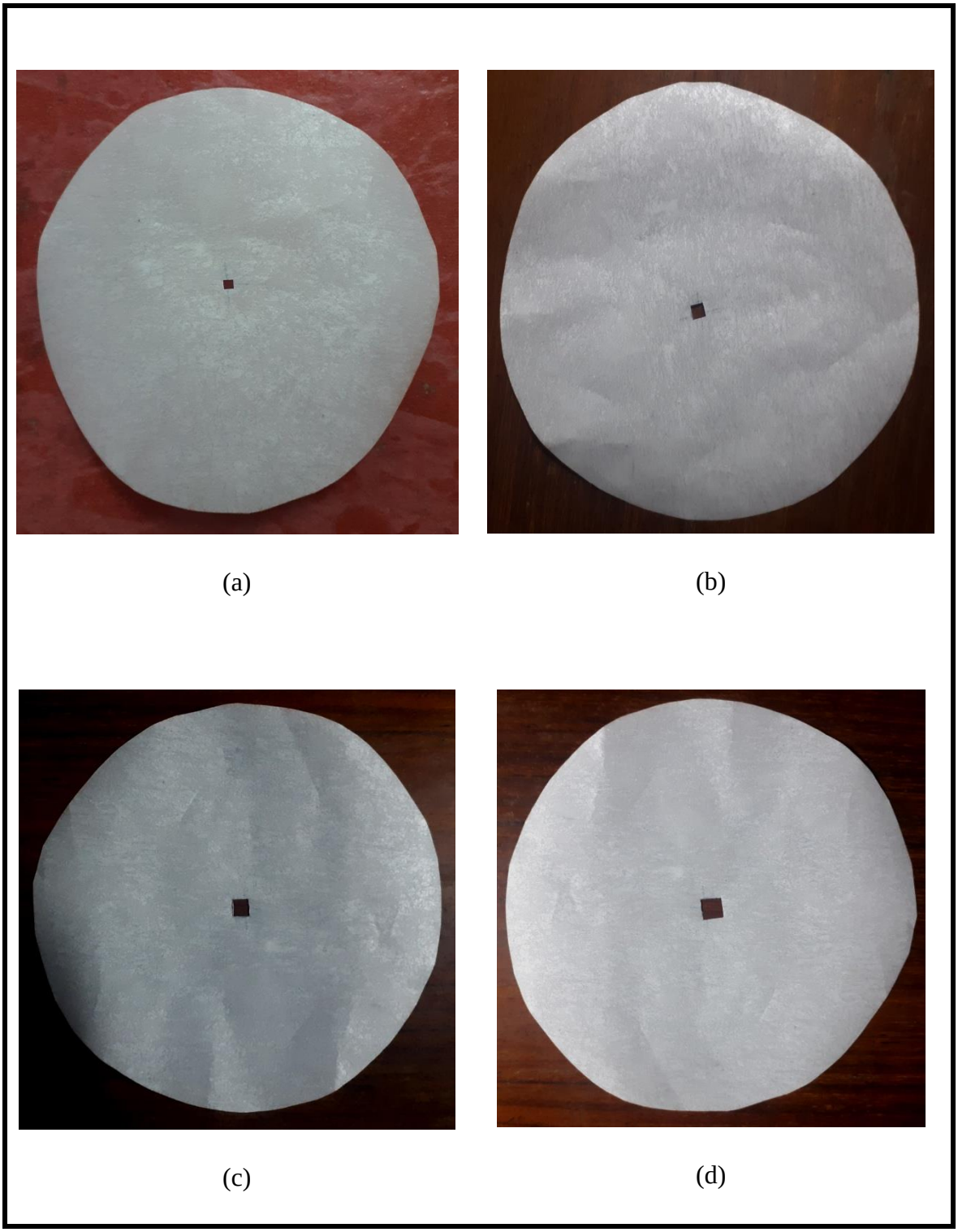

Fig. 5.12. Nomex paper samples having voids of area (a) 4sq.mm ,(b) 9sq.mm.,(c)16 sq.mm and (d) 25sq.mm.

5.4 EQUIPMENT AND COMPONENTS REQUIRED

Several types of equipment and components were used to perform the experiment in the laboratory. The High Tension Laboratory of Jadavpur University has provided a wide and diverse range of equipment to perform the PD measurement on the insulation samples. Detailed information about the equipment used has been discussed here.

Following are the equipment used are discussed in the subsequent sub-sections.

5.4.1 HIGH VOLTAGE A.C. POWER SOURCE

The high voltage a.c. power source, shown in Fig. 5.13, was used for supplying alternating voltage ranging up to 10kV. The device has a variable autotransformer that regulated and controlled the applied voltage. The insulation sample was kept between the two electrodes and high electric field stress was applied to the insulation sample with the help of this high voltage a.c. power supply.

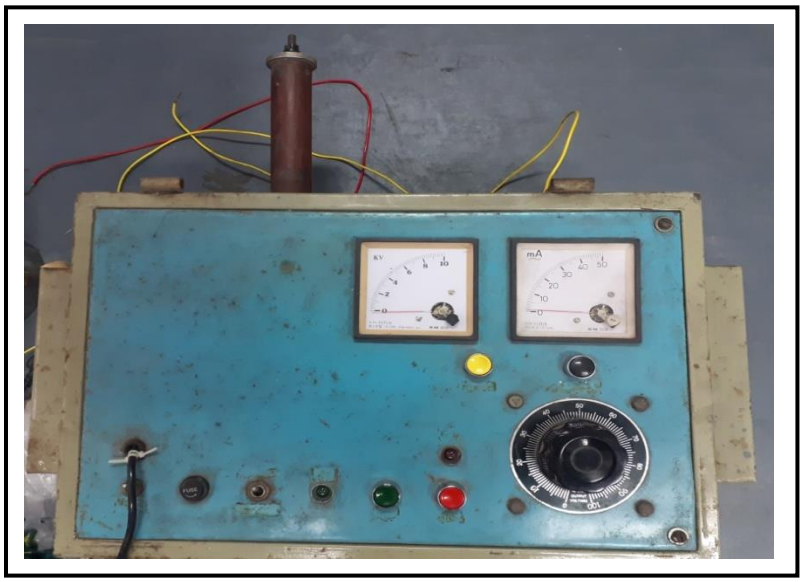

Fig. 5.13. High voltage alternating power supply.

5.4.2 CYLINDRICAL ELECTRODES

Two stainless steel electrodes, as shown in Fig. 5.14 were placed on each of the upper and bottom surfaces of the insulation test sample. The upper electrode was connected to the high voltage source and the lower electrode was grounded via a high-frequency current transformer. Application of high voltage electric stress on the insulation sample was exerted through the electrodes. The cylindrical shaped electrodes used here have a smooth

flat surface and round edges. The height and diameter of each electrode are 2.5cm and 7.5cm respectively.

Fig. 5.14. Stainless steel cylindrical electrodes.

5.4.3 PARTIAL DISCHARGE CALIBRATOR

The PD calibrator, as shown in Fig. 5.15 was a compact, battery operated discharge calibrator. It could inject a signal of known charge magnitude into the test circuit to verify the calibration of the instrument according to the standards of IEC 60270. In the High Tension laboratory of Jadavpur University, the Haefely make PD calibrator type 450, has been used.

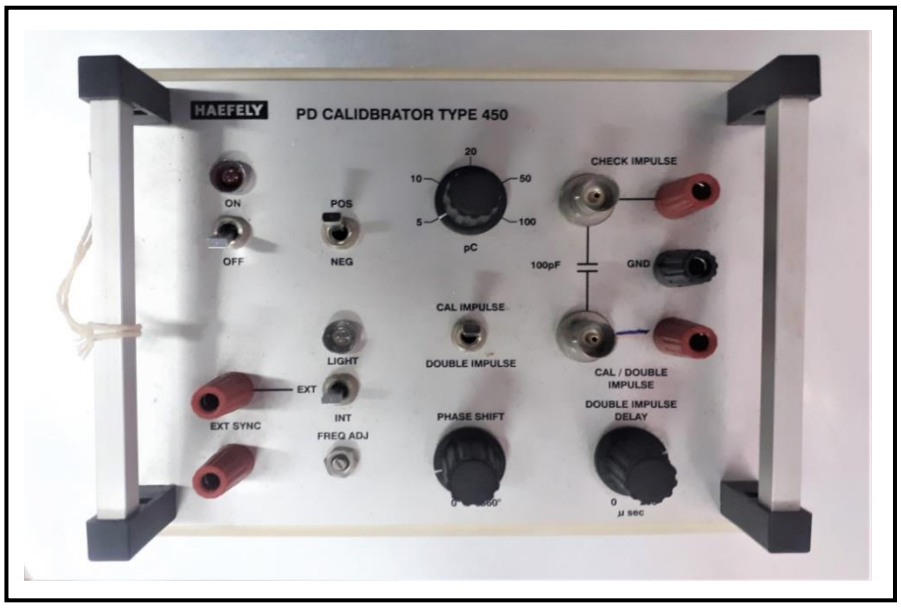

Fig. 5.15 Haefely PD calibrator type 450.

5.4.4 HIGH-FREQUENCY CURRENT TRANSFORMER (HFCT)

Conventional PD pulses have higher rise time and relatively slow decay time. HFCT was designed in such a way to measure current pulse with high bandwidth. For PD purpose, HFCT was used to measure fast current discharges with the rise time in the order of nanoseconds and pulse duration up to 10 nanoseconds quintessentially. The HFCT, as shown in Fig. 5.16 was a two winding current transformer such that both the primary and secondary windings have 35 turns each having turns ratio as 1:1. The ring core used here was of ferrite material having a mean diameter of 12mm, core thickness of 4mm and core height of 10mm. The inductance of both the winding was 11.07mH [34].

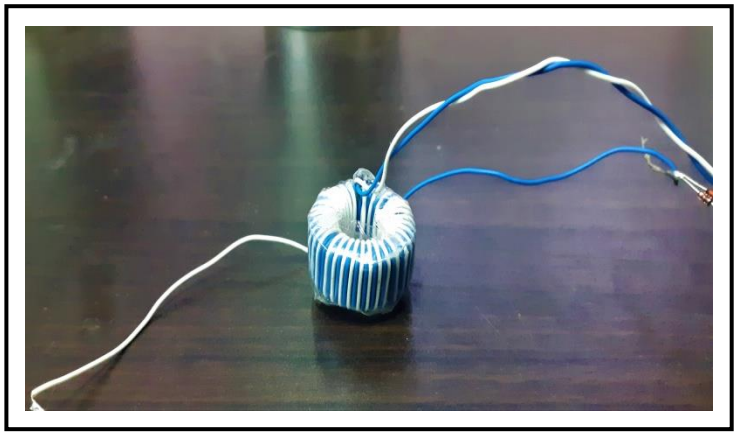

Fig.5.16 High-frequency current transformer (HFCT).

5.4.5 LCR METER

An Lcr meter is a type of electronic device used to measure the Inductance (L), Capacitance (C), And Resistance (R) of a test object. In Fig.5.17 an Lcr meter of model number Lcr-4070 of Make, Htc Instruments has been used. In the present work, Lcr Meter has been used to measure the Inductance of the high-frequency current transformer Windings.

Fig.5.17 LCR meter.

5.4.6 ANALOG-TO-DIGITAL CONVERTER (ADC)

Analog-to-Digital Converter utilizes a binary algorithm to convert continuous analog waveforms into much smaller discrete outputs. The ADC, model USB –S133, manufactured by National Instruments as shown in Fig.5.18 was used in data acquisition of PD. This ADC can be directly connected to a computer to be controlled via software.

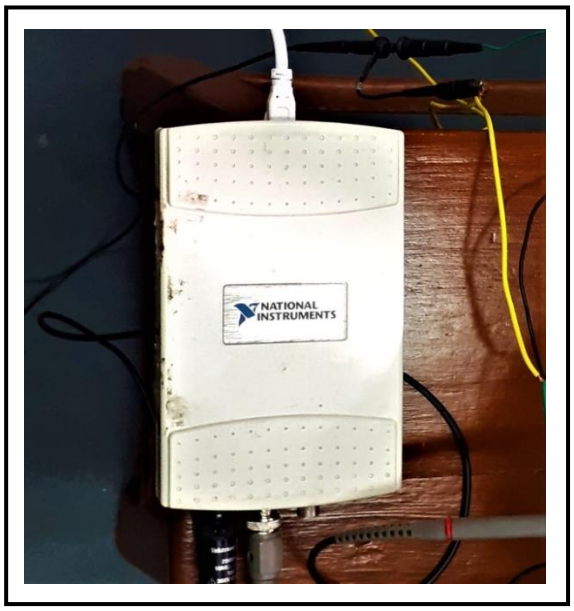

Fig.5.18. Analog-to-Digital converter.

5.4.7 TEST SET TO MEASURE TAN DELTA

The portable, reliable and highly accurate test sets STS 3000 light and TD 5000 of ISA, Altanova Group has been shown in the Fig.5.19, is a tanδ and capacitance diagnostic system which allowed performing of all tests foreseen by International Standards on electrical equipment and to measure the tanδ, dissipation factor and capacitance of any device and insulation. In the present work, this device was used to measure tanδ of all the insulation test samples at a constant voltage and frequency.

Fig.5.19. STS 3000, Tan delta measurement test set [35].

5.4.8 MEGGER

Megger is a measuring instrument used for the measurement of insulation resistance of an electrical system. The quality of insulation resistance of any electrical system deteriorates with time and other various environmental conditions including temperature, moisture, dust particles, and humidity. The device used here was Megger MIT520/2, insulation tester as shown in the Fig.5.20 which comes in a compact case and can measure Insulation Resistance upto 10MΩ.

Fig.5.20. Megger MIT520/2 [36].

5.4.9 INPUT NOISE FILTER AND VOLTAGE DIVIDER

A low pass 'T' filter was connected between the high voltage source and the pair of electrodes. The source voltage got affected by internal noises, disrupting the original sinusoid waveshape and producing a waveform erratic in nature. To eradicate the external noises,higher-order harmonics from the source voltage a filter was used. This 'T' filter consists of two 100kΩ resistors in two arms of T and one 15kV, 1000pF, high voltage disc ceramic capacitors were placed in the middle section of 'T'.The value of the capacitor was chosen such that it can protect the circuit from high voltage surges up to 15kV rms.

A voltage divider was built assembling two 1MΩ resistors and one 10kΩ resistor has been shown in Fig.5.21, such that the applied voltage could be measured easily with an oscilloscope.

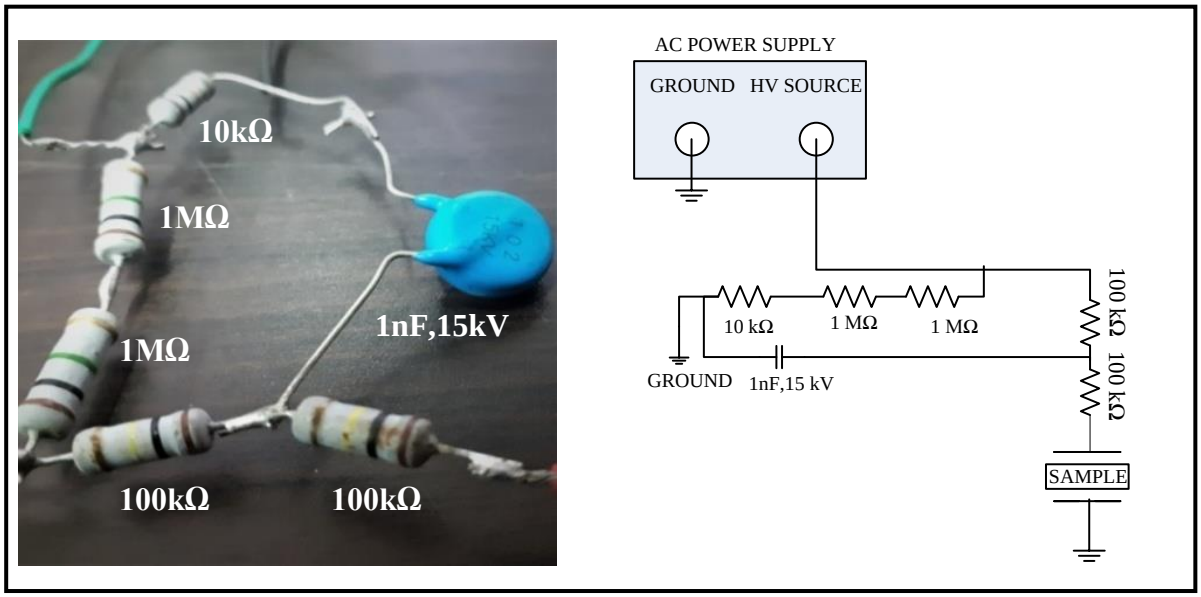

Fig.5.21. Capacitor and resistors.

5.5 EXPERIMENTAL SETUP

The experiment on PD activity on the insulation sample was carried out in the High Tension Laboratory of Jadavpur Univerisity. The set up was built assembling all the required equipment and components listed in section 5.4. The experiment setup was arranged twice, once with the PD calibrator and the other, excluding it. Here, the phase-resolved partial discharge (PRPD) pattern was implemented for evaluation and to study PD in the insulation samples. In this PRPD pattern, the PD activity was illustrated with respect to the 360° of a cycle of an a.c.waveform [4].

In the laboratory set up of PD, at first, the high voltage a.c. source was needed, which was connected to the insulation sample via the high voltage electrodes.

Since the usage of electrical products and electronic devices has increased, it has raised the problem of electromagnetic interference (EMI) also known as the electromagnetic environment pollutionSmall low-level sensitive signals such as PD signals are greatly affected by the EMI and thus show an inconsistent and unpredictable nature. To prevent that, shielding has been applied to the enclosures to isolate electrical devices from the surroundings. To set up a PD laboratory, electromagnetic shielding is indispensable [4].

Here, an aluminum cylindrical enclosure having dimensions 7.5inches of diameter and 8inches of height was used to serve the purpose of electromagnetic shielding. For the easy accessibility of the equipment inside, the shielded enclosure, aluminum cylinders were used here, such that the lid can be opened to easily change the sample inside.

The sample specimens after being prepared were placed between the two electrodes. This entire sample and electrode assembly are placed carefully inside the Aluminium shield enclosure on top of an insulator, which has been already placed in the enclosure beforehand. None of the leads of the electrodes should touch the shielded enclosure. Now, the high-frequency current transformer (HFCT) was also placed in the shielded lab. Precautions are taken such that none of the leads of the electrodes touch the HFCT. The HFCT has been employed to capture the PD pulses. The connection has been made between the current transformer primary and the low voltage electrode.

Fig. 5.22 shows the placement of the electrodes, sample and current transformer inside the cylindrical shielded enclosure.

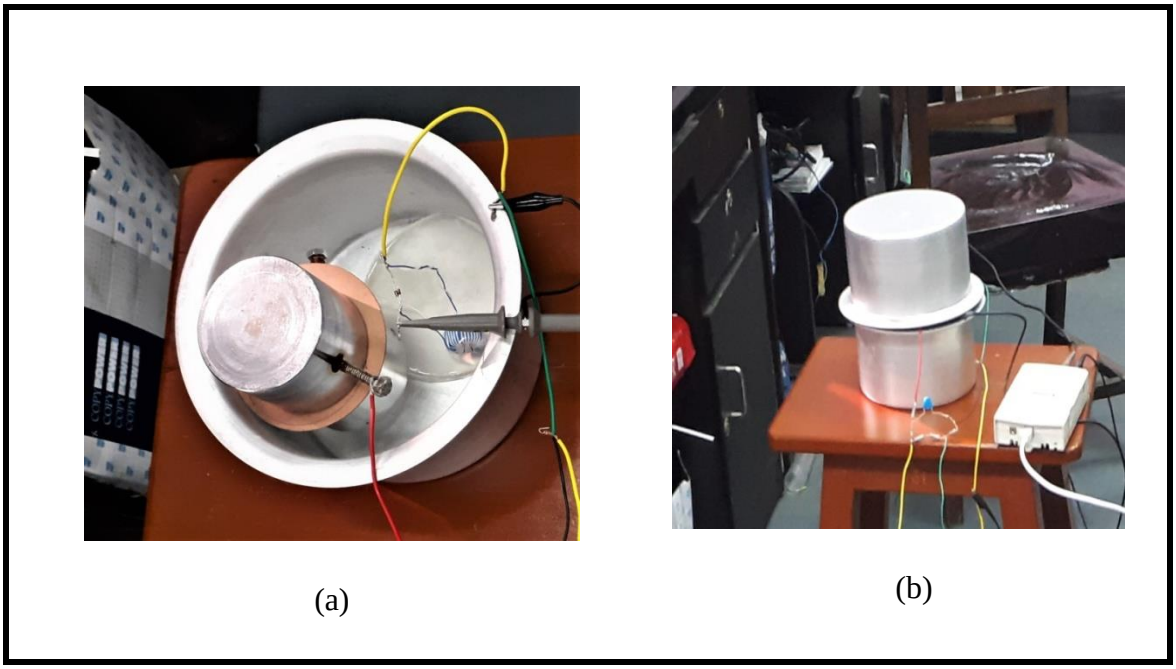

Fig.5.22. (a) A Shielded enclosure with HFCT, samples, and electrodes placed inside and (b) shielded enclosure with the lid on, while in service.

The ADC was used here to acquire data from the high-frequency current transformer (HFCT). The ADC was connected in series with the HFCT. Here, since HFCT aids in procuring the PD signals, thus ADC helped in converting the PD analog signals into PD digital signals and with the help of the LabVIEW Software, the digital PD signals were graphically displayed on the screen.

Now, in this experiment PD signals were obtained using phase resolved technique. The PD signals, those acquired experimentally and plotted on the graphs were calibrated against a

known signal whose charge magnitude was previously known. So a few modifications were done in terms of assembling the setup to take two sets of readings. The setups are mentioned in the following sub-sections.

5.5.1 The first setup was to graphically plot the signal of known charge magnitude

The Haefely make PD calibrator type 450 has been used as referred to section 5.4.3. The PD calibrator was connected to the high voltage electrode such that when a signal of known charge magnitude was applied, it was made to pass through the insulation sample and the current signal obtained by the ADC was plotted graphically. Here, the high voltage a.c. source remains connected to the electrode, but no supply was provided thus remains non-functioning. In Fig.5.23 the experimental setup for the measurement of the signal of known charge magnitude using PD calibrator is shown.

Fig. 5.23. Experimental setup for the measurement of the signal of known charge magnitude using PD calibrator.

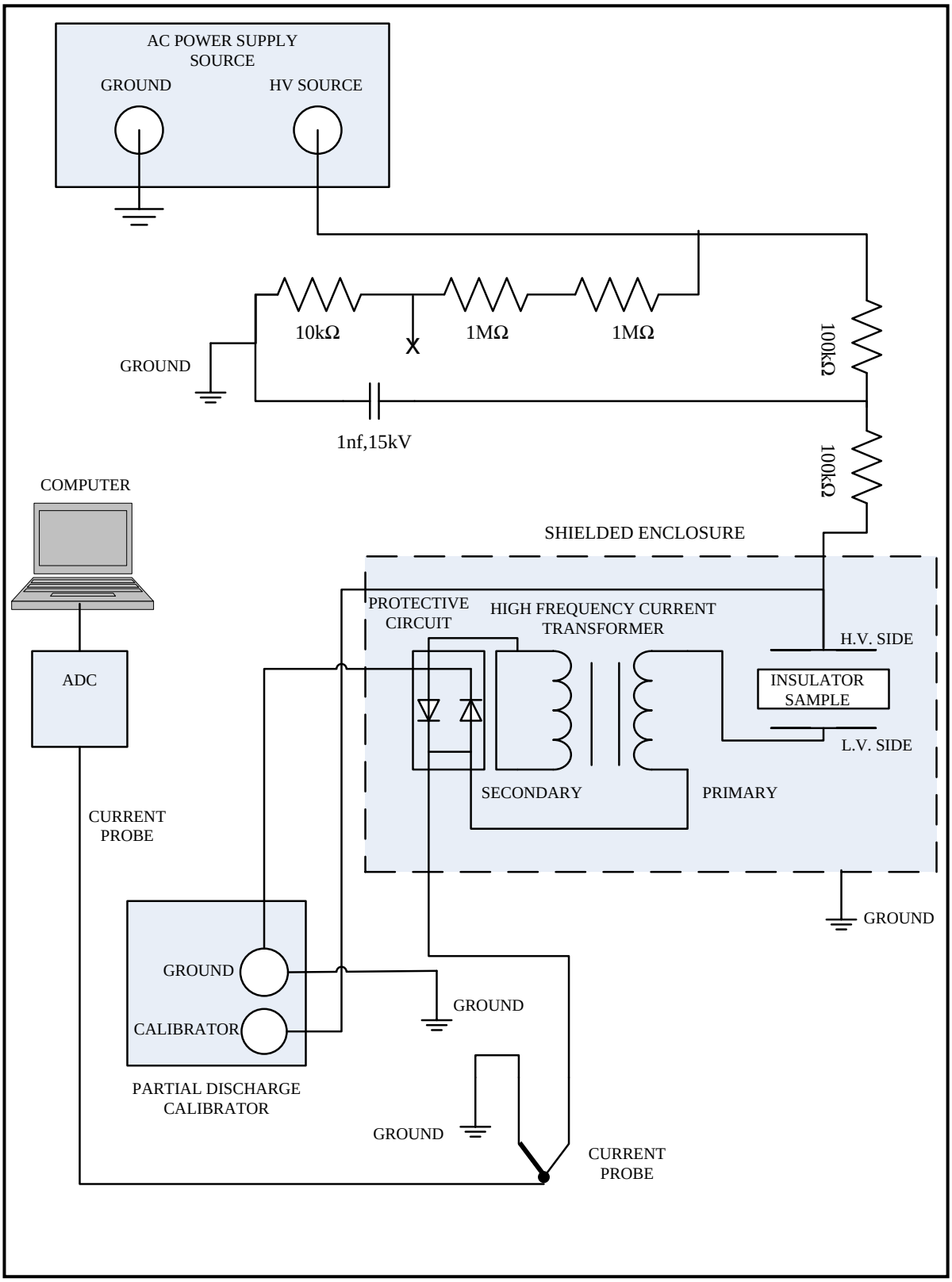

Fig. 5.24 Schematic representation for the measurement of the signal of known charge magnitude using PD calibrator.

5.5.2 The second setup assembled to record the Phase-Resolved pattern of Partial Discharges

In this case PD calibrator was not used for obtaining PRPD signals. To measure the high voltage applied across the insulation sample a potential divider was prepared using two 1MΩ and one 10kΩ resistor respectively. The voltage signal thus obtained was also represented graphically on LabVIEW with the help of ADC which converted the analog voltage signal to digital voltage signal. The applied source voltage signal and the current signal obtained from the HFCT were superimposed and displayed together graphically. In Fig.5.25 the experimental setup for the measurement of the PRPD pattern of different samples is shown.

Fig. 5.25. Experimental setup for obtaining the PRPD pattern.

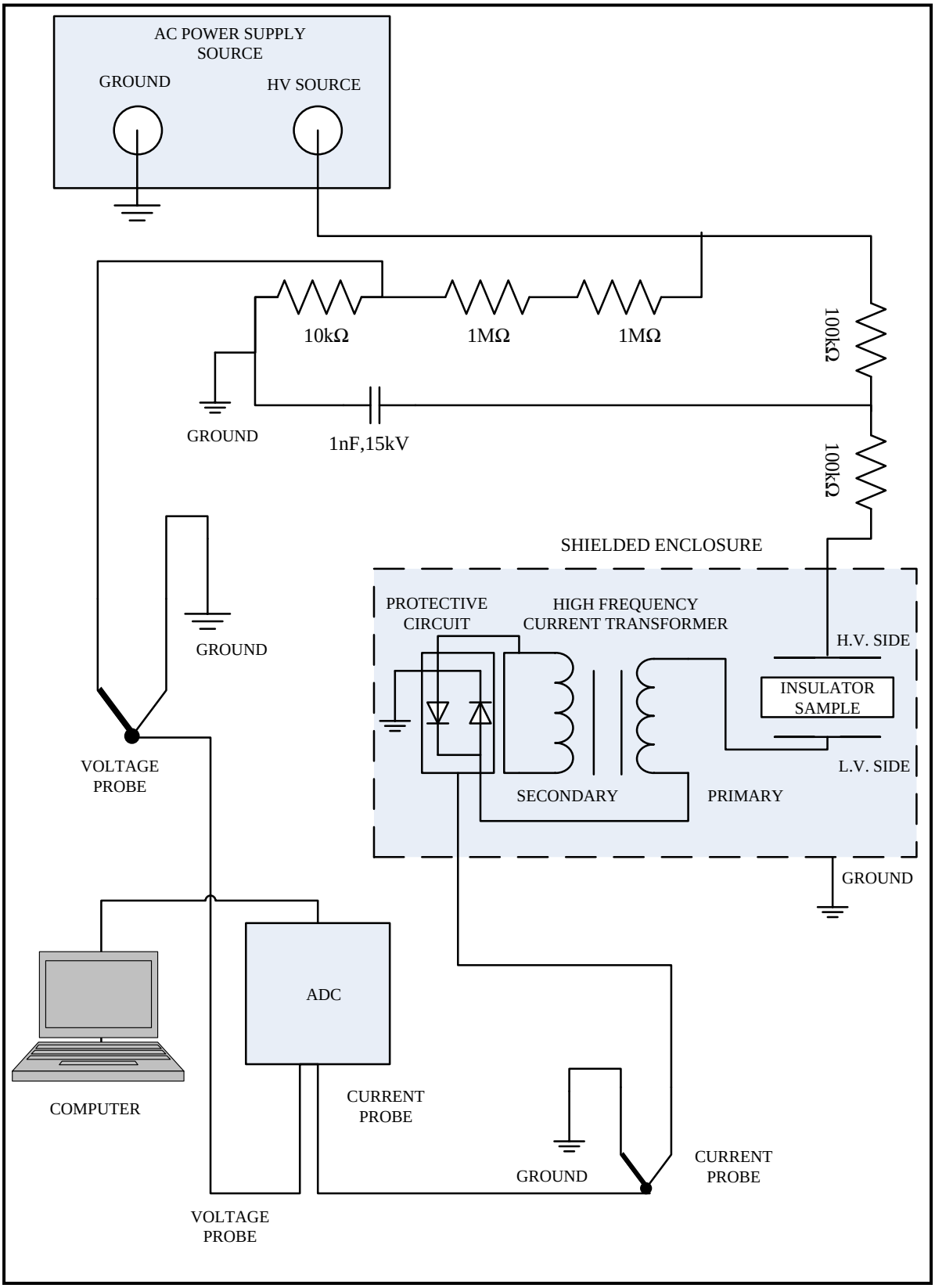

Fig. 5.26. Schematic representation of the circuit arrangement for obtaining the PRPD pattern.

5.6. EXPERIMENTAL PROCEDURE AND DATA ACQUISITION

After Assembling and setting up the equipment, the PD experiment was performed inside the laboratory. As previously mentioned in section 5.5, the data were acquired in two sets.

5.5.1 The first setup was to detect the magnitude of the graphically plotted signal of known charge magnitude.

5.5.2 The second setup was assembled to record the phase-resolved pattern of partial discharges taking place in the sample.

Now the procedure of performing the experiments in the laboratory would be explained in details.

5.6.1 PHASE RESOLVED PARTIAL DISCHARGE EXPERIMENT

It can be seen in the schematic representation in Fig.5.26, than an a.c. voltage was applied to the specimen insulation by varying the voltage with the help of autotransformer. Now, as previously mentioned, the applied voltage can be graphically displayed with the help of ADC and the LabVIEW software on the computer screen. With the application of the high voltage on the sample insulation via the electrode, PD develops in the sample due to the presence of void, impurities and air gap. These PD signals are acquired by the HFCT and were displayed on the screen with the help of LabVIEW software. This becomes easy to track the occurrence of PD in the current signal with respect to the variation of applied voltage, as both the current and voltage waveforms were displayed on the same screen [4,19].

5.6.1.1 Detection of Partial Discharge Inception Voltage

Gradually the applied a.c. voltage was increased and due to this the electric stress on the insulation sample also increased which leads to the occurrence of discharges. These discharges were projected as the spikes in the current signal which were the PD pulses. These PD pulses increased with the gradual increment of the applied voltage.

The minimum applied voltage at which the PD occurs is known as partial discharge inception voltage (PDIV). For a given sample, the applied voltage should exceed PDIV for PD to occur in the sample.

Now, PDIV value has been recorded for all the samples as mentioned in section 5.3.

The chronological sequence to find out the PDIV has been framed here in the skeleton of a Flowchart as shown in Fig. 5.27.

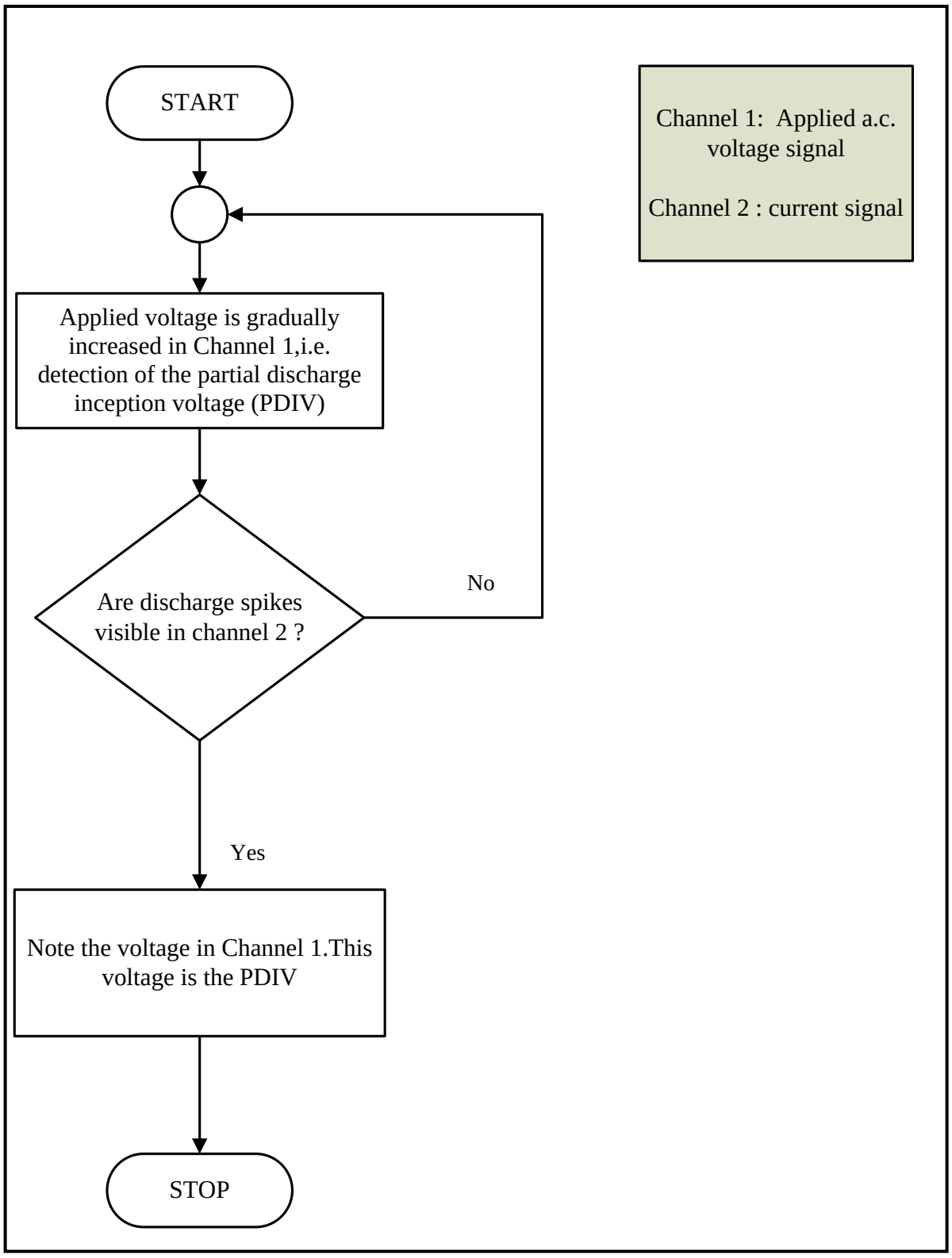

Fig. 5.27. Flowchart to detect the PDIV for a given insulation sample.

The PDIV distributions were displayed graphically with the help of LabVIEW software program. The few specifications used in the program to view the PDIV are given here :

Channel 1 and Channel 2 were the two ports in the ADC in which the applied voltage signal and the current signal of HFCT were fed respectively. The corresponding signals were graphically plotted on the LabVIEW as fed in Channel 1 and Channel 2 of the software. Triggering was done from Channel 1 having a positive slope and threshold value being 0.01V. Channel 1 ranges from ±1V to ±2V, whereas the range of channel 2 was ± 50mV. The sampling rate of the data here was 540,000 samples per second. There are 10,800 data points that represent a complete a.c. cycle of 360° and the time-gap between two adjacent data was 1.85μs.

5.6.1.2 Detection of Phase Resolved Partial Discharge pattern

PD pattern was recorded in a phase-resolved graph where each of these PD pulses was quantified by their discharge magnitude (q), the corresponding phase angle (ϕ) (at which they have occurred) and the discharge rate or pulse count (n).
The most standard univariate distributions are (a) q– ϕ, (b) n– ϕ were plotted.

The most standard bivariate distribution was ϕ - q - n plot.

In this experiment to detect the PRPD pattern, the a.c. high voltage was applied and the partial discharge inception voltage (PDIV) for each of the insulation sample was recorded as mentioned in the section 5.6.1.1 For each sample insulation, the applied voltage was kept constant at their respective PDIV value. The charge magnitude (q) has been plotted against the corresponding phase angle (ϕ) and the data was collected. Now to find out the pulse count (n), the entire process of application of high voltage on the insulation sample and the occurrence of partial discharges were repeated thousand times. The distribution plot showing pulse count(n) against the corresponding phase angle (ϕ) was also collected. Since the pulse count (n) indicates, the number of times, PD pulse of a certain charge magnitude (q) occurred at a certain phase angle (ϕ) when the process of application of high voltage on the sample was repeated a number of times.

The pulse count (n) was plotted against the corresponding phase angle (ϕ) for all the samples mentioned in section 5.3 The chronological sequence to find out the PRPD pattern has been framed here in the skeleton of a flowchart as shown in Fig.5.28.

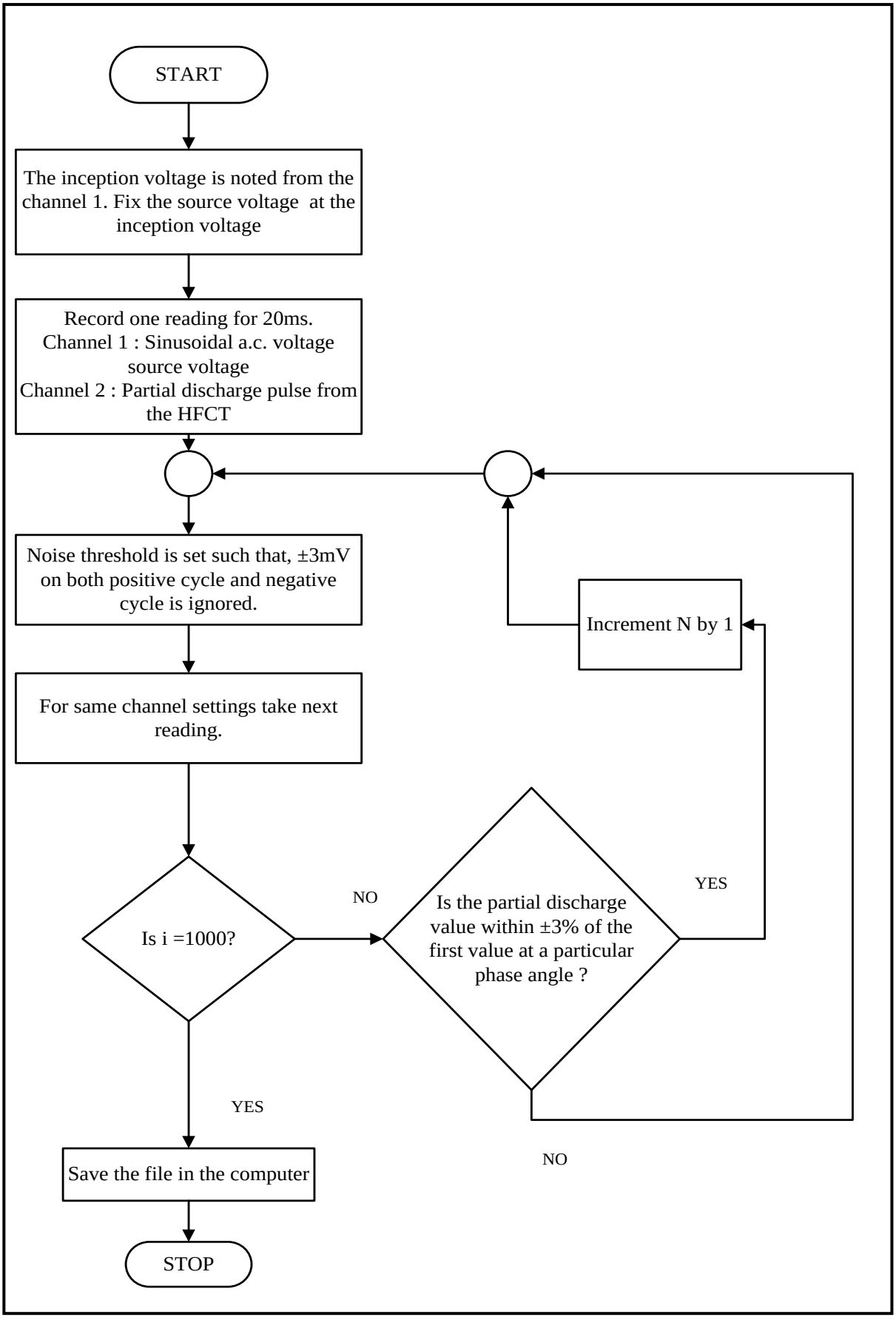

Fig. 5.28. Flowchart to detect the PRPD pattern for a given insulation sample.

The PRPD distributions were displayed graphically with the help of LabVIEW software program. The few specifications used in the program to view the PRPD patterns are given here :

Channel 1 and Channel 2 were the two ports in the ADC in which the applied voltage signal and the current signal of HFCT were fed respectively. The corresponding signals were graphically plotted on the LabVIEW as fed in Channel 1 and Channel 2 of the software. Triggering was done from Channel 1 having a positive slope and threshold value being 0.01V. Channel 1 ranges from ±1V to ±2V, whereas the range of channel 2 was ± 50mV. The sampling rate of the data here was 540,000 samples per second. There were 10,800 data points that represent a complete a.c. cycle of 360° and the time-gap between two adjacent data was 1.85μs.

5.6.1.3 Calculation of the Current Magnitude of the Known Signal

The Haefely make PD calibrator, as mentioned in section 5.4.3 provided multiple ranges of charge in pico-coulomb. After any particular charge range was selected, that charge was injected and made to flow through insulation sample via the electrodes. The waveshape of this known charge was a damped oscillating wave. Now, this waveshape was projected graphically on screen using the LabVIEW software. The highest magnitude of this current wave was calculated from the graph which was later used for the calibration purpose of the PRPD data. If the magnitude of the current signal of a known charge was found, then the quantity of charge in PD pulses whose current magnitude was already calculated from the graph. Thus, using the current magnitude of the known charge a multiplication factor has been deduced, with the help of which the charge magnitude of the PRPD data could have been calculated for all the samples using the mathematical formula of the unitary method.

The chronological sequence to calculate the current magnitude of a known charge and how that data was utilized to calibrate PRPD plots has been illustrated in a flowchart in Fig. 5.29.

The signal of a known charge applied from the PD calibrator was displayed graphically with the help of LabVIEW software program. The few specifications used in the program to view the PRPD patterns were given here :

Channel 1 was fed by the signal from the ADC. Channel 1 ranges up to ± 50mV. The sampling rate of the data was 50Msamples per second, having 4000 data points to represent the plot. Time difference between two adjacent data points being 0.02μs.

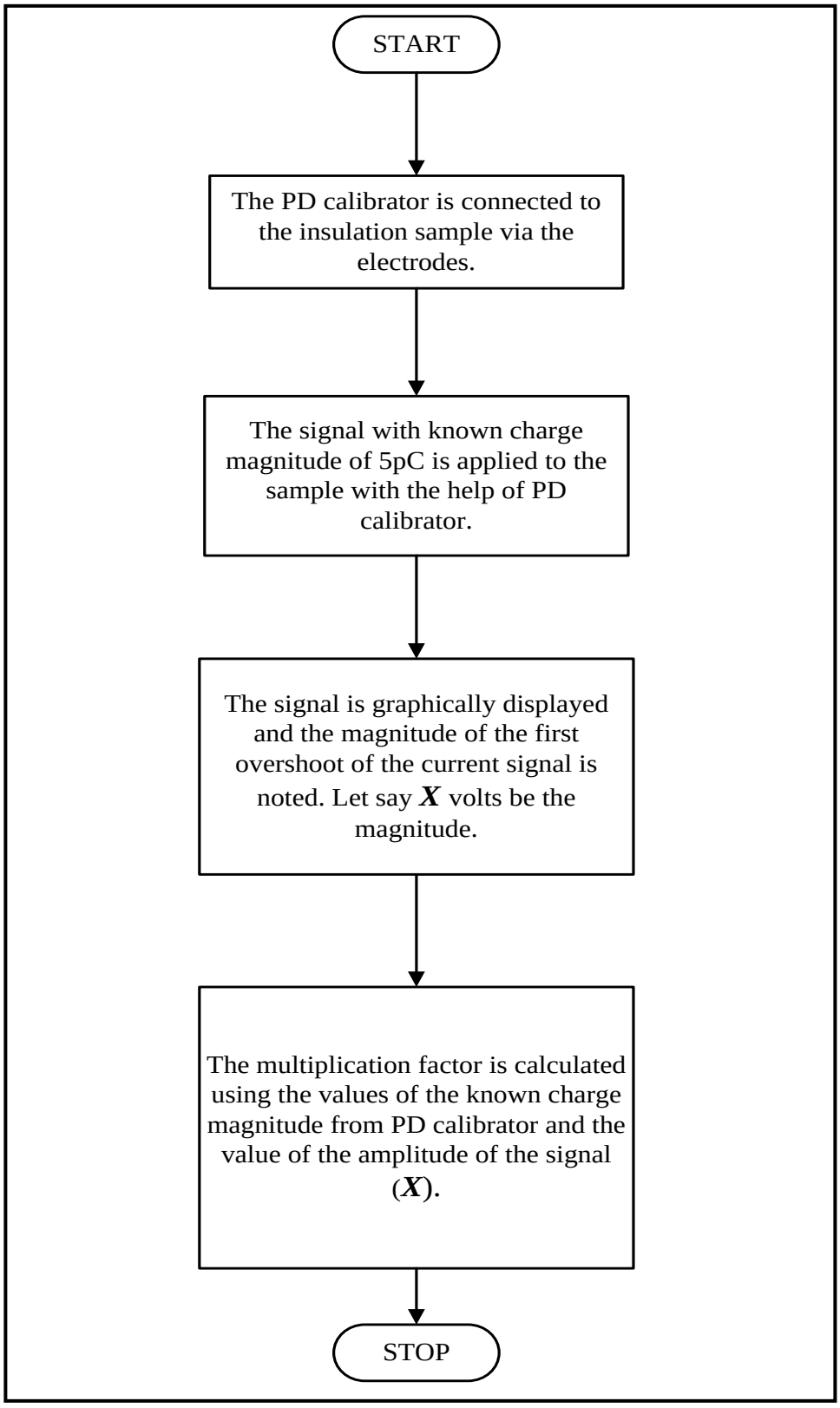

Fig. 5.29. Flowchart to plot the wave of a known charge magnitude.

5.7 Measurement Of Tan Delta and Insulation Resistance

5.7.1 Experimental Set-up for the Calculation of the Dissipation Factor

For this experiment, the test sets of STS 3000 light and TD 5000 of ISA [35] as mentioned in section 5.4.7. was used. This experiment was performed at a constant voltage of 500V and at 50 Hz. Each insulation sample was placed between the electrodes and the required voltage was applied, and the tanδ set recorded the dissipation factor which accounts for the heat loss in the sample. The arrangement for the tanδ experiment in the High Tension Laboratory of Jadavpur University is shown in Fig. 5.30.

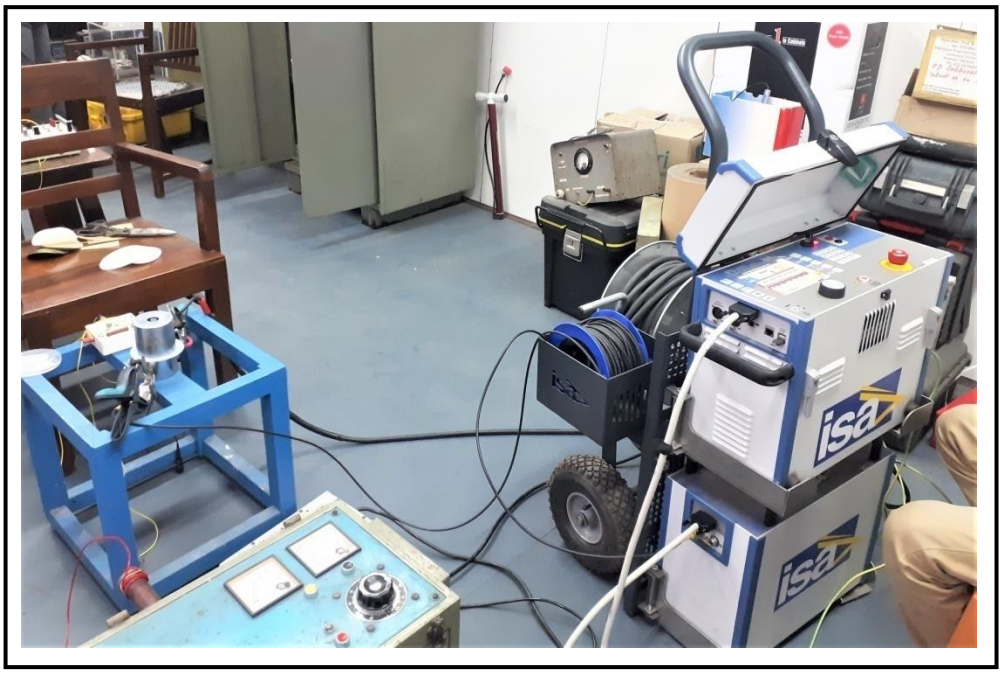

Fig. 5.30. Experimental setup for tan-delta measurement.

5.7.2 Experimental Set-up for Measuring the Insulation Resistance of the Sample

For the quality control and to understand the integrity of the insulation sample, insulation resistance test was performed on the sample. The samples were placed between two electrodes (positive and negative electrodes) and after the connections were made, a constant d.c. test voltage of 1kV was applied for 60 seconds on the samples. The experiment was performed at a room temperature of 27°C. This process was repeated after some time with d.c. test voltage of 1.5kV for 60 seconds and the data were recorded. The *Megohmmeter* or Megger MIT520/2 as mentioned in the section 5.4.8 was used to

calculate and display the value of Insulation Resistance. Fig. 5.31 shows the arrangement for the IR test [36].

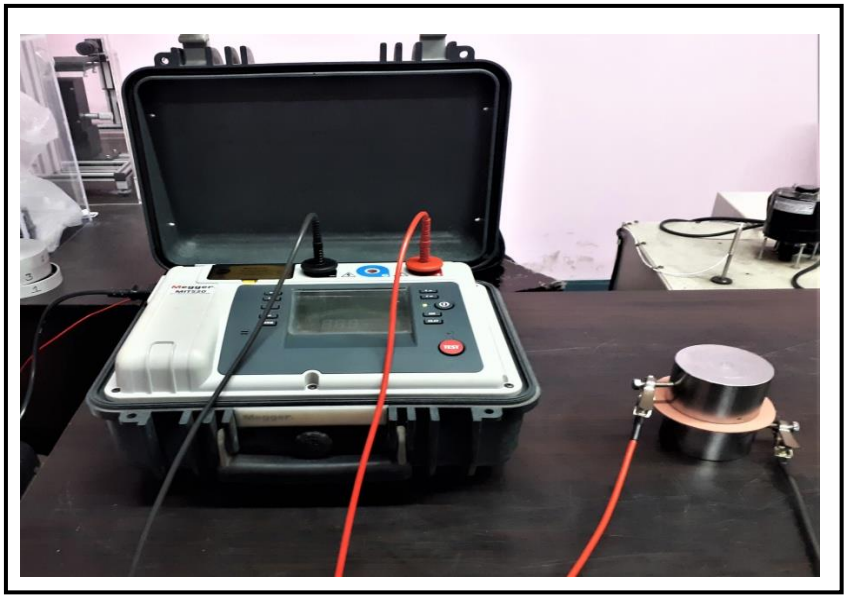

Fig. 5.31. Experimental set-up for the measurement of Insulation Resistance.

5.8 SUMMARY

In this Chapter, the procedures of sample preparation, experimental setup, and the method adapted for the partial discharge experiment have been documented. The main objective of this experiment was to capture PD occurring in different insulation samples when working under an a.c. high voltage. The quantification of PD has been the principal task here. The PRPD pattern obtained here had provided information about PD in varied samples. A database has been created in the next chapter based on the PRPD patterns obtained by performing the procedures. To learn about a few characteristics of the insulation samples, tanδ and IR tests were also performed. The complete database is represented in the next chapter.

CHAPTER - 6

Results And Discussions

Chapter 6

6.1 INTRODUCTION

The previous chapter describes the different types of insulation samples collected and preparation of these samples. It documents the assembling of the experimental set up for the detection of the PRPD pattern and the procedure for calibration of the PRPD data with the help of a PD calibrator. A small approach is also made to assess the insulation condition of the sample via the measurement of tanδ and insulation resistance [4,40].

Diverse insulation samples are used and when the experiment of partial discharge detection is carried out on these samples, different sets of data are recorded. With these data, different uni-variate and bi-variate PRPD distributions can be graphically plotted.

Now, the results obtained are explored and analyzed in this chapter and a comparative study of different types of samples is drawn on the basis of the data acquired. A database of different insulation samples is created based on the characteristics of the partial discharge pattern. A comparative study has also been done based on the dissipation factor and insulation resistance result of each sample.

6.2 QUANTIFICATION OF THE PARTIAL DISCHARGE BASED ON THE MEASURED CALIBRATOR READING

As previously stated, PD calibrator is employed to calibrate and quantify the amount of discharge in a PD current waveform. The procedure by which the unknown PD current is calibrated and converted into charge is explained in details in section 5.6.1.3 of the previous chapter.

With the help of an example, this method of conversion is demonstrated.

The insulation sample used here is a single layer pressboard sample having a width of 0.89mm and a diameter of 10.5mm. A charge of the known magnitude of 5pC is applied to an insulation sample with the help of PD calibrator. The current waveform corresponding to this applied known charge is plotted graphically and the maximum value of the current is noted as $I_{max.}$ In Fig. 6.1, I_{max} denotes the maximum magnitude of the current signal when a 5pC charge is injected in the single layer thin pressboard.

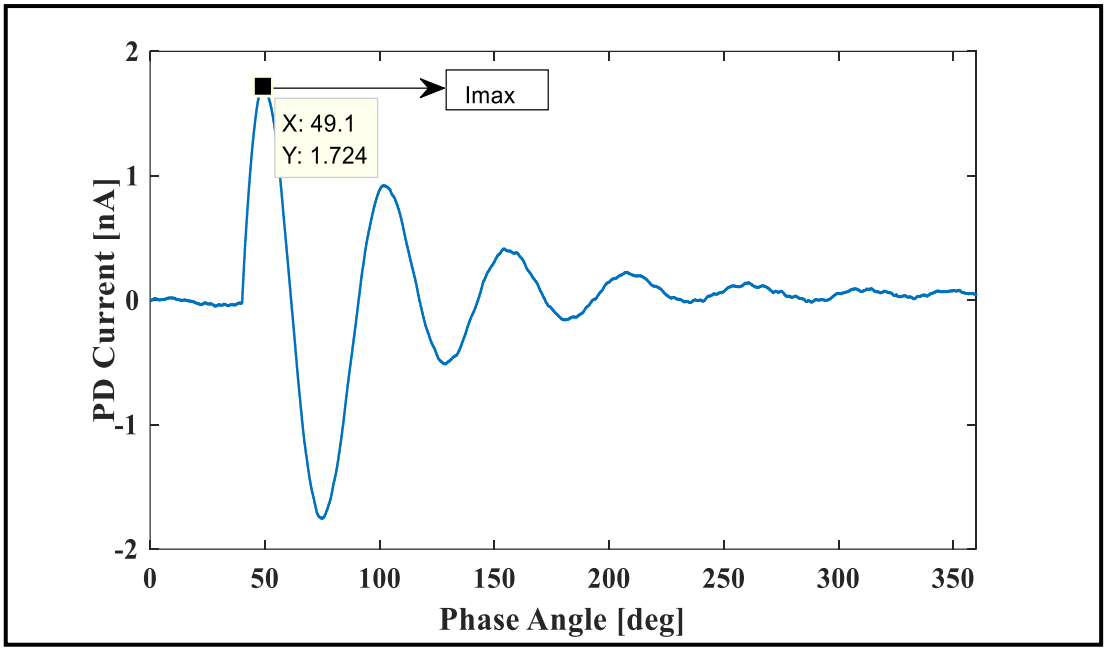

Fig. 6.1. The current waveform of a 5pC charge applied on a single layer of thin pressboard.

Now, when a high voltage is applied on the pressboard layer, PD discharges tend to occur when the applied voltage crosses the PDIV. In Fig 6.2, the PD current versus the phase angle is plotted graphically. From Fig.6.2 , the current magnitude of this PD pattern can be deduced. Let this current magnitude be I_{known}.

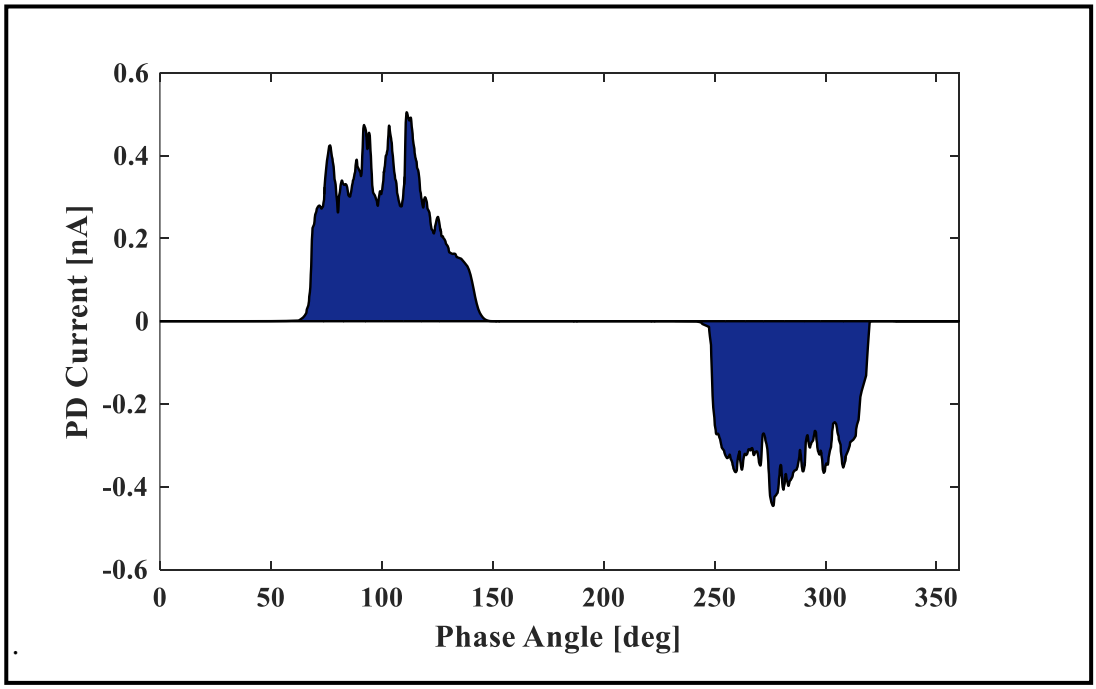

Fig. 6.2. The PD current waveform when voltage is applied on a single layer of thin pressboard.

Now, with the value of $I_{max,}$ I_{known} and the known charge of 5pC, a multiplication factor is calculated following the unitary method. This multiplication factor is utilized to convert the current waveform, would give us the quantitative value of charge present in the PD pattern. Thus conversion of current to charge takes place. Fig. 6.3 shows the calibrated PD charge graph plotted versus phase angle.

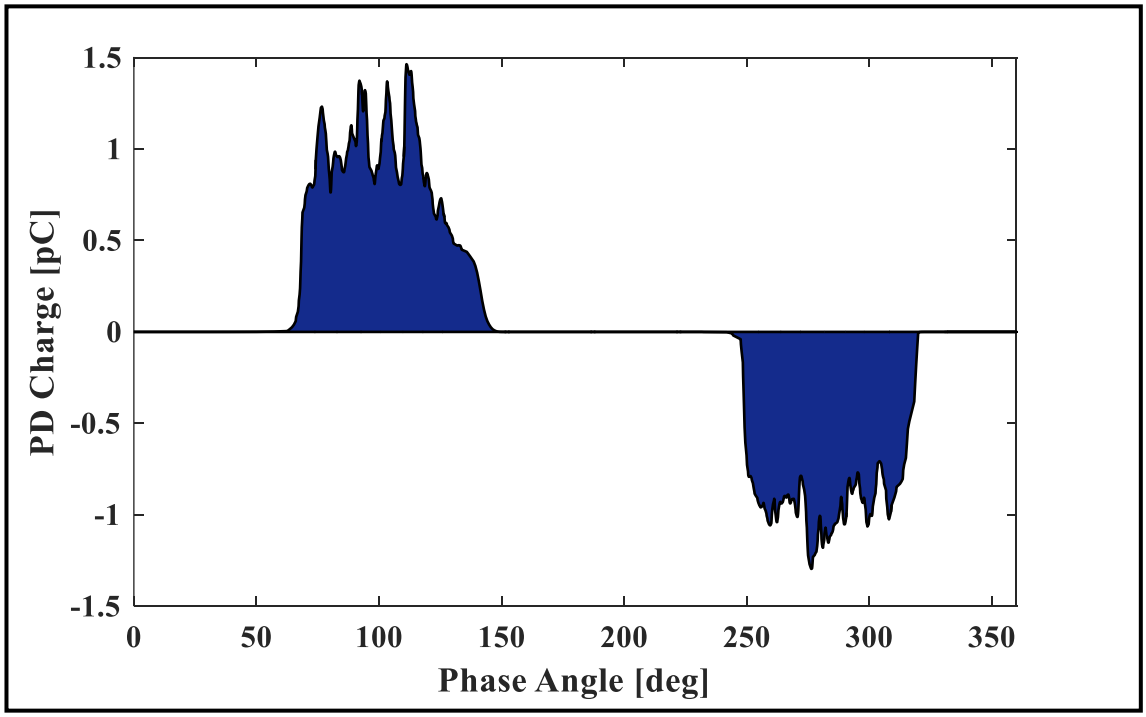

Fig. 6.3. The charge magnitude plot of a single layer of thin pressboard.

The current signal is obtained for the known charge of 5pC for all the samples and applying the same process the discharge value is calculated for all the samples. This way the process of quantitative measurement of PD by calibrating the PD waveform with the help of a PD calibrator is performed.

6.3 Comparative Study on Condition Monitoring of Different Dry Type Insulating Material Based on Their PRPD Pattern [37,38,39]

The objective of this comparative study is to create a database on various dry type insulation after their distinguished PRPD pattern is explored and analyzed. The data graphically plotted here are, uni-variate and bi-variate distribution of the discharge magnitude of PD (q), the corresponding phase angle (ϕ) and the discharge rate of the pulses (n) over some selected time range.

The samples are reported in the subsequent subsections.

6.3.1 PRESSBOARD

Here based on the thickness two types of Pressboard is used. The samples are prepared as described in section 5.3 in details.

6.3.1.1 Comparative Study on Discharge Magnitude (Q)

The PRPD pattern is obtained as stated in section 5.6.1.2 of the previous chapter. These uni-variate ϕ-q distributions for thin pressboard (a) single-layered (b) double-layered and (c) triple-layered has been shown in Fig. 6.4 and for the thick pressboard (a) single-layered and (b) double-layered has been shown in Fig. 6.5.

As mentioned before, with an increase in the number of layers in an insulation sample, the overall insulation thickness is said to be increased. From the PD patterns shown in Fig. 6.4 and Fig. 6.5 it is noticed that as the number of layers are increasing, the partial discharge inception voltage is also increasing. Hence, with more number of layers, the insulation has been able to withstand a higher voltage which could be an advantage.

At the layer interface and also at the interface between the layers and the electrode, there is a possibility of the presence of the air layer, irregularities due to the insulation manufacturing defects. These together increase the amount of discharge during PD. So as the number of layers is increased, the presence of these irregularities, contaminants and air layer also increases. Hence from the PD patterns in Fig. 6.4 and Fig. 6.5, it is observed that the overall charge magnitude increases abruptly with an increase in layers and the maximum PD magnitude also increases as the number of layer increases in case of both positive cycle and negative cycle. But this is not a desirable feature and considered disadvantageous for the insulation system.

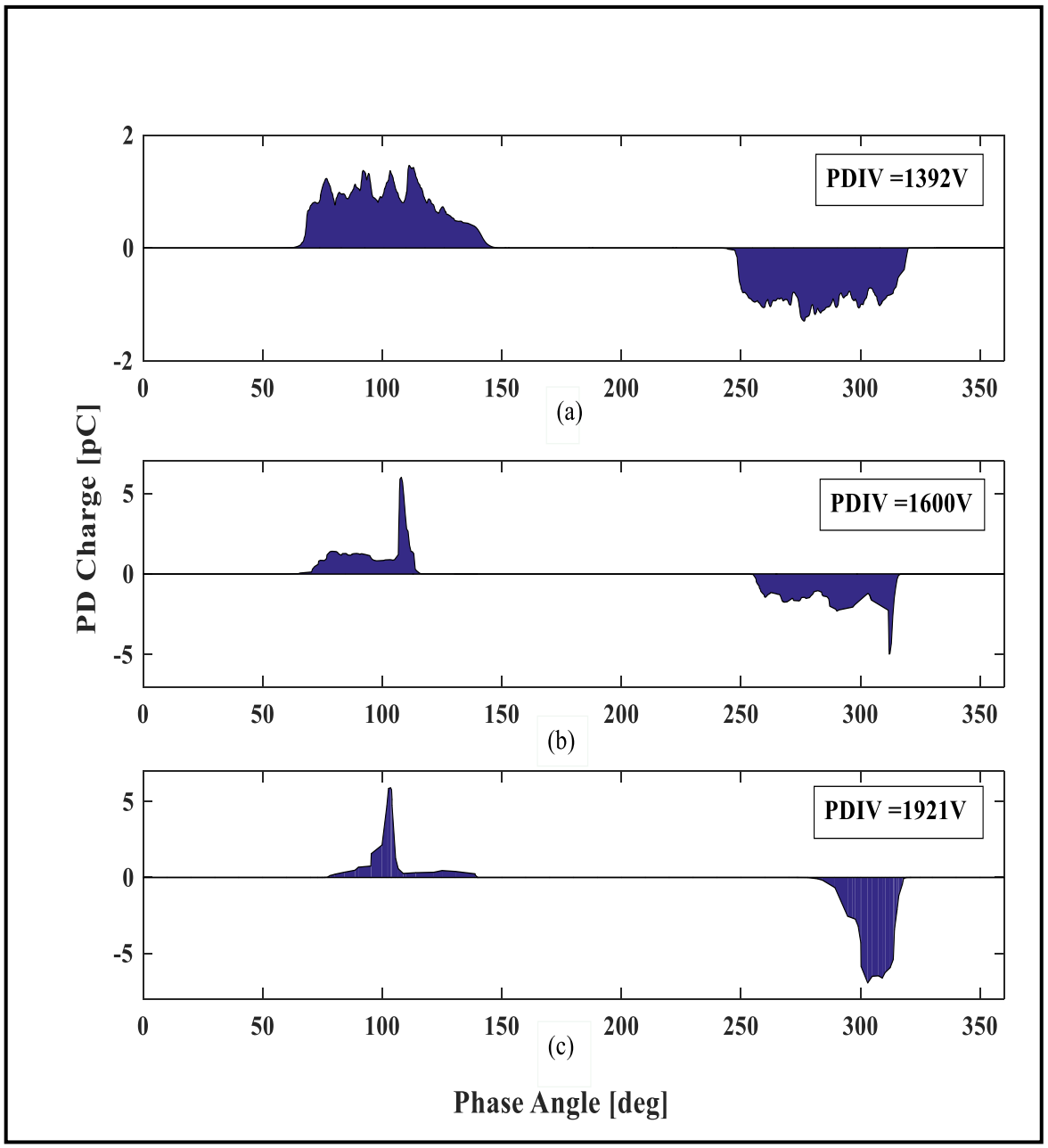

Fig. 6.4. The phase angle- PD charge (ϕ-q) plot for (a) single-layered, (b) double -layered and (c) triple -layered thin pressboard.

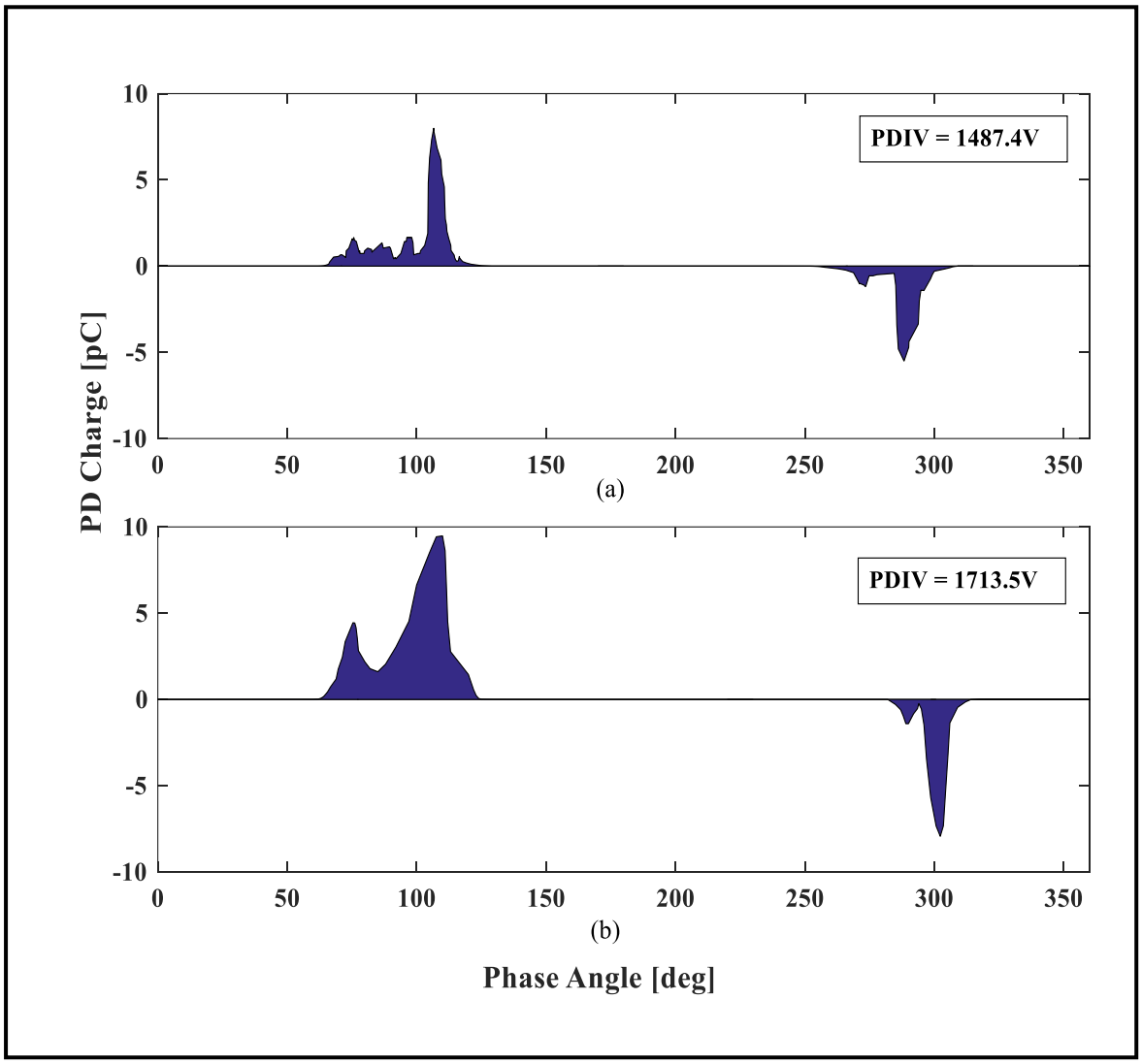

Fig. 6.5. The phase angle - PD charge (ϕ-q) plot for (a) single-layered and (b) double-layered thick Pressboard.

6.3.1.2 Comparative Study on Discharge Pulse Count (N)

In Fig. 6.6 and Fig. 6.7, the pulse count of PD (n) is plotted against the corresponding phase angle (ϕ) for different layers of thin pressboard. In the ϕ-n plot of Fig. 6.6 and Fig. 6.7, the pulse count rate is observed to increase in magnitude with the addition of layers as both the charge magnitude and PDIV increase with the addition of layers. From the pattern shown in Fig. 6.7 it can be stated that the number of pulse count is more in the positive cycle than in the negative cycle. Regarding the waveshape of ϕ-n, no proper conclusion can be drawn as the magnitude of pulse rate is not showing any relation.

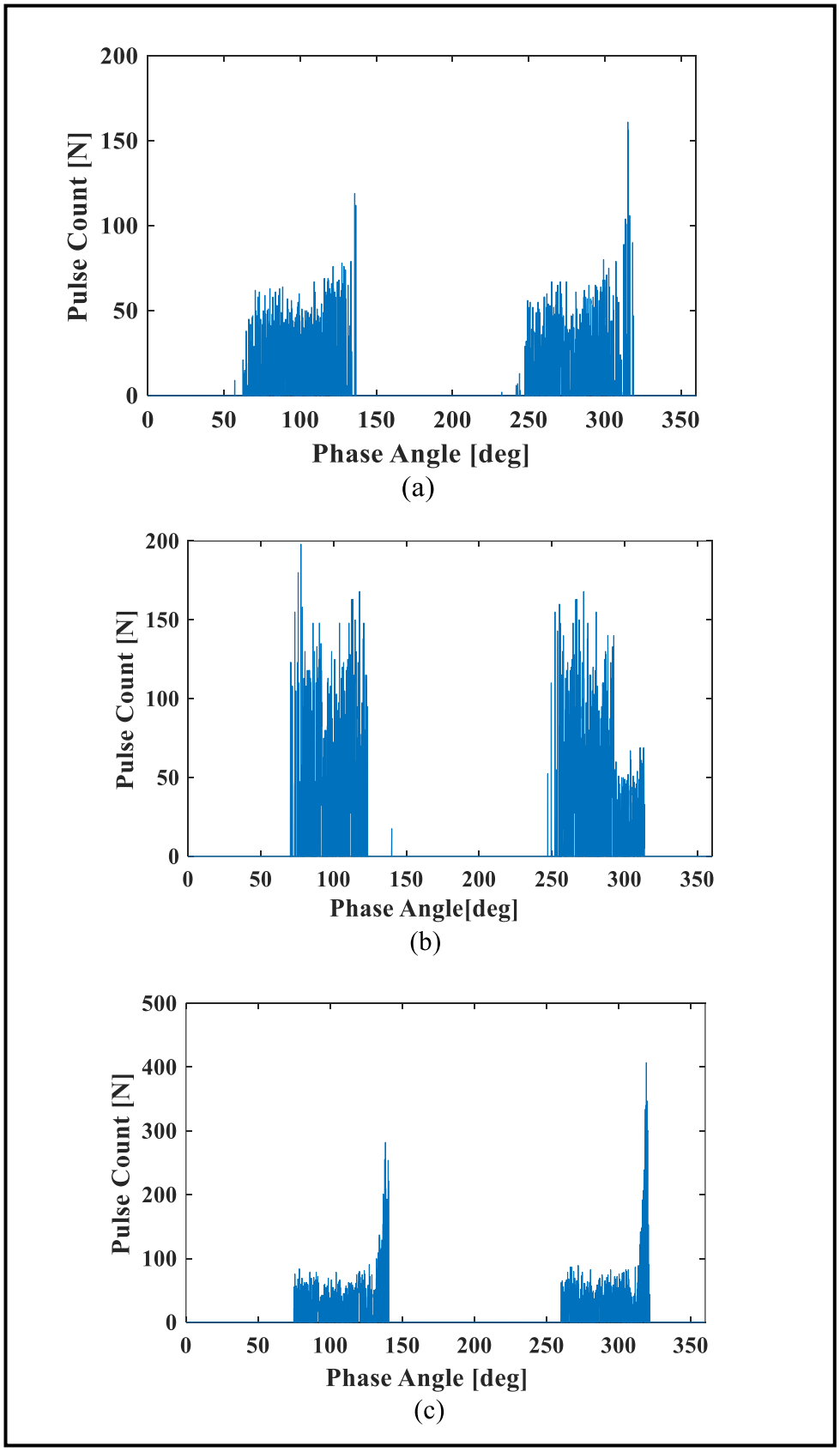

Fig. 6.6. The pulse count– phase angle (ϕ-n) for (a) single- layered, (b) double -layered and (c) triple-layered thin Pressboard.

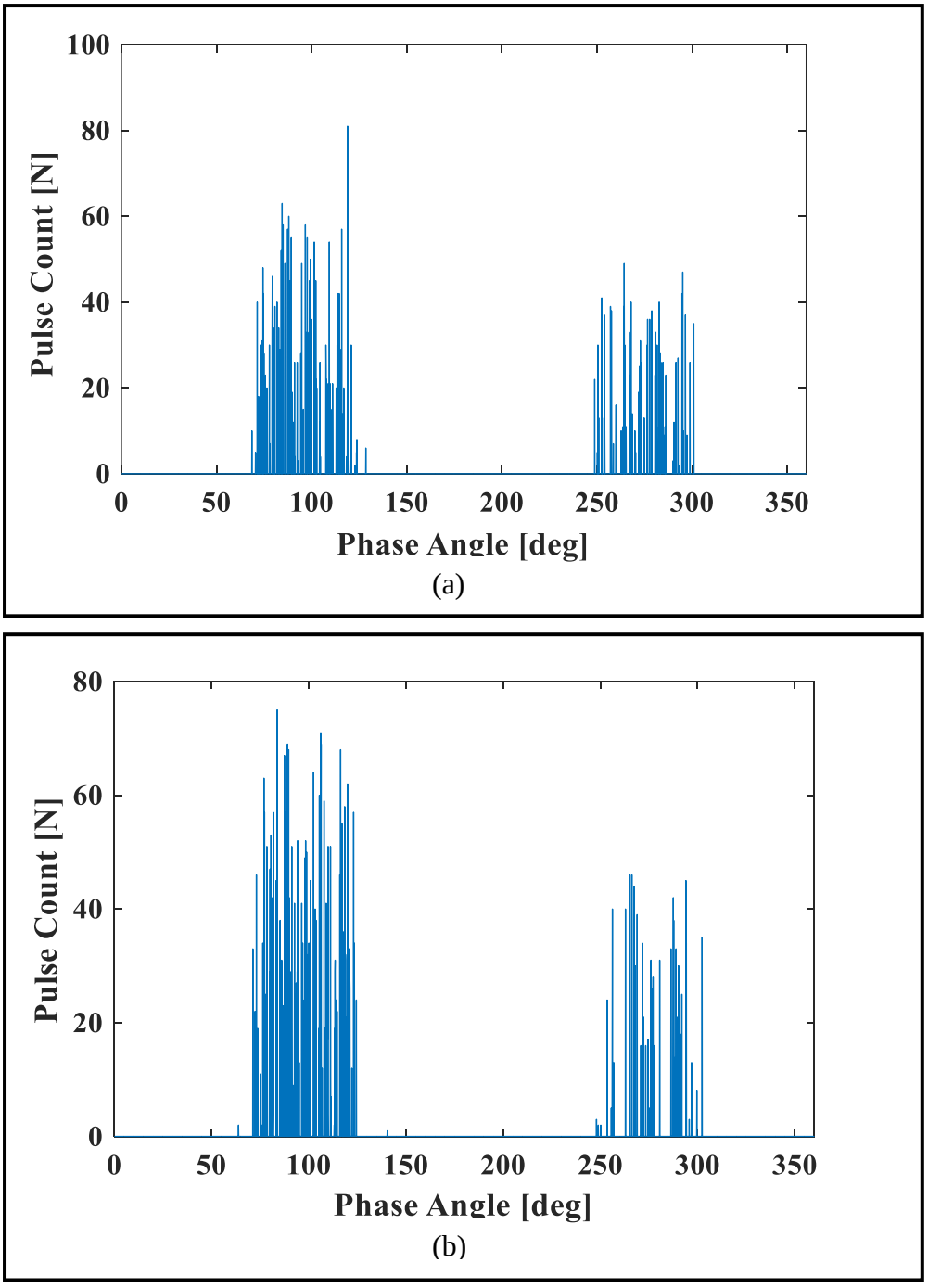

Fig. 6.7. The pulse count– phase angle (ϕ-n) for (a) single-layered and (b) double-layered thick Pressboard.

6.3.2 LEATHEROID PAPER

Here samples were prepared with leatheroid in two sets. In the first set, only layers are added and the second set artificial void is created in a double-layered sample as described in sections 5.3.1 and 5.3.2 of Chapter 5.

6.3.2.1 Comparative Study on Discharge Magnitude (Q)

The uni-variate ϕ-q distributions for the Leatheroid paper (a) double-layered and (b) triple-layered are shown in Fig. 6.8.

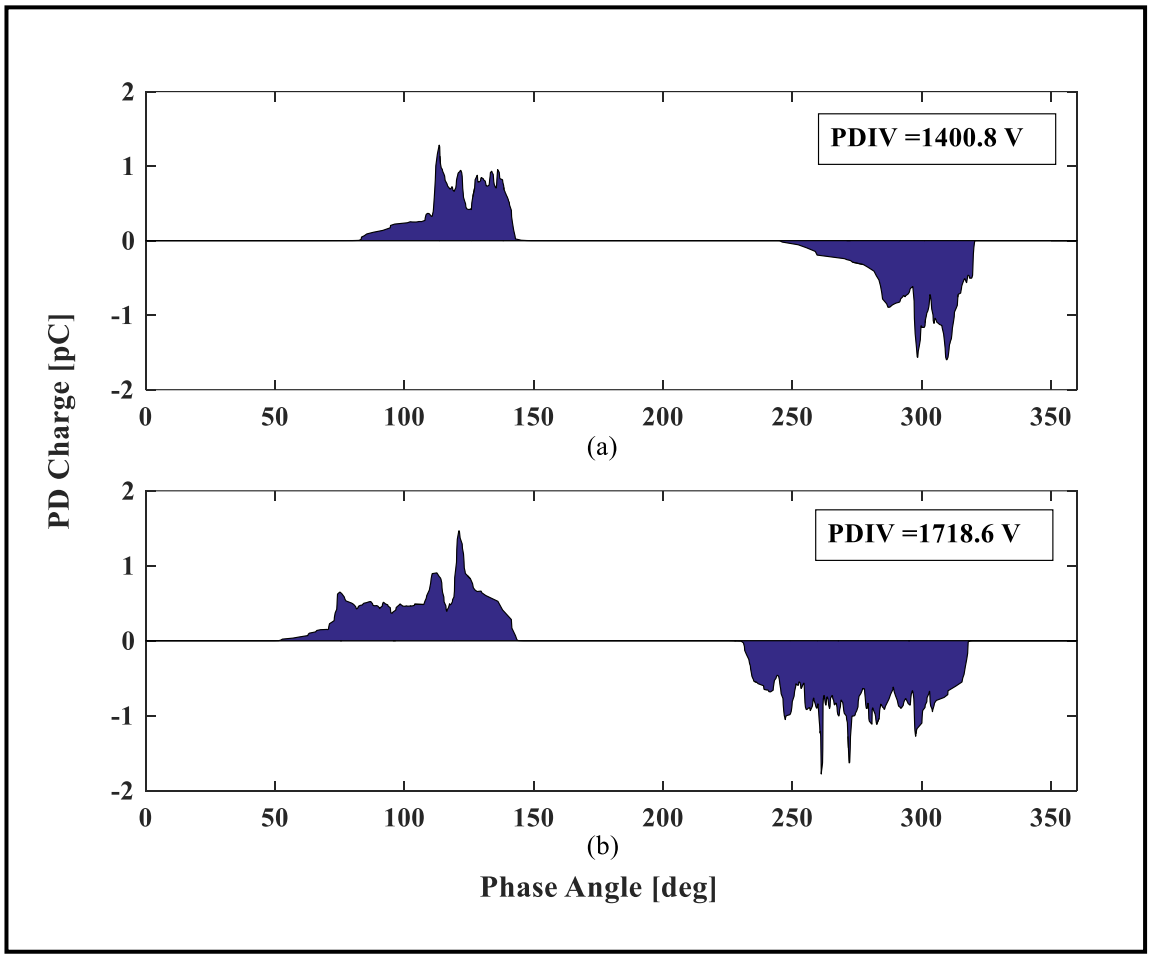

Fig. 6.8. The phase angle- PD charge (ϕ-q) plot for (a) double-layered and (b) triple- layered Leatheroid paper.

From the PD pattern shown in Fig. 6.8, it can be seen that double-layered and triple-layered samples have a different value of PDIV, which means that if the number of layers is increased, the sample can endure higher operating voltage which would definitely be considered as one of the vital advantages of increasing the number of layers. But on the contrary, it can be seen that with an increase in the number of layers, the discharge quantity increases, as well as the maximum discharge value of PD, also increases, which could further damage the insulation sample and aid in the breakdown of the sample. From the PD patterns shown in Fig. 6.8 (a) and (b) it is observed that the phase angle range corresponding to the occurrence of discharge increases in the triple layer in both the negative and positive cycle.

The uni-variate ϕ-q distributions for an artificial void created in a double-layered Leatheroid sample is shown in Fig. 6.9.

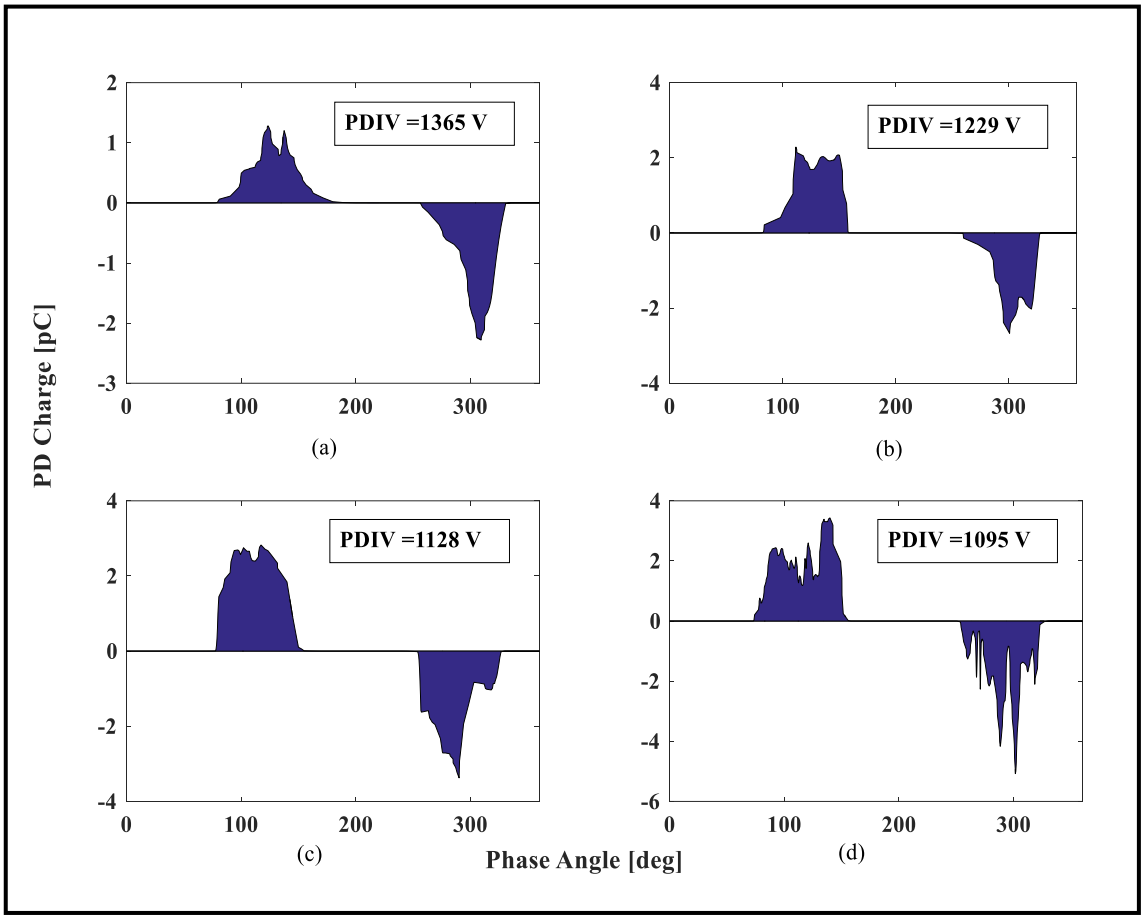

Fig. 6.9. The phase angle-PD charge (ϕ-q) plot for a void of area (a) 4sq.mm., (b) 9sq.mm., (c)16sq.mm. and (d) 25 sq.mm. in a double-layered Leatheroid paper.

From Fig. 6.9, the ϕ-q plot of gradually increasing void can be seen. It is apparently observed that discharges are occurring around almost the same range of the phase angle. With an increase in void size, the number of PDs and total discharge increases abruptly in both the positive and negative cycle. The maximum magnitude of the PD increases with an increase in void dimension. The value of PDIV decreases which indicates due to the presence of void partial discharge occurs at a much lower voltage. If the PD pattern in Fig. 6.8 (a) is compared with the PD pattern in Fig. 6.9 (a), it is observed PDIV is low in case of the void, even though both the samples are double-layered. With an increase in the area of the void, PDIV value falls. If the comparison is drawn between the PD patterns in Fig. 6.8 (a) and Fig. 6.9 (a) it can be seen that the maximum charge magnitude is more in the case of the double-layered sample having a centrally placed void. Therefore, it could be said that a sample having void can expedite the breakdown mechanism of an insulation

sample. In the samples, referred to Fig. 5.11 of section 5.3.2 it is seen that the void is located in the center. Due to this the electric field on the surface of the void is symmetrical. Hence the ϕ-q pattern obtained for both the negative cycle and positive cycle of the applied voltage is apparently almost symmetrical [21].

6.3.2.2 Comparative Study on Discharge Pulse Count (N)

In Fig. 6.10 the pulse count of PD (n) is plotted against the corresponding phase angle (ϕ) for double and triple layers of Leatheroid paper.

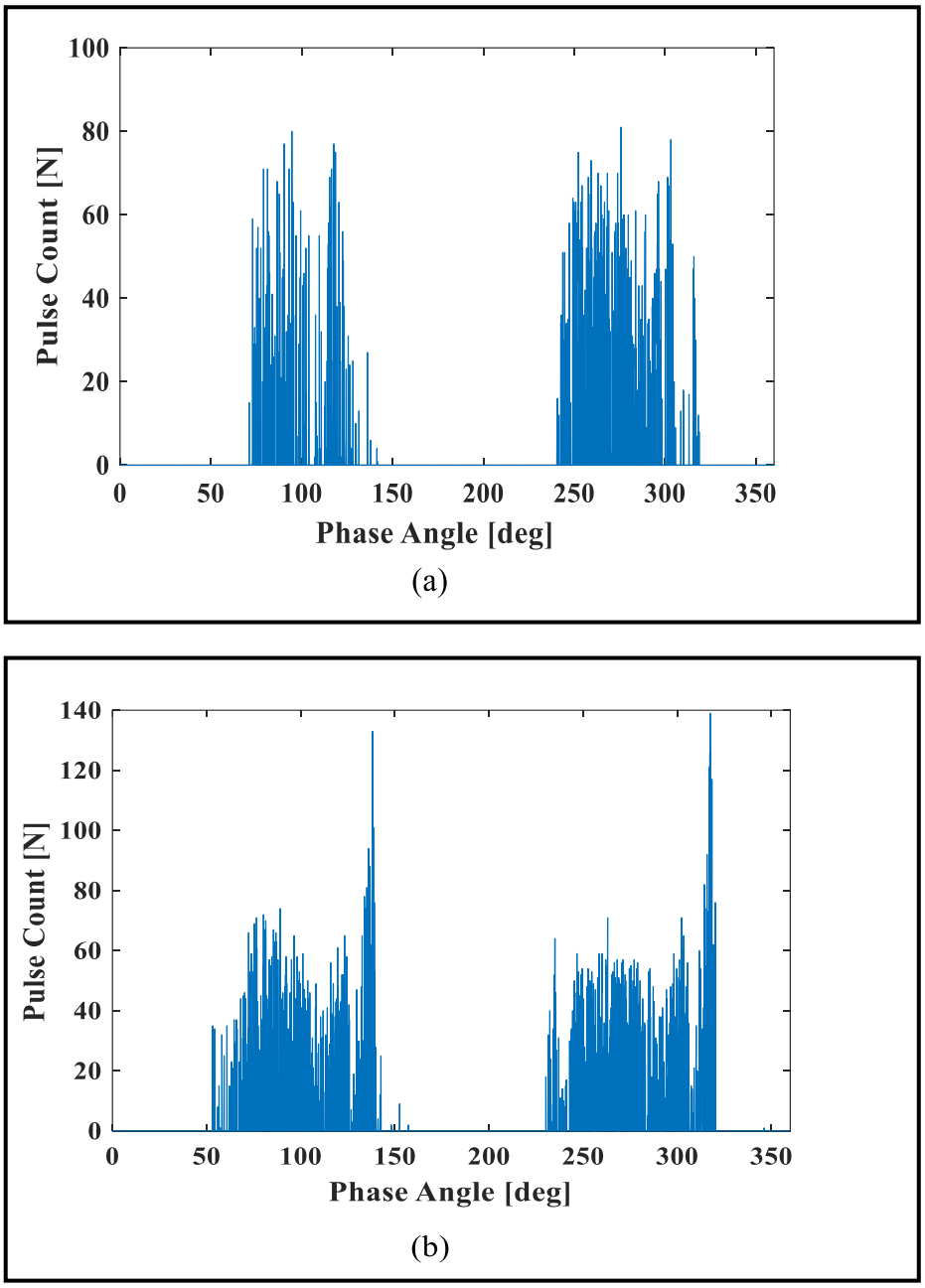

Fig. 6.10. The pulse count-phase angle (ϕ-n) for (a) double-layered and (b) triple-layered Leatheroid paper.

From Fig. 6.10, it is observed that with an increase in the layer of the sample, the number of pulse count (n) increases. The PDIV is also different for two layers and it is apparent that pulse count is dependent on the applied voltage.

In Fig. 6.11 the pulse count of PD (n) is plotted against the corresponding phase angle (ϕ) for a void of area (a) 4sq.mm., (b) 9sq.mm.,(c)16sq.mm. and (d) 25sq.mm. in a double-layered Leatheroid paper.

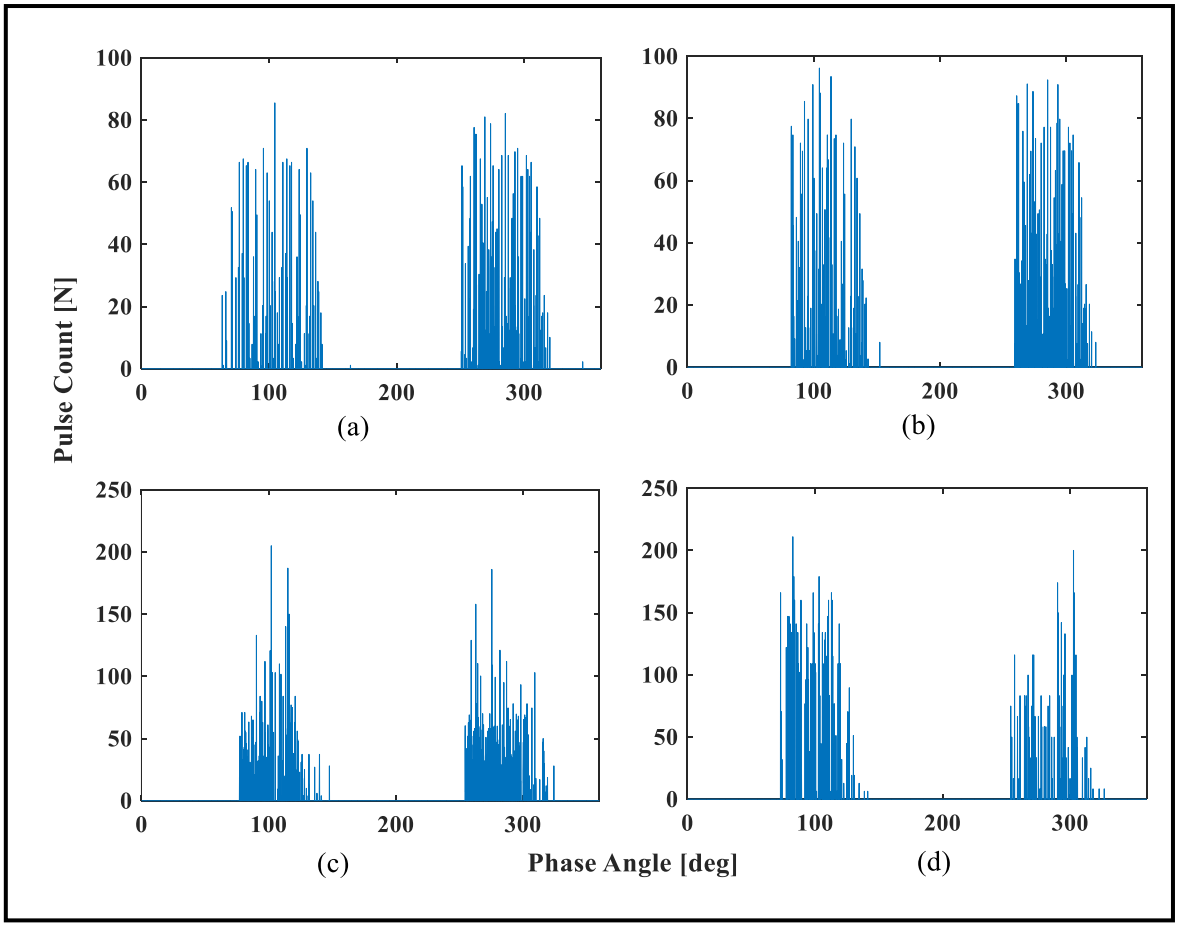

Fig. 6.11.The pulse count– phase angle (ϕ-n) for a void of area (a) 4sq.mm. ,(b) 9sq.mm., (c)16sq.mm. and (d) 25sq.mm. in a double-layered Leatheroid paper.

It is observed from the distribution in Fig. 6.11 that as the void area is increasing in size there is an increased rate of occurrence of PD such that the pulse count is extensively high. The pulse count increases abruptly with an increase in the area of the void. The distribution pattern of the pulse count gradually increases and reaches the crest, and then it seems to gradually decrease in nature.

6.3.3 NOMEX FILM

Two types of Nomex films are used here based on their thickness. The thick Nomex film is used to prepare samples with layers only. Samples prepared with the thin Nomex film in two sets. In the first set, only layers are added and in the second set, an artificial void is created in a double-layered sample as described in sections 5.3.1 and 5.3.2.

6.3.3.1 Comparative Study on Discharge Magnitude (Q)

The uni-variate ϕ-q distributions for Nomex film (thick) (a) double-layered and (b) triple-layered has been shown in Fig. 6.12.

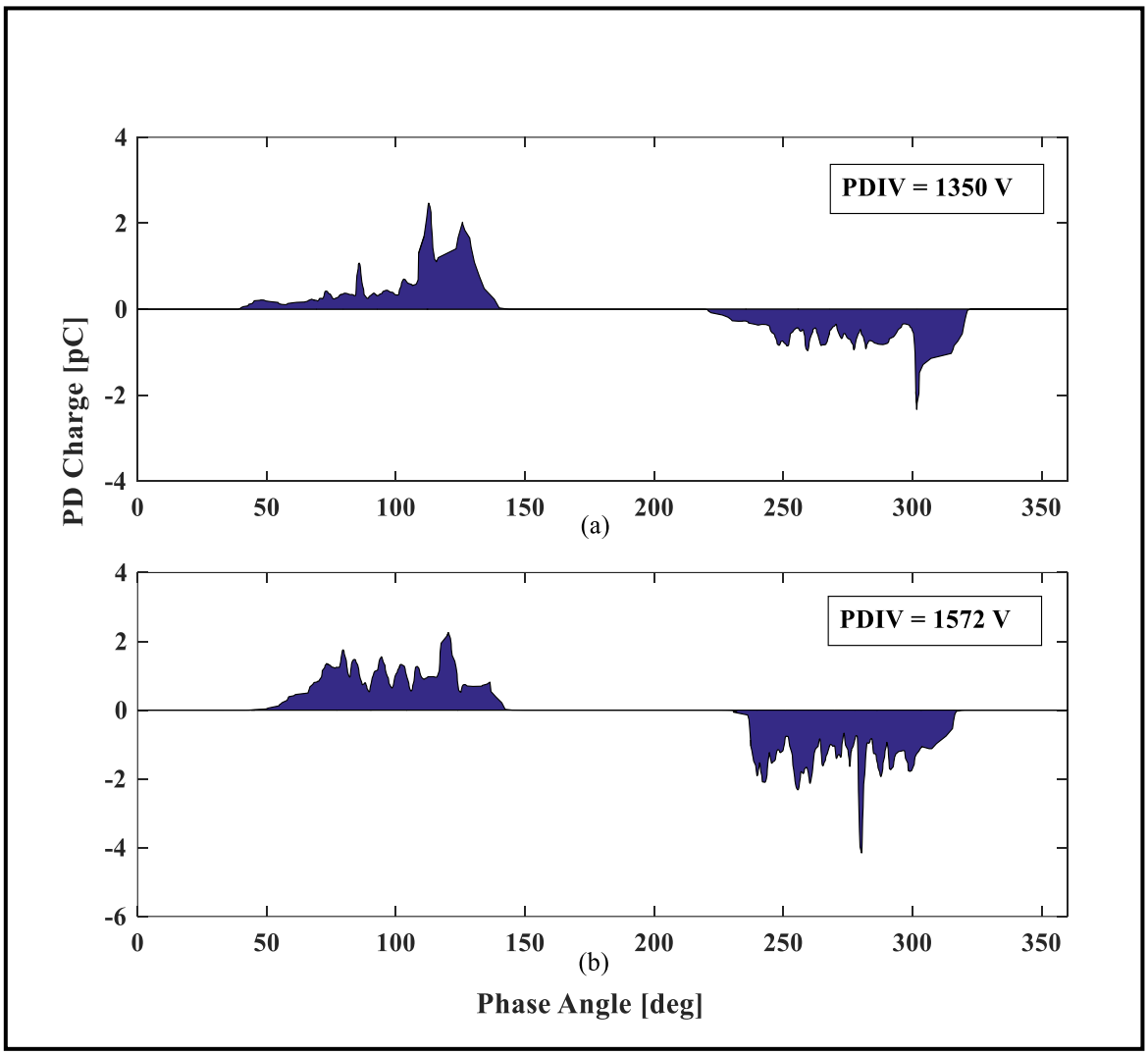

Fig. 6.12. The phase angle- PD charge (ϕ-q) plot for (a) double-layered and (b) triple- layered thick Nomex film.

From the patterns shown in Fig. 6.12, it can be said that with an increase in just one layer of the sample, the PDIV value increases by more than 20% which is highly beneficial as

the insulation can withstand higher operating voltage. But with an increase in the number of layers, the discharge quantity increases as seen in the PD patterns from Fig. 6.12 (a) and (b). The maximum discharge value of PD also increases as the number of layers increases. From the PD patterns inFig. 6.12 (a) and (b) it is observed that the phase angle range corresponding to the occurrence of discharge remains nearly the same in both the layers in both the negative and positive cycle.

The uni-variate ϕ-q distributions for Nomex film (thin) (a) double-layered and (b) triple-layered has been shown in Fig. 6.13.

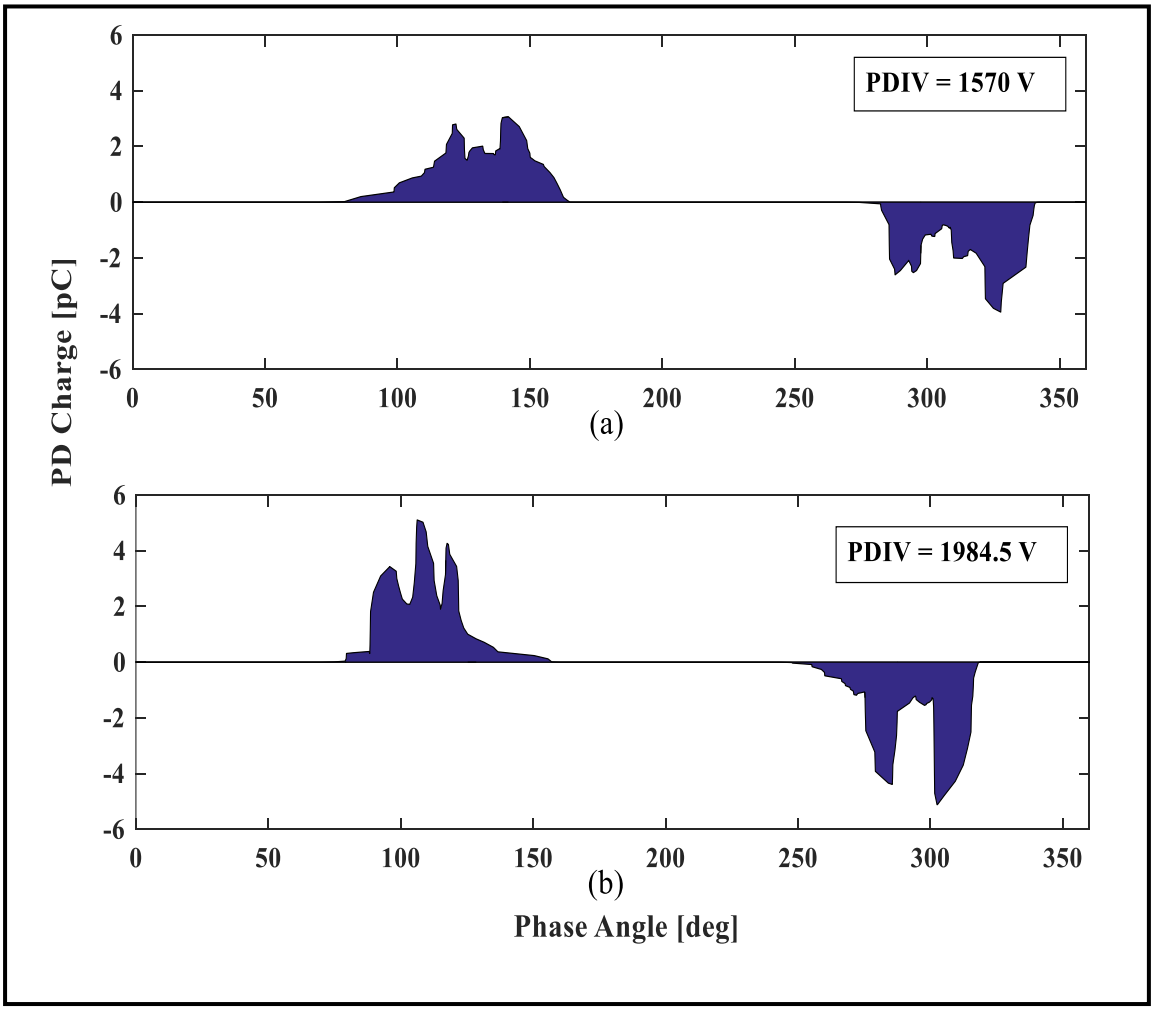

Fig. 6.13. The phase angle- PD charge (ϕ-q) plot for (a) double-layered and (b) triple- layered thin Nomex film.

From the PD patterns shown in Fig. 6.13, it can be seen that PDIV increases by almost 15% in case of usage of the triple-layered sample instead of the double-layered sample. This is a great advantage as the sample can endure more working voltage. But, from the PD pattern in Fig. 6.13, it can be seen that in the triple-layered the quantity of discharge is

much more than that in case of the double layer. The maximum magnitude of discharge is also much higher in the case of the triple-layered sample for both positive and negative cycle. In the case of Nomex film (thin), it is observed that in both the sample the range of phase angle corresponding to PD is similar.

From the PD patterns in Fig. 6.12 and Fig. 6.13, it is seen that the PDIV of the thin Nomex film is higher than the thick Nomex film which makes thin Nomex film a better choice. But if the comparison is drawn between the quantity of discharge, then thick Nomex paper is a better choice.

The uni-variate ϕ-q distributions for an artificial void created in a double-layered thin Nomex film sample is shown in Fig. 6.14.

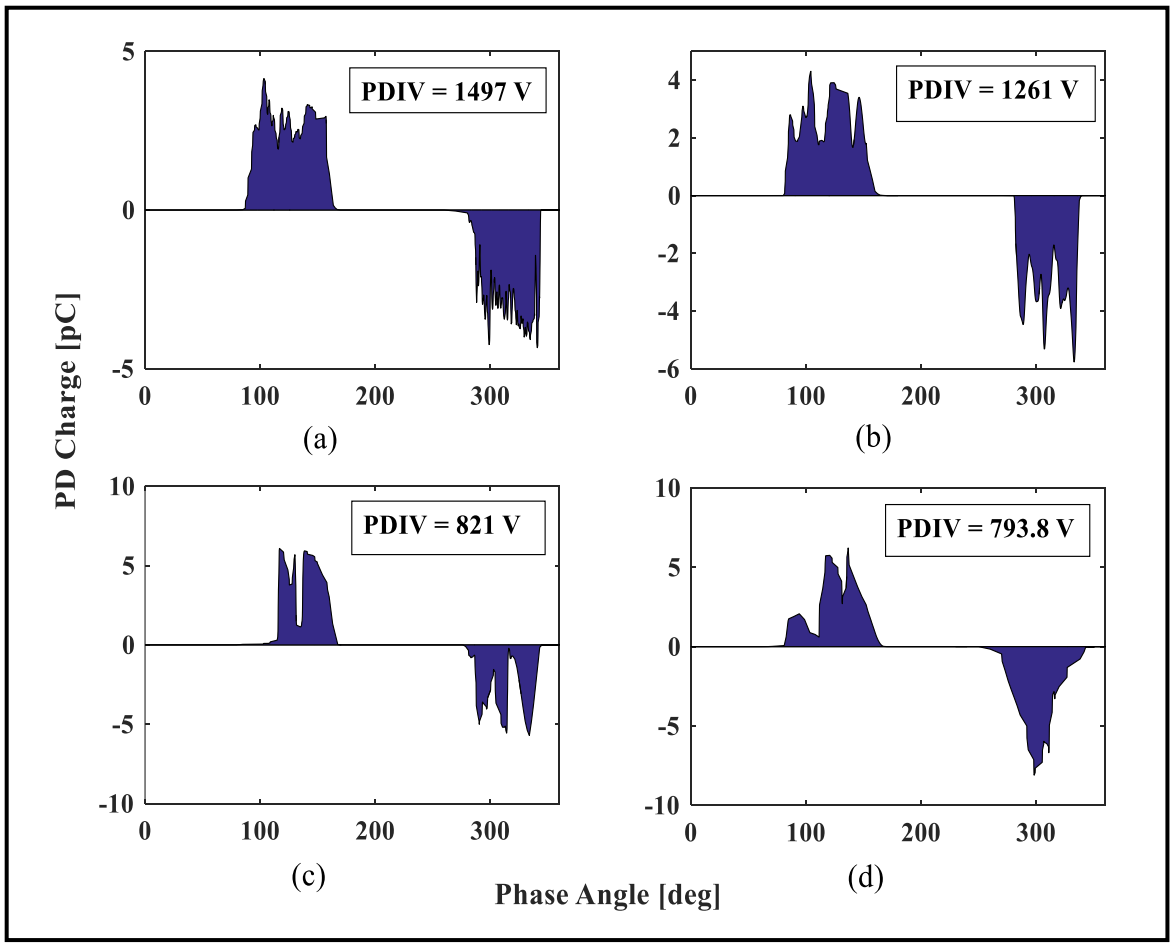

Fig. 6.14. The phase angle- PD charge (ϕ-q) plot for a void of area (a) 4sq.mm., (b) 9sq.mm., (c)16sq.mm. ,(d) 25sq.mm. in a double-layered thin Nomex film.

The ϕ-q plot for gradually increasing void area has been shown in Fig. 6.14. The PDIV for individual void size was recorded and it is observed that the PDIV decreases as the void area increases. For this sample, it is seen that the PDIV for the void size of 9sq.mm.

decreases by a substantial amount. If the PD patterns are observed carefully, it is seen that the quantity of PD increases with the increase in void size. The maximum magnitude of PD also increases with an increase in void dimension for both positive and negative cycles. The phase angle of occurrence of PD is increasing with the void size as shown in the PD patterns in Fig. 6.14. Thus it can be concluded that as the void size increases, the breakdown of that insulation sample becomes faster. If a comparison is drawn between the PD patterns from Fig. 6.13 and Fig. 6.14, it is seen that although a void of 4sq.mm. is present in the sample, the PDIV has not decreased by a huge amount in the PD pattern of Fig. 6.14 (a) than the PD pattern in Fig. 6.13 (a). From the PD distribution patterns of the double-layered sample in Fig. 6.13 (a) and the PD patterns of the samples with a void in Fig. 6.14, it is seen that the quantity of discharge is more in case of the sample with the centrally placed void and also the maximum magnitude of PD is more. Thus it can be concluded that PD can speed up the process of sample degradation when the dimension of the void increases.

6.3.3.2 Comparative Study on Discharge Pulse Count (N)

In Fig. 6.15 the pulse count of PD (n) is plotted against the corresponding phase angle (ϕ) for double and triple-layered samples of thick Nomex film.

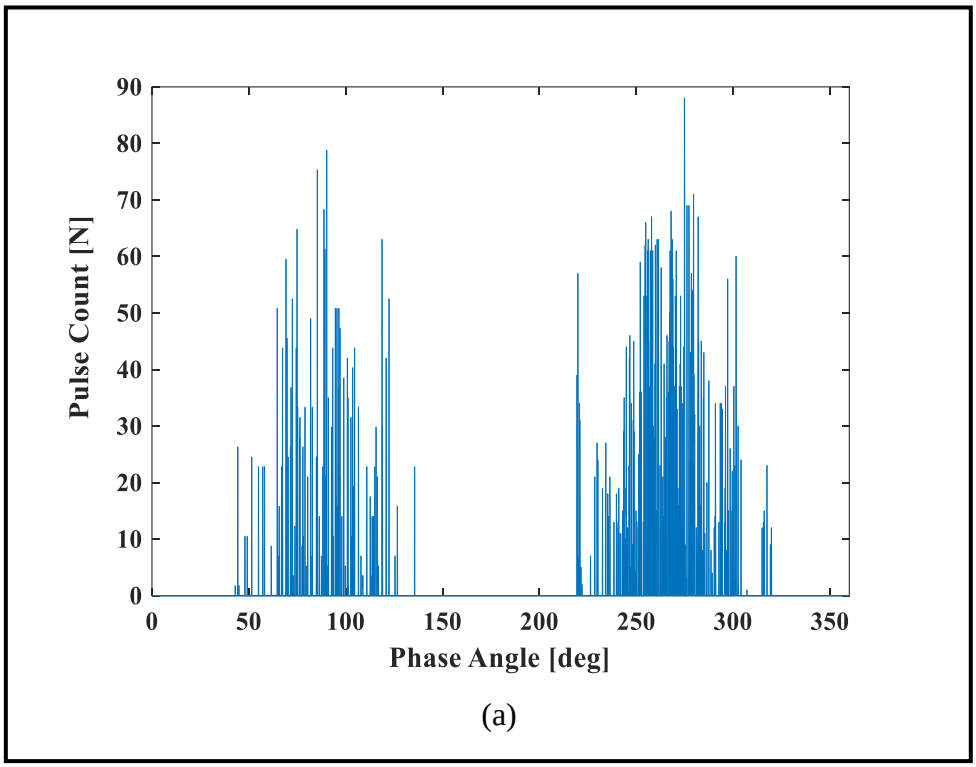

(a)

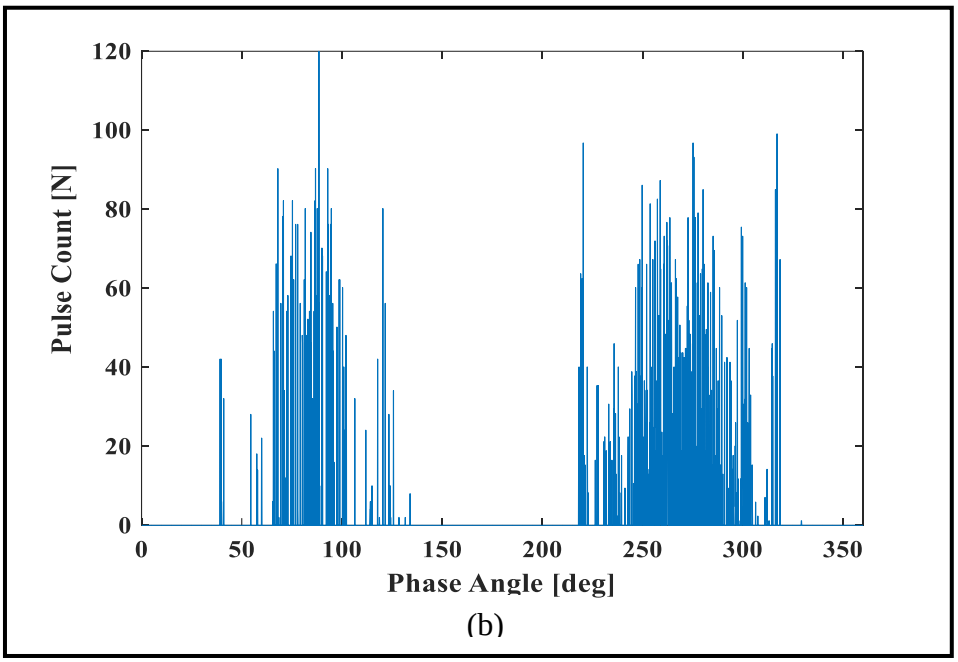

Fig. 6.15. The pulse count– phase angle (ϕ-n) for (a) double- layered and (b) triple- layered thick Nomex film.

From the distribution patterns in Fig. 6.15 (a) and (b) it is observed that with increase in layer the pulse count rate (n) increases. The PDIV is different for both the samples. The span of pulse count on the a.c. cycle and the maximum magnitude of the pulse count increase with the addition of layers. Here, from the distribution patterns in Fig. 6.15 it is seen that the pulse count in the negative cycle is more than in the positive cycle for both the samples.

In Fig. 6.16 the pulse count of PD (n) is plotted against the corresponding phase angle (ϕ) for double and triple-layered samples of thin Nomex film.

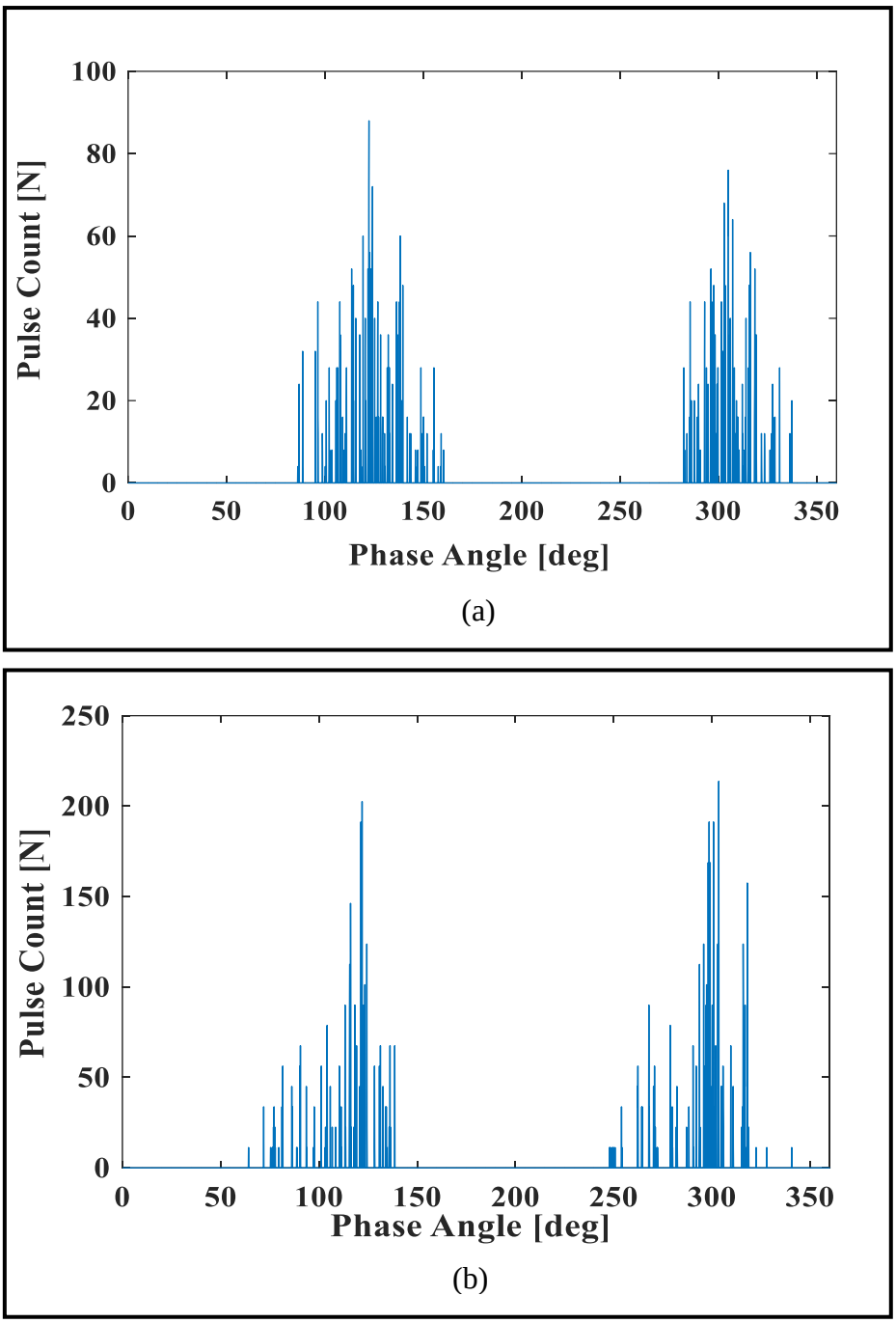

Fig. 6.16. The pulse count– phase angle (ϕ-n) for (a) double- layered and (b) triple -layered thin Nomex film.

From the patterns shown in Fig. 6.16, it is observed that the pulse count rate (n) increases with the addition of layers and also the highest magnitude of the pulse count increases abruptly. In the case of thin nomex film, it is seen that the pulse count rate pattern is sparsely distributed in both the positive and negative cycle but the span on the a.c. the cycle is almost similar for both the layers. If the distribution patterns in Fig. 6.15 and Fig. 6.16 are compared, it is observed that the pulse count rate is higher in the case of the thin

nomex film. In both the nomex films the pulse count patterns have a shape in which the distribution gradually increases, reaches the crest and then decreases gradually.

In Fig. 6.17 the pulse count of PD (n) is plotted against the corresponding phase angle (ϕ) for a void of area (a) 4sq.mm. ,(b) 9sq.mm., (c)16sq.mm. and (d) 25sq.mm. in a double-layered thin Nomex film.

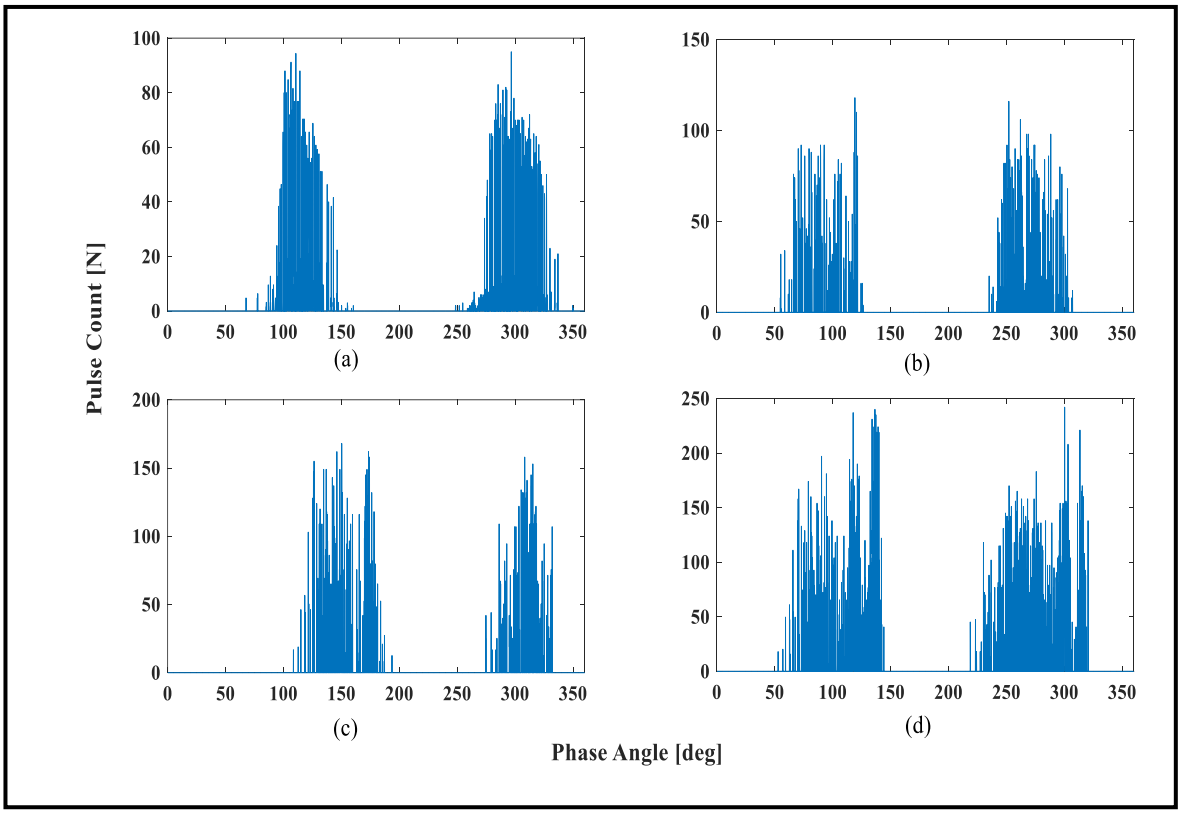

Fig. 6.17. The pulse count–phase angle (ϕ-n) for a void of area (a) 4sq.mm.,(b) 9sq.mm.,(c)16sq.mm. and (d) 25sq.mm. in a double-layered thin Nomex Film.

From the distribution in Fig. 6.17, it is observed that the magnitude and also the quantity of pulse count rate increases rapidly with increase in the void size. The span of the phase angle corresponding to the pulse count increases with an increase in the void size. The shape of the distribution is more or less similar in the case of the different types of voids.

6.3.4 NOMEX PAPER

Two types of nomex paper samples are used here. One having double and triple-layered samples. The other is a double-layered sample with centrally placed void as shown in section 5.3.1 and 5.3.2.

6.3.4.1 Comparative Study on Discharge Magnitude (Q)

The uni-variate ϕ-q distributions for Nomex Paper (a) double layer and (b) triple layer are shown in Fig. 6.18.

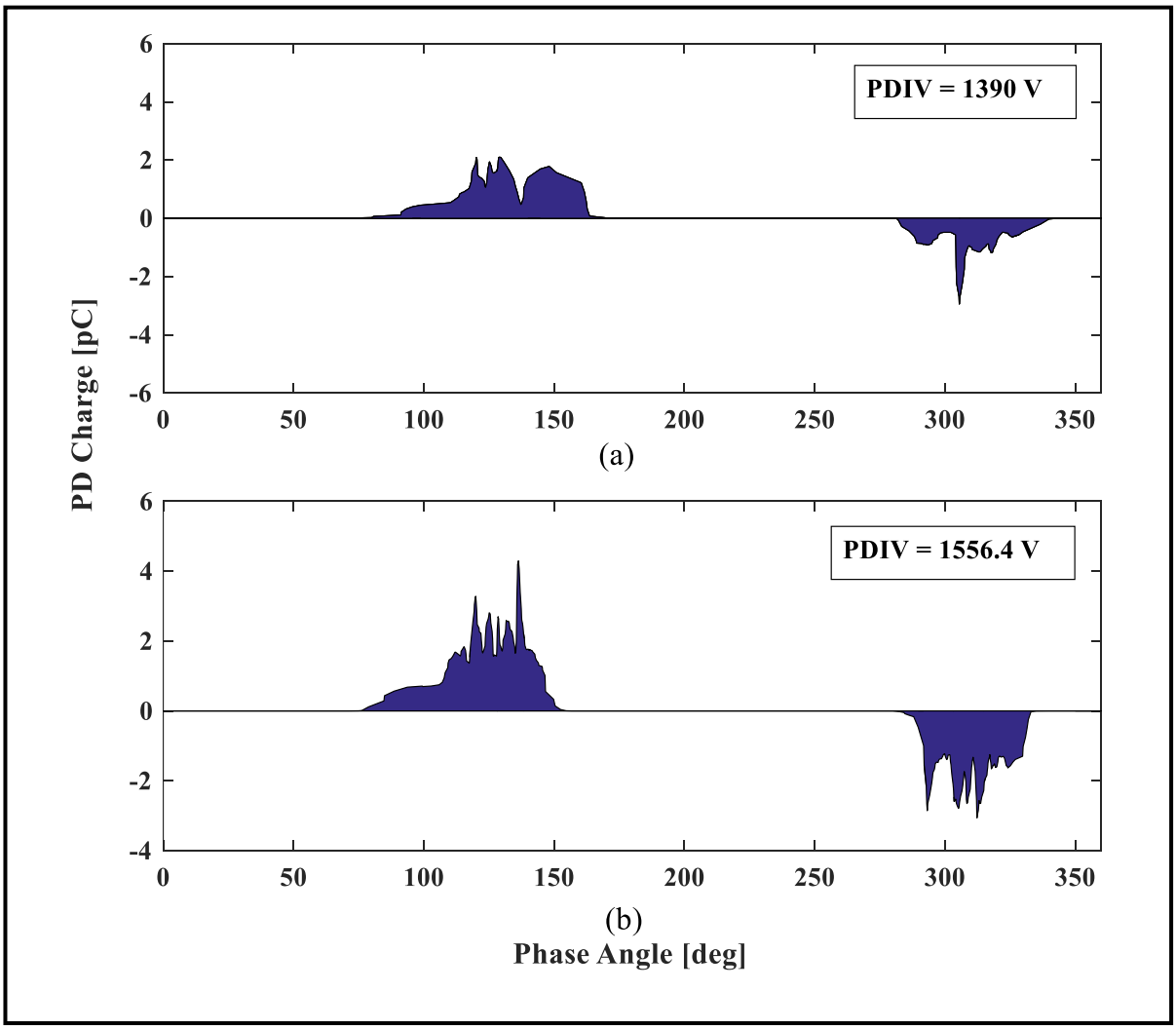

Fig. 6.18. The phase angle- PD charge (ϕ-q) plot for (a) double-layered and (b) triple- layered Nomex paper.

In Fig. 6.18, the PDIV for the two different layered samples are shown and it is observed that with an addition of another layer, the sample can work at 15% higher operating voltage. This makes the triple layer an extremely good choice of insulation. But, in the case of the triple-layered sample, the quantity of discharge is more than in the double-layered sample. The maximum magnitude of discharge is also high in the case of the triple layer. The span of the angle of occurrence of PD in both the layers is almost similar. There PD occurrence is more in case of the triple-layered sample which will ultimately lead to the breakdown of the insulation.

The uni-variate ϕ-q distributions for an artificial void created in a double-layered Nomex paper sample is shown in Fig. 6.19.

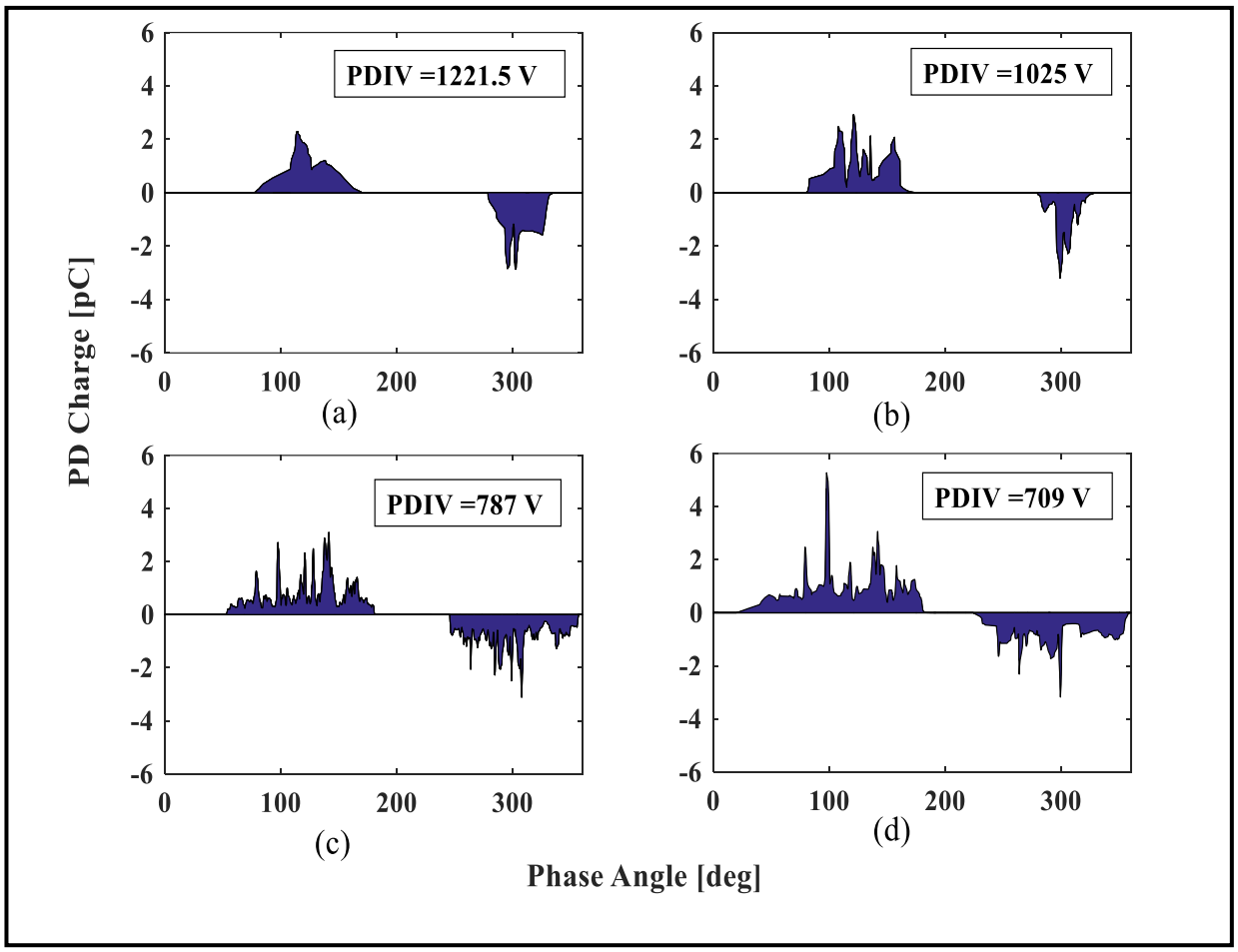

Fig. 6.19. The phase angle- PD charge (ϕ-q) plot for a void of area (a) 4sq.mm., (b) 9sq.mm.,(c)16sq.mm. and (d) 25 sq.mm. in a double-layered Nomex paper.

From the PD patterns shown in Fig. 6.19, it is observed that PDIV value decreases as the void area increases. For void of 16sq.mm, PDIV falls rapidly so it can be said that PD starts to occur earlier for this void size. The quantity of discharge increases with void size and the maximum magnitude of discharge also increases with an increase in the void size for both positive and negative cycles. From the PD distribution pattern in Fig. 6.19,if observed carefully it can be seen that the span of the phase angle corresponding to the PD pulses is gradually increasing such that for the void of area 25sq.mm, PD occurs almost throughout the 360° of the a.c. cycle. If the PD patterns in Fig. 6.18 (a) and Fig. 6.19 (a) are observed it is seen that for a small void of 4sq.mm. , the PDIV decreases by almost 12% both being double layered and also the maximum PD magnitude and PD quantity are higher in case of PD pattern shown in Fig. 6.19 (a) than that in Fig. 6.18 (a). Looking at all

the waveforms in Fig. 6.19 it can be concluded that the PD activity increases with an increase in void dimension.

6.3.4.2 Comparative Study on Discharge Pulse Count (N)

In Fig. 6.20 the pulse count of PD (n) is plotted against the corresponding phase angle (ϕ) for

double and triple layers of thin Nomex paper.

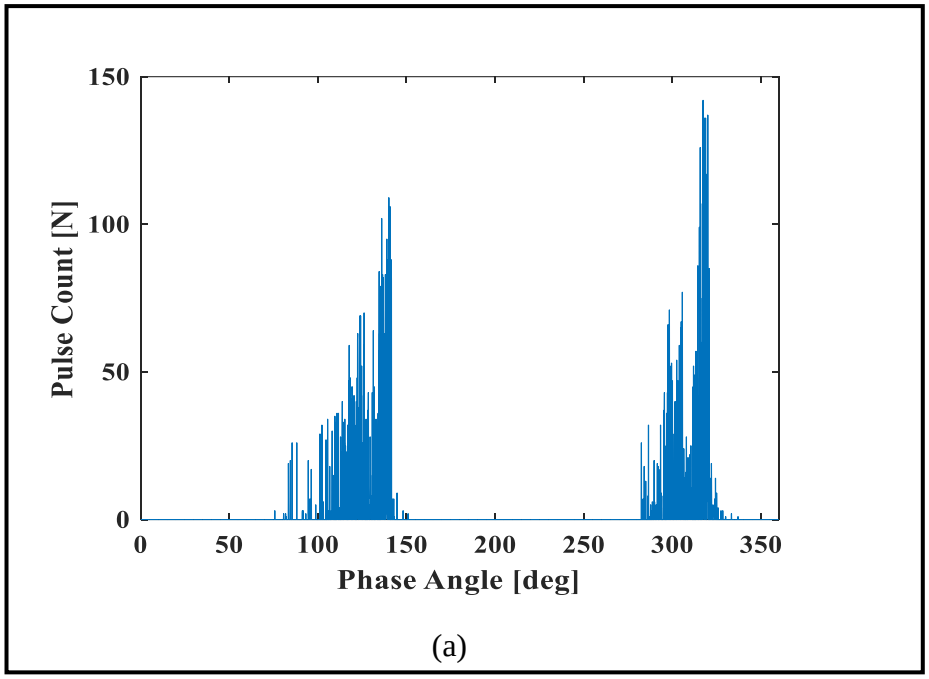

(a)

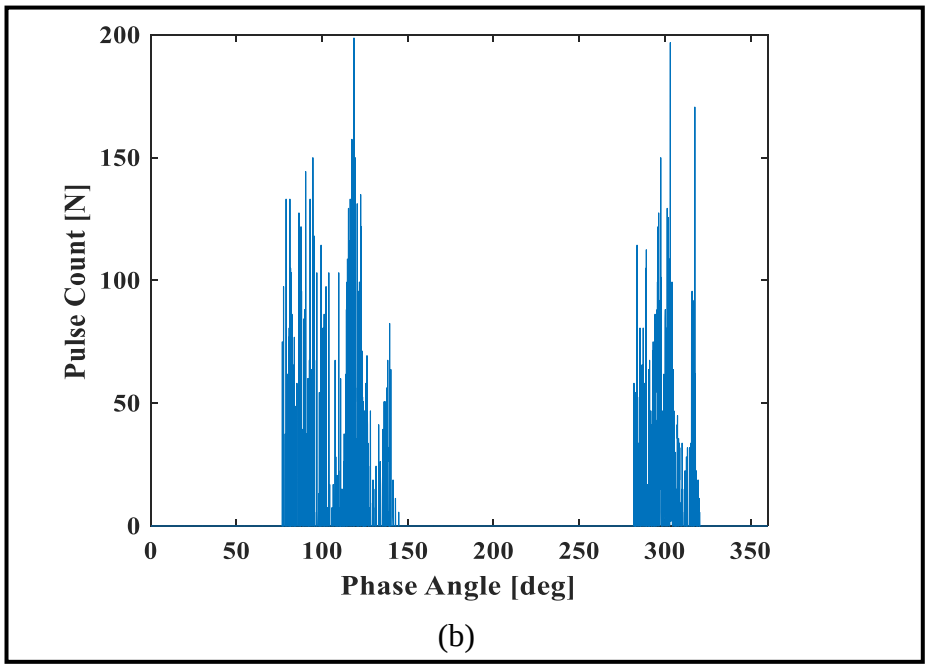

(b)

Fig. 6.20. The pulse count– phase angle (ϕ-n) for (a) double- layered and (b) triple-layered Nomex paper.

From the pulse rate distribution in Fig. 6.20, it is observed that the pulse count rate is much higher in the case of the triple-layered sample. From the PD patterns Fig. 6.18 it is observed that the PD charge quantity is more in the case of the triple-layered sample, hence the pulse count is also high here. The maximum magnitude of the pulse in case of triple-layered sample is also higher than the double-layered sample.

In Fig. 6.21 the pulse count of PD (n) is plotted against the corresponding phase angle (ϕ) for a void of area (a) 4sq.mm. (b) 9sq.mm. (c)16sq.mm. (d) 25sq.mm. in a double-layered Nomex paper

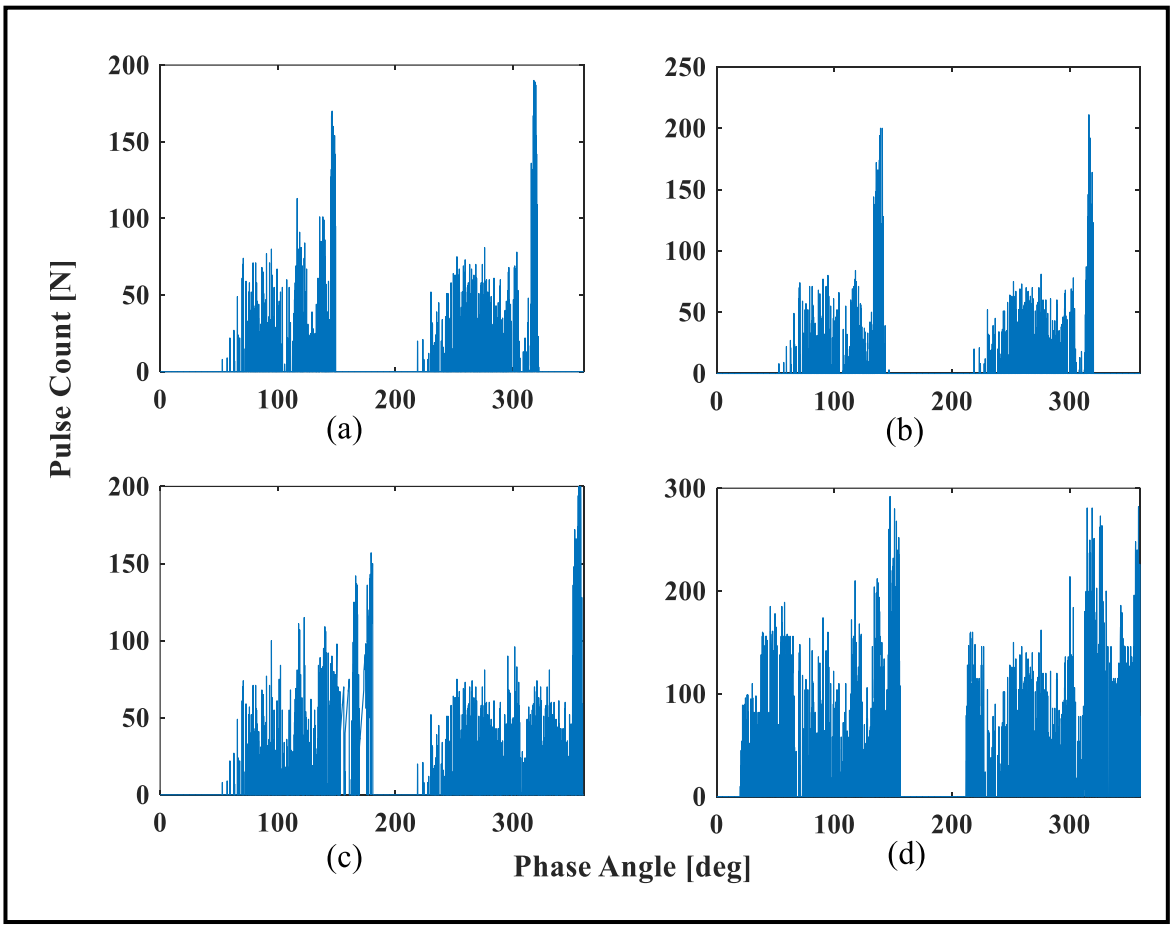

Fig. 6.21. The pulse count– phase angle (ϕ-n) for a void of area (a) 4sq.mm., (b) 9sq.mm. ,(c)16sq.mm., and (d) 25sq.mm. in a double-layered Nomex paper.

From the distribution patterns shown in Fig. 6.21 it has been observed that with an increase in the void area, the rate of pulse count increases in magnitude as well as throughout the a.c. cycle. In the case of 25sq.mm. void area, the PD pulse occurred spreading almost throughout the a.c. cycle. From the pulse count pattern in Fig. 6.21 (d) it is seen that distribution ranges almost throughout the a.c. cycle. Thus it is observed that

Nomex paper with centrally placed void has a distinct pulse count pattern as shown in Fig. 6.21.

6.3.5 KRAFT PAPER

Eight layers of kraft paper are layered together and used as a sample as mentioned in section 5.3.1.

6.3.5.1 Comparative Study on Discharge Magnitude (Q)

The uni-variate ϕ-q distributions for eight-layered kraft paper is shown in Fig. 6.22.

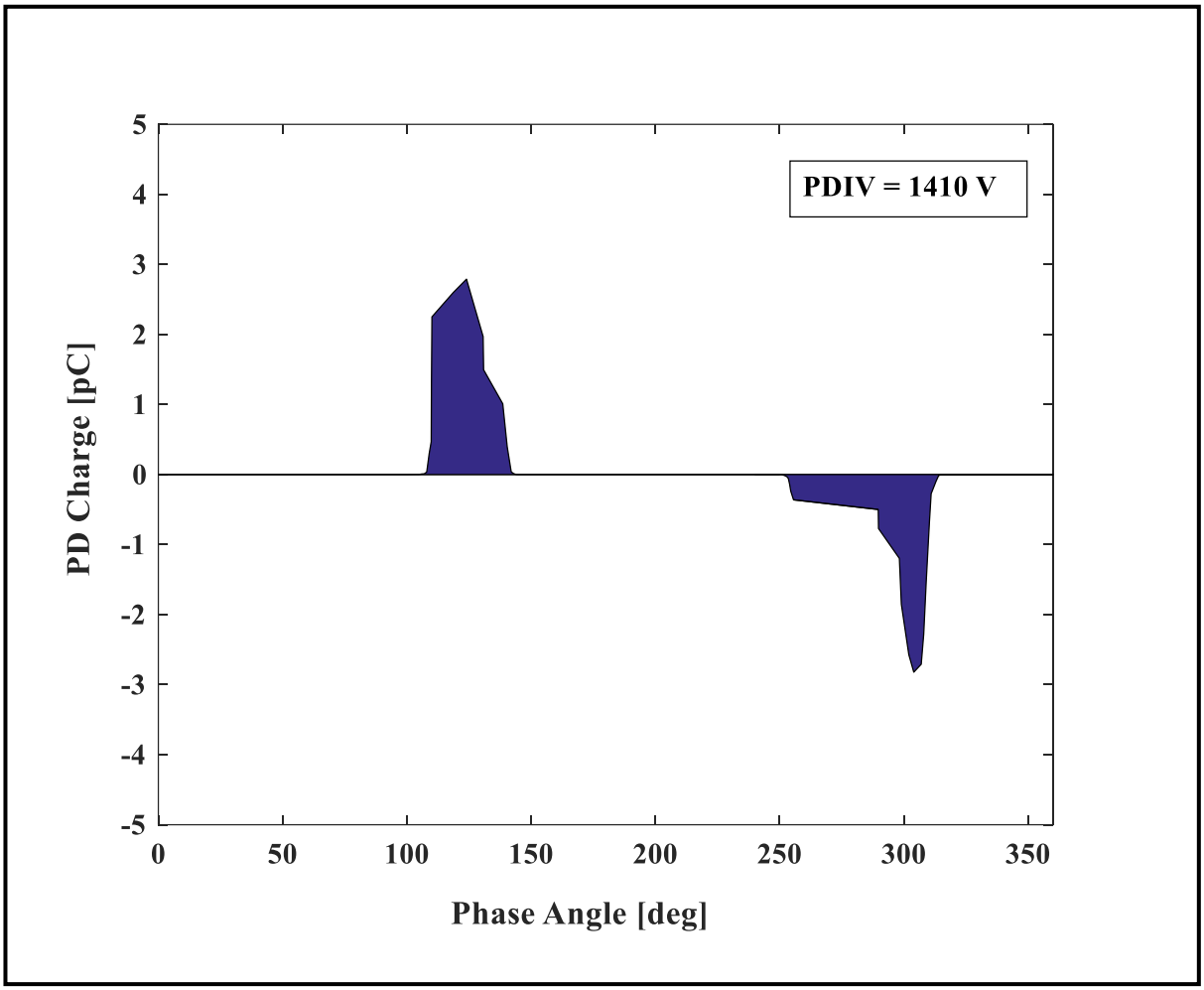

Fig. 6.22. The phase angle- PD charge (ϕ-q) plot for eightfold Kraft paper.

Eightfold kraft paper has been selected to increase the thickness of the insulation. Breakdown of single-layered kraft paper occurred with a little application of voltage Now, in Fig. 6.22 it is seen that PD in the sample occurs at 1.4kV. From the PD pattern shown in Fig. 6.22, the quantity of PD in both the positive and negative cycle is seen, and this is due

to the presence of weak zones between the layers. The maximum PD amplitude is also quite high, but the span of the phase angle corresponding to the occurrence of PD is small.

6.3.5.2 Comparative Study on Discharge Pulse Count (N)

In Fig. 6.23 the pulse count of PD (n) is plotted against the corresponding phase angle (ϕ) for eightfold kraft paper.

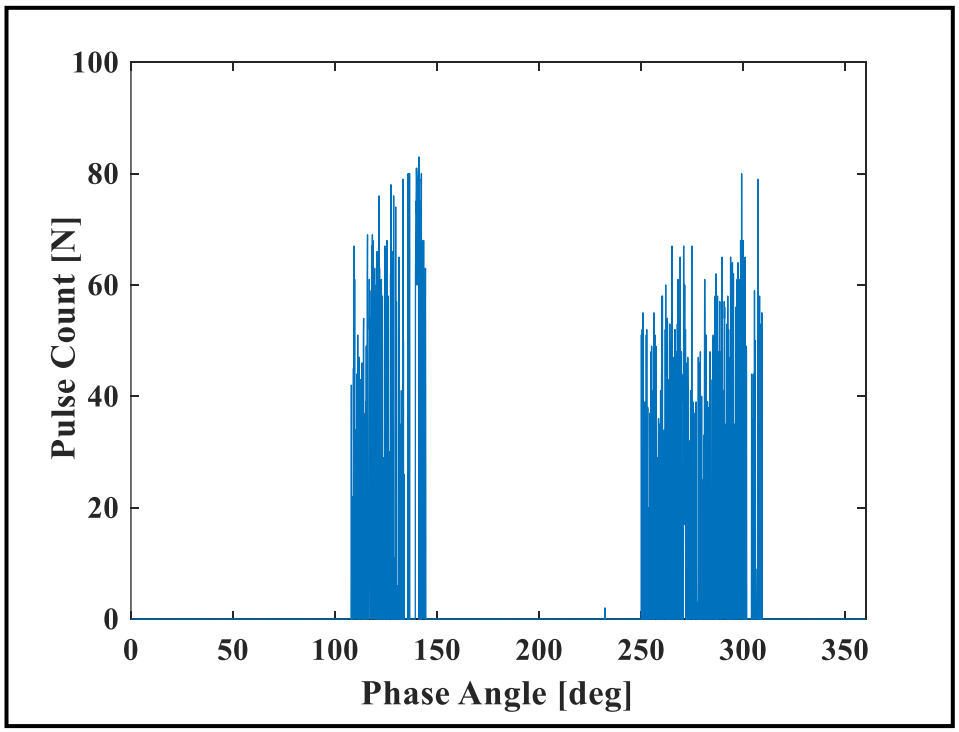

Fig. 6.23. The phase angle- PD charge (ϕ-n) plot for eightfold Kraft paper.

From the pattern in Fig. 6.23, the pulse count rate could be seen quite high and it spread out more in the negative cycle that in the positive cycle. No particular pattern is observed in this case.

The results obtained from the experiment on a different type of dry type insulation specimen were graphically plotted her and analyzed. A database has been created which projects all the different PRPD distribution patterns. An attempt has been made to assess the ϕ-q and ϕ-n plots of different samples. A comparison is drawn among different samples made with the same insulation material. The varied samples showed a variety of PRPD pattern, but still, an attempt was made to group them on the basis of the distribution pattern. The PDIV of every sample was recorded when the experiment was performed and the quantity of discharge or maximum magnitude of discharge for that particular PDIV is

graphically shown in the waveforms. The pulse count rate was also recorded, which may be later used to plot the ϕ-q-n plot.

The Phase angle –PD charge (ϕ-q) patterns for all the different types of samples are showed here. But, to check the integrity of the experiment, the repeatability of the process to produce a similar PD pattern is examined here. Thus multiple times data were fetched for a similar sample applying the same voltage. An example is shown in Fig. 6.24 for the sample single-layered thin pressboard.

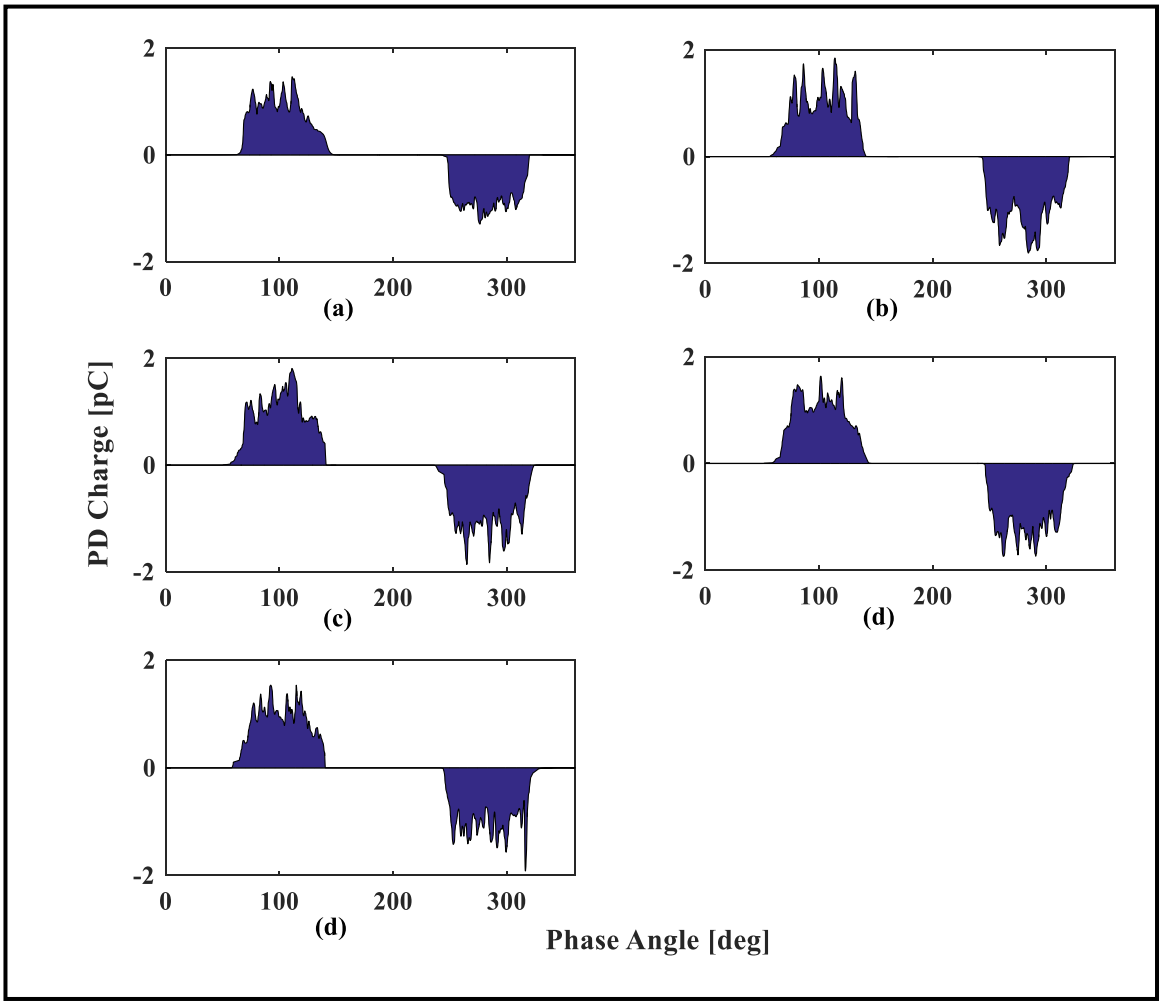

Fig. 6.24. The phase angle- PD charge (ϕ-q) plot for five readings corresponding to a fixed voltage in a single-layered thin Pressboard.

In Fig 6.24, It is seen that five readings for the same sample are taken. The ϕ-q patterns obtained for all the five readings are more or less similar, thus creating a distinct pattern for a particular sample. This repetition is true for all the other samples used here.

6.4 COMPARATIVE STUDY ON CONDITION MONITORING OF DIFFERENT DRY TYPE INSULATING MATERIAL BASED ON DISSIPATION FACTOR (Tanδ)

Tanδ is a diagnostic measure which helps in quality control of the insulation sample. The objective of the tanδ test is to measure the deterioration of an insulation sample due to the presence of impurities, defects, etc. A variation in tanδ with applied voltage helps to find the source of imperfection in the sample. The insulation samples prepare in section 5.3.1 and 5.3.2 have undergone this test to check the dissipation factor. A low dissipation factor indicates good quality of insulation. Here, a database is created on the basic of dissipation factor for different insulation used.

6.4.1 COMPARATIVE STUDY ON LAYERED SAMPLES

In Fig. 6.25 a comparative study is done on various dry type solid insulation used. The procedure has been described in subsection 5.7.1. The stacked bar chart helps to show the increasing or decreasing value of dissipation factor with the addition of layers in the sample.

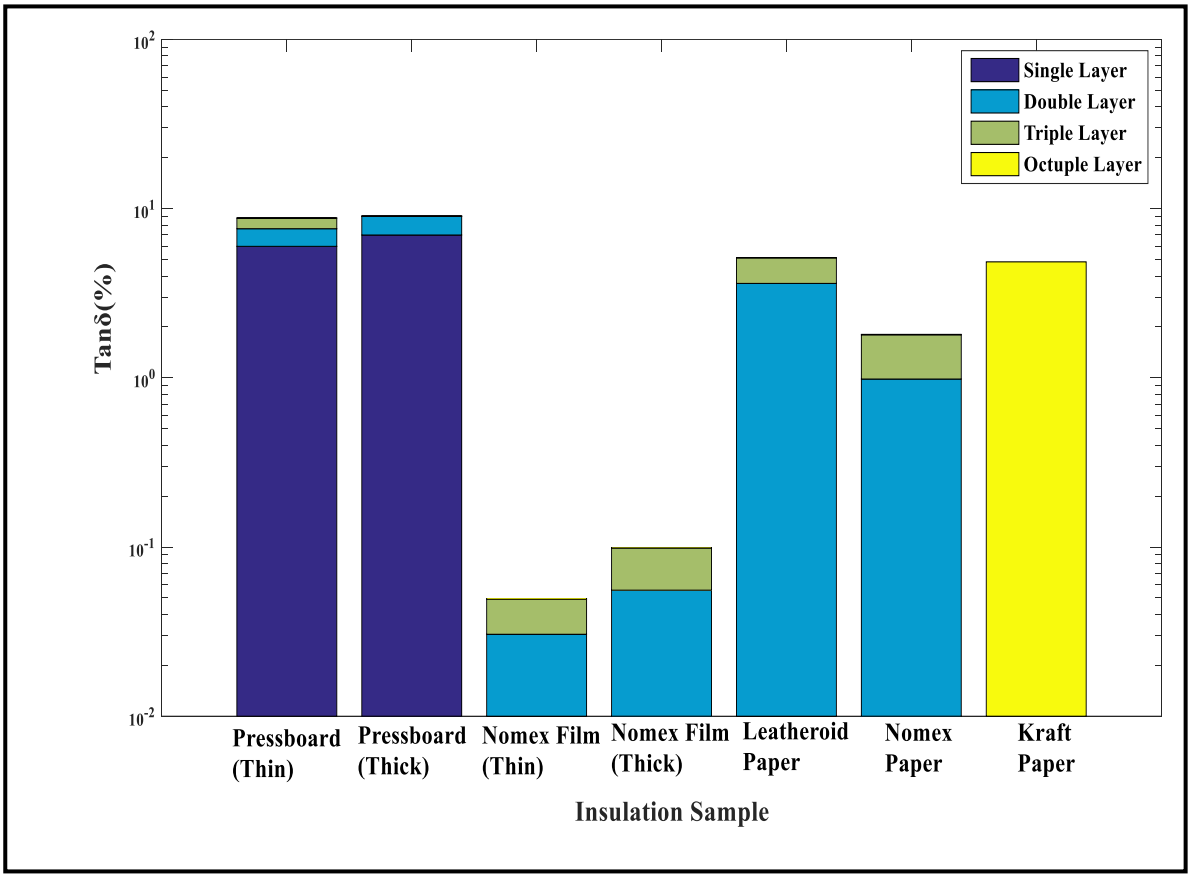

Fig. 6.25. Tanδ values of different Insulation Samples

Fig. 6.25 shows that with an increase in the layer the value of tanδ(%) also increases. This would happen since, with addition in the layer, creation of voids, impurities between the interfaces of the layers are created which increases the overall heat losses of the sample. Due to the different heat losses, the value of tanδ changes significantly. Tanδ value is independent of the geometry of the sample, but if the tanδ value starts increasing at a certain applied voltage then it indicates the presence of voids and impurities in the sample [11].

6.4.2 Comparative Study on Samples with Centrally Placed Void

In Fig. 6.26 a comparative study is done on various dry type insulation used with a centrally placed void in the top layer. For the procedure, subsection 5.7.1 is referred**.** The stacked bar chart helps to show the increasing or decreasing value of dissipation factor with the increment in the void area of the sample.

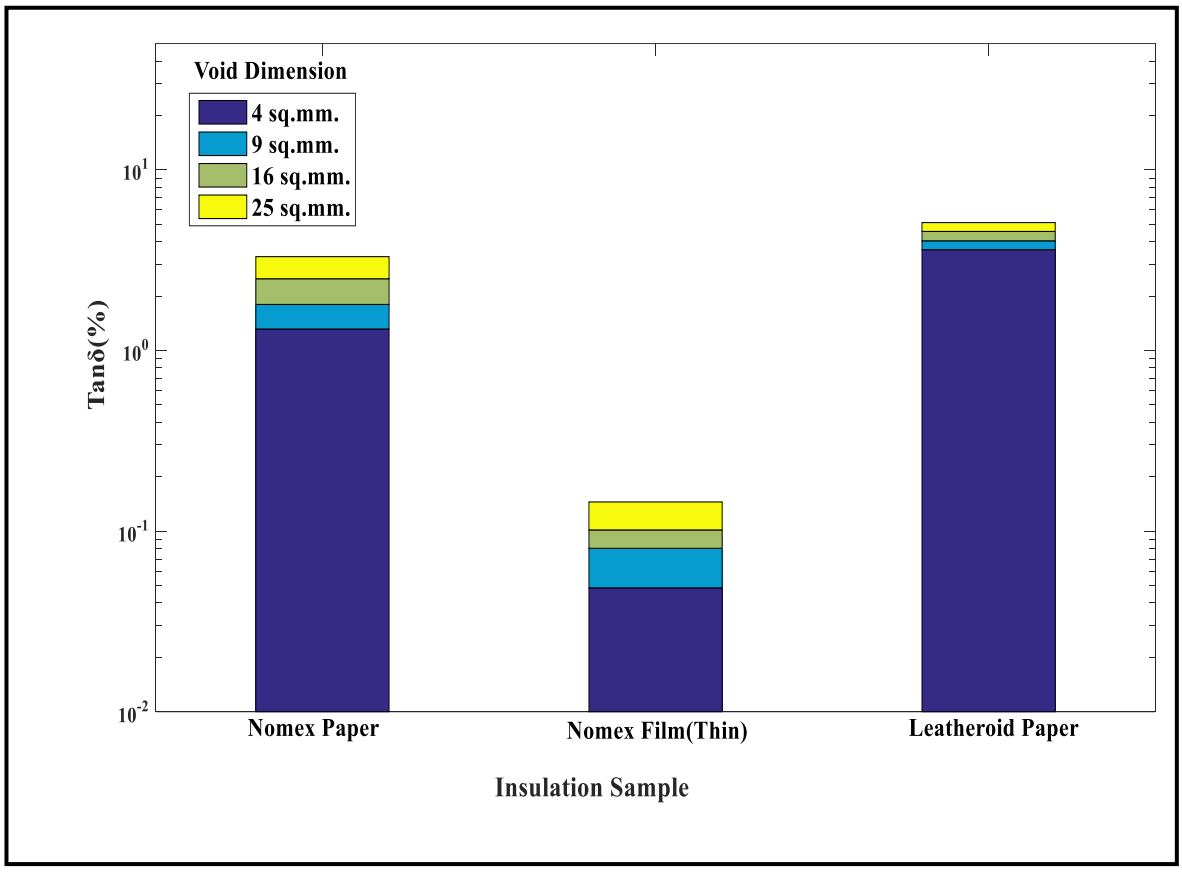

Fig. 6.26. Tanδ values of different Insulation Samples with a centrally placed void.

If Fig. 6.26 is referred, it is seen that the value of tanδ(%) increases with increase in the area of the void. This is because when a voltage is applied, the overall heat loss is more in the sample. These heat losses affects the tanδ value. Thus tanδ value increases with void size. But again tanδ is independent of the geometry of the sample and thus for an applied voltage if the value starts to increase, then it means void is present in the sample [11].

6.5 Comparative Study on Condition Monitoring of Different Dry Type Insulating Material Based on Insulation Resistance (IR)

Insulation resistance is an important test to assess the condition of the insulation used. In Fig. 6.27 the IR values of different samples are shown.

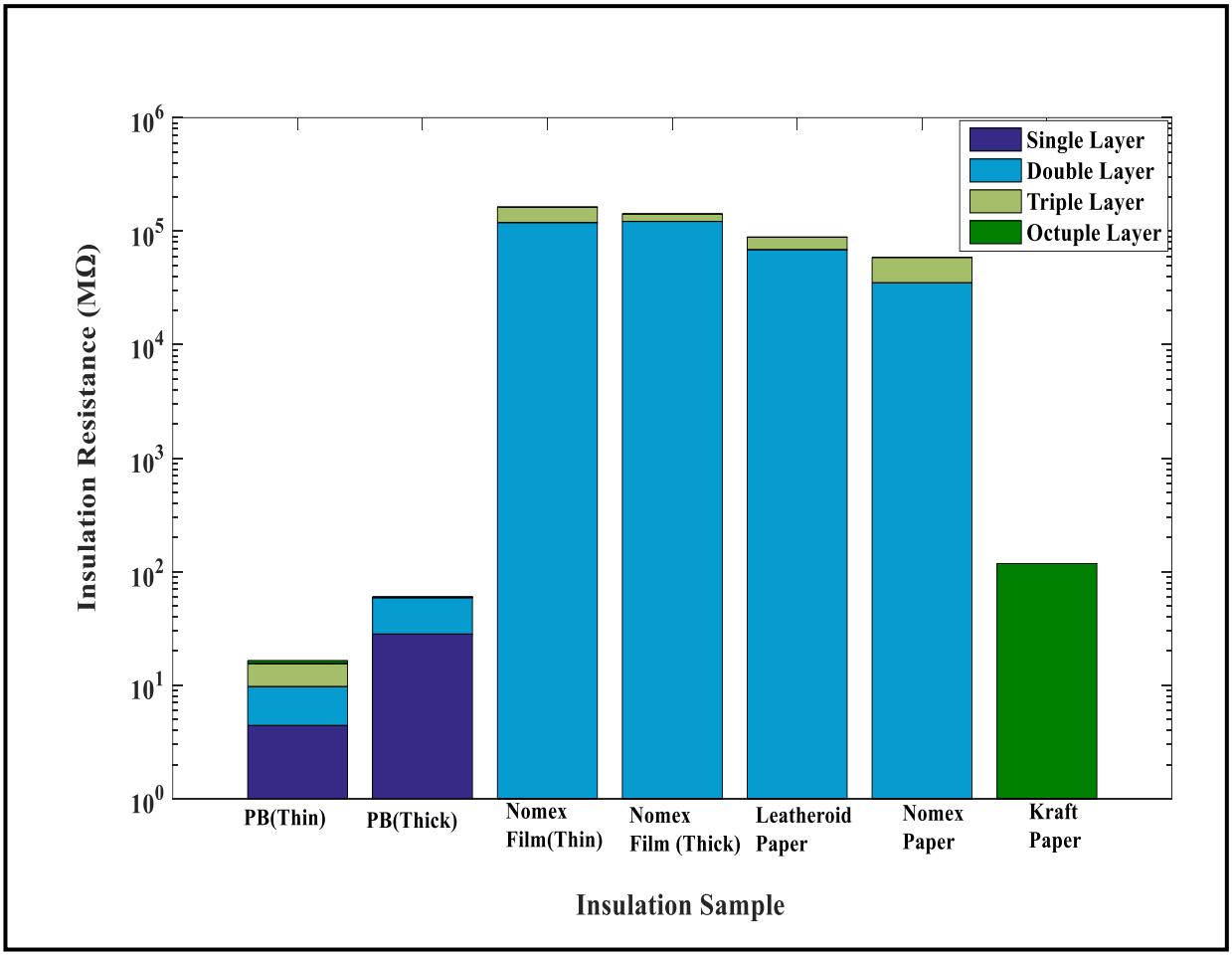

Fig.6.27. The IR values of different solid dielectric samples.

From Fig. 6.27, it can be concluded that with the increase in layers in the sample, the IR value of the sample gets increased, but this increment is not very significant. With the addition of layering, there must be some contamination, moisture present between the interfaces which would decrease its value. This experiment was performed at two different d.c. voltage levels, but the difference in IR values for two sets of reading are negligible

which indicates the absence of significant voids in the sample [11]. Thus IR is an important diagnostic method that helps in understanding the present condition of the insulation.

6.6 INFERENCE

In this Chapter, a comparative study has been made among the insulation samples. The PRPD patterns obtained for different insulation samples have their own distinctive ϕ-q, ϕ-n distribution. From these reported patterns, an idea about the PD activity of the sample could be obtained as these patterns are sample specific. Later these patterns from the database could be used to identify any insulation material.

It is observed that with the addition of layers in the sample, basically the thickness is increased which is increasing the PDIV of the sample. Then the sample can be made to operate at high working voltage. Thus this is considered to be a great advantage. But again it is seen that with the increase in layering, air layer, contaminants, manufacturing defects, air bubble, impurities between the interfaces increases, which would ultimately lead to the high discharge of PD pulses which in turn ultimately be the cause breakdown of the sample. It is also seen that with the increase in the void area, the insulation sample degrades faster as the PD activity increases. The tanδ(%) and insulation resistance of different samples are recorded for the quality control and condition monitoring of the samples. Following the results obtained, the analysis of the data is done in Chapter 7.

CHAPTER - 7

Analysis

Chapter 7

7.1 INTRODUCTION

PD detection and measurement have been one of the most important diagnostic methods for the quality assessment of the Insulation system. In order to ensure reliable and durable operation of high voltage equipment, it was vital to relate the observable statistical characteristics of PDs to the properties of the defect or void. In the previous chapter, the PRPD pattern of the PD pulses was extracted and explored for various samples. The quantification of PD pulses by their magnitude (q) and discharge rate of the pulse(n) was done and various ϕ-q and ϕ-n plots for various samples were obtained in relation to the applied a.c. voltage [43].

In this Chapter, a few features have been studied from the already obtained PRPD distribution to assimilate the PD pattern. Statistical analysis is adapted for the characterization of several univariate PRPD distributions. A visual representation of a bi-variate ϕ-q-n plot is also presented here.

7.2 CHARACTERIZATION OF PRPD PATTERNS BASED ON STATISTICAL ANALYSIS

Statistical methods are best applied for PRPD data. Several statistical operators are calculated applying standard statistical analysis, which had helped in characterizing uni-variate distribution. Since PD occurs in both the positive and negative cycle of a test a.c. cycle, these parameters are evaluated separately for both half cycles. The profile of all these discrete distribution functions is put together in a general structure $y_i = f(x_i)$. The statistical operators are discussed in the subsequent subsections [42,43].

7.2.1 Mean Value (μ)

For the given data of a discrete set of numbers, Mean value is defined as the sum of the values divided by the number of values. This is also known as the average value. This statistical operator can be calculated as shown in equation 7.1.

$$\text{Mean (Average) Value } (\mu) = \frac{\sum_{i=1}^{N} x_i \, f(x_i)}{\sum_{i=1}^{N} f(x_i)} \qquad 7.1$$

Where, x = pulse rate count (n); $f(x)$ = charge magnitude of PD ; N = number of phase windows in half cycle (negative or positive).

The PRPD graphs were obtained and plotted graphically in Chapter 6 for varied samples as mentioned in subsection 5.3.1 and 5.3.2. From the ϕ-q plots of these samples, the mean value of discharges in one complete a.c. cycle is calculated using the equation 7.1. The mean (average) value of the discharge is calculated individually for the positive and negative cycle and are represented in a tabular format in Table 7.1 and Table 7.2.

TABLE 7.1 MEAN VALUE (μ) OF PD PULSES FOR LAYERED SAMPLES.

Sl. No.	Sample Type	Mean PD Magnitude (pC)	
		Positive Cycle	Negative Cycle
1	Pressboard Thin Single Layer	0.89	0.90
2	Pressboard Thin Double Layer	1.40	1.43
3	Pressboard Thin Triple Layer	1.45	2.64
4	Pressboard Thick Single Layer	1.52	1.07
5	Pressboard Thick Double Layer	3.08	2.47
6	Leatheroid Double Layer	0.63	0.79
7	Leatheroid Triple Layer	0.75	0.81
8	Nomex Film Thin Double Layer	1.56	1.50
9	Nomex Film Thin Triple Layer	2.25	1.96
10	Nomex Film Thick Double Layer	0.47	0.65
11	Nomex Film Thick Triple Layer	0.99	1.37
12	Nomex Paper Double Layer	1.22	0.91
13	Nomex Paper Triple Layer	1.38	1.44
14	Eightfold Kraft Paper	5.01	8.24

From Table 7.2, it is seen that for every insulation material when layers of the sample are added to it, the mean PD discharge value increases for both the positive and negative half cycles in a complete a.c. cycle. It is observed in some samples the mean value of PD is more in the positive cycle and in some mean value of PD is more in the negative cycle.

TABLE 7.2 MEAN VALUE (μ) OF PD PULSES FOR SAMPLES WITH AN ARTIFICIAL VOID.

Sample Type	Area Size(sq.mm.)	Mean PD Magnitude(pC)	
		Positive Cycle	Negative Cycle
Leatheroid Paper	4	0.68	1.13
	9	1.46	1.29
	16	1.86	1.48
	25	1.80	1.45
Nomex Paper	4	1.26	1.58
	9	1.30	2.41
	16	1.47	4.52
	25	3.30	5.41
Nomex Film (Thin)	4	2.42	2.75
	9	2.54	3.18
	16	4.92	3.35
	25	0.00	4.20

From Table 7.2, it is observed that for every sample type, as the size of the area increases, PD discharge and hence the mean PD value also increases in both positive and negative half cycle. PD mean value gives an estimate of the PD discharge occurred in one complete a.c. cycle.

7.2.2 Standard Deviation (σ)

Standard deviation gives a measure that quantifies the amount of dispersion is present in a set of data. A low value of standard deviation indicates that the data points tend to be close to the mean value of the set of data, while a high standard deviation indicates that the data points are spread out over a wider range of values. The statistical operator can be calculated as shown in equation 7.2.

$$\text{Standard Deviation } (\sigma) = \sqrt{\frac{\sum_{i=1}^{N} (x_i - \mu)^2 f(x_i)}{\sum_{i=1}^{N} f(x_i)}} \qquad 7.2$$

Where, x = pulse rate count(n); $f(x)$ = charge magnitude of PD ; N = number of phase windows in half cycle (negative or positive) ; μ = mean value of PD pulse.

From the ϕ-q plots of the samples, as represented in Chapter 6, the standard deviation of discharges in both positive and negative half cycle of one complete a.c. cycle is calculated using the equation 7.2. The standard deviation value of the discharge is calculated individually for the positive and negative cycle and are represented in a tabular format in Table 7.3 and Table 7.4.

TABLE 7.3 STANDARD DEVIATION (σ) OF PD PULSES FOR LAYERED SAMPLES.

Sl. No.	Sample Type	Standard Deviation (pC)	
		Positive Cycle	Negative Cycle
1	Pressboard Thin Single Layer	0.33	0.24
2	Pressboard Thin Double Layer	1.50	1.12
3	Pressboard Thin Triple Layer	2.05	2.65
4	Pressboard Thick Single Layer	2.08	1.89
5	Pressboard Thick Double Layer	3.26	3.52
6	Leatheroid Double Layer	0.30	0.43
7	Leatheroid Triple Layer	0.30	0.32
8	Nomex Film Thin Double Layer	0.91	1.14
9	Nomex Film Thin Triple Layer	1.66	1.46
10	Nomex Film Thick Double Layer	0.51	0.38
11	Nomex Film Thick Triple Layer	0.44	0.62
12	Nomex Paper Double Layer	0.69	0.70
13	Nomex Paper Triple Layer	0.70	0.59
14	Eightfold Kraft Paper	1.06	1.25

TABLE 7.4 STANDARD DEVIATION (σ) OF PD PULSES FOR SAMPLES WITH AN ARTIFICIAL VOID.

Sample Type	Area Size(sq.mm.)	Standard Deviation(pC)	
		Positive Cycle	Negative Cycle
Leatheroid Paper	4	0.40	0.80
	9	0.81	0.94
	16	1.06	1.16
	25	0.86	1.23
Nomex Paper	4	0.73	0.82
	9	0.88	0.83
	16	0.63	0.48
	25	0.45	0.28
Nomex Film(Thin)	4	0.82	1.01
	9	1.05	1.31
	16	2.05	1.47
	25	2.27	2.58

7.2.3 Skewness (S_k) and Kurtosis (K_u)

These two statistical operators are a descriptor of the shape of the PD distribution pattern. Both skewness and kurtosis are evaluated with respect to a standard normal distribution.

Skewness is used to quantify the extent to which a distribution differs from a normal distribution. It measures the quantity of asymmetry or degree of tilt of the data. Skewness can be calculated as shown in equation 7.3.

For a symmetric distribution, S_k =0.

For a distribution to be asymmetric to the left, S_k >0.

For a distribution to be asymmetric to the right, S_k <0.

$$\text{Skewness } (S_k) = \frac{\sum_{i=1}^{N} (x_i - \mu)^3 f(x_i)}{\sigma^3 \sum_{i=1}^{N} f(x_i)} \qquad 7.3$$

Where, x = pulse rate count(n); $f(x)$ = charge magnitude of PD ; N = number of phase windows in half cycle (negative or positive) ; μ = mean value of PD pulse; σ = standard deviation.

Kurtosis acts as an indicator of sharpness of distribution and compares the distribution with the normal distribution. It tells us the extent to which the distribution is heavier or light-tailed than the normal distribution. Kurtosis can be calculated as shown in equation 7.4.

If the distribution has the same sharpness as a normal distribution, then K_u=0.
If the distribution is sharper than the normal distribution, then K_u >0.
If the distribution is flatter than the normal distribution, then K_u <0.

$$\text{Kurtosis } (K_u) = \frac{\sum_{i=1}^{N} (x_i - \mu)^4 f(x_i)}{\sigma^4 \sum_{i=1}^{N} f(x_i)} - 3.0 \qquad 7.4$$

Where, x = pulse rate count(n); $f(x)$ = charge magnitude of PD ; N = number of phase windows in half cycle (negative or positive) ; μ =mean value of PD pulse; σ = standard deviation.
The skewness and kurtosis value of the PD distribution is calculated individually for samples for both the positive and negative cycle and are represented in a tabular format in Table 7.5 and Table 7.6.

TABLE 7.5 SKEWNESS (S_K) AND KURTOSIS (K_U) VALUES OF PD DISTRIBUTION FOR LAYERED SAMPLES.

Sl. No.	Sample Type	Skewness (Sk)		Kurtosis (Ku)	
		Positive Cycle	Negative Cycle	Positive Cycle	Negative Cycle
1	Pressboard Thin Single Layer	-0.7267	-2.1077	3.5199	8.6477
2	Pressboard Thin Double Layer	2.2544	3.3629	7.1429	21.1844
3	Pressboard Thin Triple Layer	1.4271	0.4207	3.3097	1.5805
4	Pressboard Thick Single Layer	2.1194	2.1642	7.0795	6.7254
5	Pressboard Thick Double Layer	1.2139	1.5834	3.6824	4.1435

Sl. No.	Sample Type	Skewness (Sk)		Kurtosis (Ku)	
		Positive Cycle	Negative Cycle	Positive Cycle	Negative Cycle
6	Leatheroid Double Layer	-0.2735	0.0337	2.8152	2.418
7	Leatheroid Triple Layer	1.0551	2.334	5.4609	23.4996
8	Nomex Film Thin Double Layer	0.189	0.8397	3.0293	3.6383
9	Nomex Film Thin Triple Layer	0.1571	1.1155	1.8839	3.0384
10	Nomex Film Thick Double Layer	2.5534	2.163	9.3271	11.2933
11	Nomex Film Thick Triple Layer	0.1918	1.4391	3.7192	8.6193
12	Nomex Paper Double Layer	0.0229	2.1777	1.9717	9.0305
13	Nomex Paper Triple Layer	0.739	-0.0978	4.8011	3.3214
14	Eightfold Kraft Paper	2.6865	1.7052	9.6256	4.7758

TABLE 7.6 SKEWNESS (S_K) AND KURTOSIS (K_U) VALUES OF PD DISTRIBUTION FOR SAMPLES WITH AN ARTIFICIAL VOID.

Sample Type	Area Size(sq.mm.)	Skewness (Sk)		Kurtosis (Ku)	
		Positive Cycle	Negative Cycle	Positive Cycle	Negative Cycle
Leatheroid Paper	4	-0.1454	-0.0845	2.1112	1.6775
	9	-0.8815	-0.1173	2.2037	1.7693
	16	-0.7785	0.3931	2.084	1.7206
	25	-0.1513	1.2002	2.8323	3.9741
Nomex Paper	4	-0.1771	-0.0231	1.9837	2.5399
	9	0.4341	1.4871	1.9869	4.4593
	16	1.6247	2.0223	5.2228	8.8709
	25	2.2208	2.0259	10.7425	9.3615
Nomex Film(Thin)	4	-1.5302	-1.0212	6.1594	3.5473
	9	-0.5313	-0.5155	3.195	3.4984
	16	0.8273	0.8273	2.2983	1.9224
	25	0.2948	-0.0769	1.5768	1.8434

From Tables 7.5 and 7.6, a brief idea about the ϕ-q pattern can be drawn regarding the degree of its tilt towards the left or right side and about the sharpness of pattern.

7.3 VISUAL REPRESENTATION OF A 3-D PLOT

The bi-variate distribution of ϕ-q-n is generally graphically represented in a three-dimensional plot. The aforementioned 3D plot has been considered to be a complete form of graphical representation of a PD pulse distribution. The pulse magnitude (q) and pulse count rate (n) can be derived indirectly from this plot.

The 3-D representation of a Leatheroid triple layered sample is shown in Fig. 7.1.

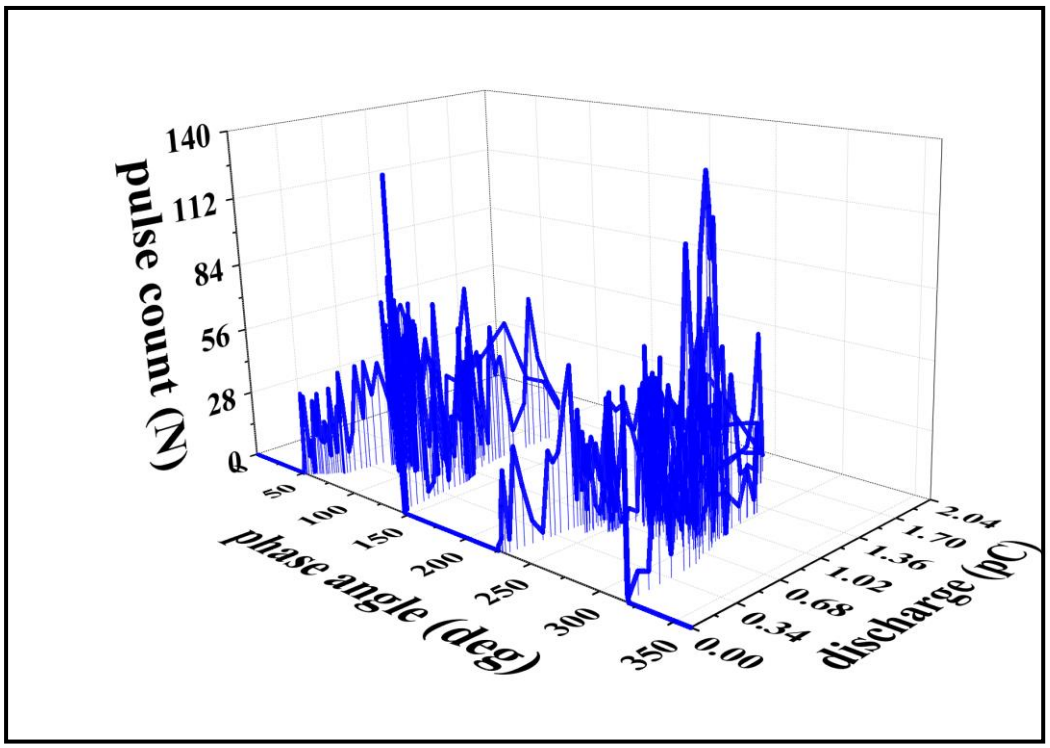

Fig. 7.1. A 3D representation of a ϕ-q-n plot of triple-layered Leatheroid sample

In this Fig. 7.1, the pulse count rate (n) can be seen for the corresponding PD magnitude (q) with respect to the phase angle.

7.4 DISCUSSIONS

In this Chapter, a few statistical operators are computed for the different PRPD patterns obtained for varied samples. A 3-D ϕ-q-n plot that presents a complete form of representation of the PRPD pattern is also shown in this chapter.

CHAPTER - 8

Conclusions

Chapter 8

8.1 CONCLUSIONS

Degradation of the solid insulation is one of the main causes behind the failure of different high voltage devices. Thus, condition monitoring of the insulation is imperative to ensure reliable operation of the equipment.

Solid insulating materials which are used in various high voltage equipment are already under a lot of stresses like electrical, electromechanical, thermal, etc when in service. It has been established partial discharge is another phenomenon other than these stresses that have been an active instigator in the degradation processes of solid insulation. PD in high voltage insulating systems originate from various local defects, which results in further degradation of the insulation.

There have been various diagnostic methods developed for quality control of the insulation. The PD measurement is considered as one of the most important diagnostic tools for condition monitoring of the insulation as it provides critical information regarding the degradation stage and location of the PD source and also produces insight into the aging condition of the solid insulating material. Thus with the help of PD activity data, an overall predictive diagnosis of the sample is possible.

In the present work, the aim was to measure the PD activity in different solid insulation samples with the help of a very cost-effective PD test setup. This PD setup has been assembled in the High Tension Laboratory of Jadavpur University. The PD experiment was performed on different samples and after the data acquisition has been done, quantification of PD pulses by their magnitude (q) and discharge rate of the pulse (n) was accomplished. Various ϕ-q and ϕ-n distribution for different samples have been obtained in relation to the applied a.c. voltage. These distributions are also known as PRPD patterns.

A database has been created on different samples on the basis of their PD characteristics and a comparative study was drawn among the samples based on the PRPD patterns. The PRPD patterns which were obtained for different samples are unique and sample specific. The objective of this PD experiment was to create a database where distinct PD activity patterns of the samples could be reported. In the database, the unique PRPD patterns of the different samples comprising of multiple layers, as well as void, are presented along with

their respective PDIV. Later in the future, a sample could be easily identified with the help of these reported PRPD patterns. An example is taken from Fig. 6.8 from section 6.3.2.1.

From Fig. 6.8 from section 6.3.2.1, the ϕ-q patterns for double and triple-layered Leatheroid paper has been seen respectively. These two plots are different and distinctive for double and triple layers of leatheroid paper. Thus it can be deduced that a sample has different PRPD for a different arrangement of layers and voids in the sample. These patterns are distinctive in nature such that no two patterns are the same. An insulation sample could later be easily identified by looking at these pattern of PRPD reported in the database.

The tanδ and IR values help in getting a better insight into the condition of the insulation and indicates the presence of defects. Thus, a comparative study based on tanδ and IR values of different samples has been drawn here in the thesis for the quality control and condition monitoring of the samples.

Statistical analysis has been adapted here for the characterization of several uni-variate PRPD distributions. Mean value and standard deviation of the PD pulses of different samples gives a measure of the PD activity in the sample. Skewness and kurtosis help in defining the shape of the PD pattern. With the help of the PRPD data, a 3-D representation of the plot was depicted which has been considered to be a complete form of graphical representation of a PD pulse distribution.

In this present work, an attempt has been made to measure PD activity in solid insulation in the most cost-effective way without using expensive oscilloscopes and high-end sensors. Though the accuracy and quality in the data acquisition process were not compromised, a certain degree of uncertainty remains in the process due to human error and error due to environmental conditions. The data acquisition process can be made more accurate if the shielding of the entire set up is made better eg, using Faraday's cage to mitigate all the external noises.

8.2 FUTURE SCOPES OF WORK

In this present work, a database has been created reporting a comparative study among the different PRPD characteristics of different solid insulation material. From this study, a basic idea about the PD activity in different solid dielectrics could be obtained. The devices and components in the experimental setup play an integral part in the deduction of

PD activity. A system with superior precision would have helped in capturing PD activity with better accuracy. This research work could be extended further in the future in the area are given here.

- Condition based monitoring of thermally aged solid insulation using PD measurement as the diagnostic tool.
- Condition based monitoring of solid insulation by varying the temperature as well as the relative humidity using PD measurement as the diagnostic tool.
- Condition monitoring of solid insulation based on the application of wavelet signal processing in the elimination of external noises and recovering the PD signal.
- Processing of the PD signal using discrete wavelet transforms in time-frequency domain such that both time and frequency characteristics can be studied simultaneously.
- Different algorithms like the nearest neighbor and genetic algorithm can be applied for identifying the location of PD activity from the data obtained from PRPD pattern.

REFERENCES

[1] M. Wang, A.J.Vandermaar and K.D. Srivastava, "Review of condition assessment of power transformers in service", IEEE Electrical Insulation Magazine, vol. 18, no. 6, pp.12 - 24, 2002.

[2] M. Arshad and S.M. Islam, "Significance of cellulose power transformer condition assessment", IEEE Transaction on Dielectrics and Electrical Insulation, vol.18, no.5, pp. 1591 -1598, 2011.

[3] T. Shioiri, J. Sato, T. Ozaki, O. Sakaguchi, T. Kamikawaji, M. Miyagawa, M. Homma and K. Suzuki, "Insulation technology for medium voltage solid insulated switchgear", Proceedings of IEEE Annual Report Conference on Electrical Insulation and Dielectric Phenomena (CEIDP), pp. 341 – 344, 2003.

[4] S.Chakravorti, D. Dey and B.Chatterjee, "Recent Trends in the Condition Monitoring of Transformers", Springer-Verlag London 2013.

[5] E.Kuffel, W.S. Zaengl and J. Kuffel, "High Voltage Engineering Fundamentals", Butterworth-Heinemann 2000.

[6] General Electric Measurement and Control - online workbook "Electrical equipment – Condition Monitoring and Diagnostics" ,"www.industrial.ai/sites/g/files/cozyhq596/files/acquiadam_assets/gea13907d_electrical_equipment_system_1_application_package_r1.pdf".

[7] IEC Standard 60270 (third edition, 2000). Partial Discharge Measurements. International Electrotechnical Commission (IEC), Geneva, Switzerland.

[8] L.L.Alston, " High-Voltage Technology", Oxford University Press,1968

[9] Megger- guidebook, "The complete guide to Electrical Insulation Testing", 2006

[10] M.S.Naidu and V. Kamaraju, "High-Voltage Engineering", McGraw Hill Education Pvt. Ltd., 5th edition, 2013.

[11] R.Menon, S.S. Kolambekar, and N.J. Buch, "Diagnostic testing of High Voltage Insulation for Condition Monitoring."

[12] S. Ren, X.Yang, W. Yang, B. Xi, and Xi. Cao, " Research on Insulation Condition Monitoring System for Power Transformers", Proceedings of International Conference on Condition Monitoring and Diagnosis, pp. 21-24, 2008.

REFERENCES

[13] G.C. Stone, " Partial discharge diagnostics and electrical equipment insulation condition assessment", IEEE Transactions on Dielectrics and Electrical Insulation, Vol. 12, no. 5, pp. 891 – 904, 2005.

[14] P. Su. , " Diagnostic Tests and Condition Monitoring of Electrical Machines".

[15] B. Yazici, " Statistical pattern analysis of partial discharge measurements for quality assessment of insulation systems in high-voltage electrical machinery", IEEE Transactions on Industry Applications, Vol. 40, No. 6, pp. 1579 - 1594, 2004.

[16] IEEE P1434™/D13Draft Guide for the Measurement of Partial Discharges in AC Electric Machinery.

[17] S.Ray, "An Introduction to High-Voltage Engineering", PHI Learning Pvt. Ltd., 2nd Edition, 2013.

[18] EEEGuide.com, online document, "www.eeeguide.com/breakdown-of-solid-dielectrics-in-practice".

[19] T.Joyo, T.Okuda, N. Kadota, R. Miyatake, S.Okada, and K. Mio, " Phase-resolved partial discharge patterns for various damage of winding insulation detected with different measuring devices", Proceedings of IEEE Conference on Electrical Insulation (EIC), 2017.

[20] D.Adhikari, D.M. Hepburn, and B.G. Stewart, " Analysis of Partial Discharge Characteristics in Artificially Created Voids", Proceedings of International Universities Power Engineering Conference (UPEC), 2010.

[21] H. Illias, T.S. Yuan A.H.A Baker, H. Mokhlis, G. Chen and P.L.Lewin, " Partial discharge patterns in high voltage insulation", Proceedings of IEEE Conference on Power and Energy (PECon), 2012.

[22] IEC Standard 60085 (fourth edition, 2007). Electrical Insulation –Thermal Evaluation and Designation. International Electrotechnical Commission (IEC), Geneva, Switzerland.

[23] G.L. Moses, "The Purpose Of Electrical Insulation", Proceedings of EI National Conference on the Application of Electrical Insulation, pp. 112 - 114, 1960.

REFERENCES

[24] I.E. Kuimov and V.M. Pak, " Current trends of production development as regards to the electrical insulation materials for high voltage electrical machines winding insulation: test results on long-term electrical strength", Proceedings of IEEE Conference on International Symposium on Electrical Insulation, 2000.

[25] DuPont Nomex Pressboard - Technical data sheet

[26] IndiaMart –Technical data sheet, online document, "pdf.indiamart.com/impdf/203553

42933/MY-36894643/insulating-press-board.pdf".

[27] DuPont Leatheroid paper - Technical data sheet.

[28] DuPont Nomex Paper - Technical data sheet

[29] DuPont Nomex Laminates - Technical data sheet

[30] H.C.Lauroesch, General Electric Company,"Insulation Systems For Dry Type Transformers.

[31] Technical Associates Limited, Guidebook, " Dry Type transformers".

[32] DuPont, online document, "Dry Type Transformer Insulation".

[33] IEEE Draft Standard Test Code for Dry-Type Distribution and Power Transformers.

[34] A. Rodrigo, P. Llovera, V. Fuster and A. Quijano, "Study of partial discharge charge evaluation and the associated uncertainty by means of high-frequency current transformers", IEEE Transactions on Dielectrics and Electrical Insulation, Vol.19, No. 2, pp. 434 – 442, 2012.

[35] ISA Altanova group, online document, "www.isatest.com/products-container/power-transformer-testing /sts-3000-light-td-5000".

[36] Megger Group, online document, "megger.com/5-kv-diagnostic-insulation-resistance-tester-megger-mit520/2".

[37] P. Das and S. Chakravorti, "FDM based simulation of PD patterns due to narrow void considering stochastic parameters", Proceedings of IEEE Power India Conference, 2006.

[38] S. Das and P. Purkait, "φ-q-n Pattern Analysis for Understanding Partial Discharge Phenomena in Narrow Voids", Proceedings of IEEE Power and Energy Society General Meeting - Conversion and Delivery of Electrical Energy in the 21st Century.

REFERENCES

[39] Y. H. Md. Thayoob, S. K. Ahmed and C. C. Piau, " Characterization of Phase Resolved Partial Discharge waveforms from instrument transformer using statistical signal processing technique", Proceedings of IEEE International Conference on Signal and Image Processing Applications (ICSIPA),2015.

[40]R. Piccin, A. Rodrigo, P. Morshuis, A. Girodet, and J. Smit, "Partial discharge analysis of gas insulated systems at high voltage AC and DC", IEEE Transactions on Dielectrics and Electrical Insulation, Vol. 22, No.1, pp. 218 – 228,2015.

[41] A.Masood, M.U.Zuberi, M.S.Alam, E.Husain, and M.Y.Khan, "Practices of Insulating Materials in Instrument Transformers", Proceedings of Conference on National Power Systems, 2002.

[42] P. M. Kothoke, N.R. Bhosale, A. Deshpande and Dr. A. N. Cheeran, "Analysis of Partial Discharge using Phase-Resolved (n-q) Statistical Techniques ", International Journal of Engineering Research and Applications (IJERA), Vol. 3, No. 3, pp.1317-1323, 2013.

[43] N. C. Sahoo, M. M. A. Salama, and R. Bartnikas, "Trends in Partial Discharge Pattern Classification: A Survey".